Hydraulic Capacity of Drainage Channels with Lateral Inflow

M Escarameia
Y Gasowski
R W P May
A Lo Cascio

Report SR 581
February 2001

HR Wallingford

Address and Registered Office: HR Wallingford Ltd. Howbery Park, Wallingford, OXON OX10 8BA
Tel: +44 (0) 1491 835381 Fax: +44 (0) 1491 832233

Registered in England No. 2562099. HR Wallingford is a wholly owned subsidiary of HR Wallingford Group Ltd.

Contract

This report describes work funded by the Construction Directorate of the Department of the Environment, Transport and the Regions, DETR, under research contract CI 39/5/124 for which the DETR nominated officer was Mr P B Woodhead and the HR Wallingford nominated officer was Dr S W Huntington. The HR job number was MBS 0419. The report is published on behalf of DETR, but any opinions expressed in this report are not necessarily those of the funding department. The work was carried out by M Escarameia, Y Gasowski, RWP May and A Lo Cascio in the Water Management Department.

Prepared by ....Manuela Escarameia..........

(name)

..........Senior Engineer..........

(Title)

Approved by ....RWP. May..........

(name)

..........Principal Engineer..........

(Title)

Date..........30 January 2001

Summary

Hydraulic Capacity of Drainage Channels with Lateral Inflow

M Escarameia
Y Gasowski
R W P May
A Lo Cascio

Report SR 581
February 2001

A drainage channel or linear drainage system is defined as a linear assembly that collects surface water along its length and conveys it to a suitable point of discharge. This definition, which is adopted by the new European Standard prEN1433 "Drainage channels for vehicular and pedestrian areas", includes channels that can either be manufactured (those covered by the above Standard) or constructed in situ. The Standard classifies the channels into three categories according to the type of cover: kerb units, grid units and slot units. Being a product standard, prEN1433 does not, however, provide guidance on the hydraulic capacity of the channels.

Drainage channels are one of the most common means of draining run-off from paved areas such as car parks, pedestrian precincts, roads and airports. They are also installed in floors of buildings to drain water used in various industrial and processing operations or to dispose of water used for fire fighting. In spite of their increased use, independent guidance on the hydraulic capacity of drainage channels has not been available and therefore designers have so far relied on the commercial information provided with the systems. Formulae suitable for flow in pipes or in open channels of constant flow have been recommended for design but the hydraulics of those systems are very different from those of channels with continuous inflow along their length.

This report describes a study carried out by HR Wallingford with the following objectives: 1. To obtain data on the flow and self-cleansing capacities of drainage channels commercially available in the UK; 2. To develop a general numerical method for predicting the hydraulic capacity of the channels; 3. To make recommendations on how the results should be incorporated in a relevant British or European Standard.

The methodology adopted for the study was a combination of laboratory tests and numerical simulations using a computer program that was specifically developed for spatially varied flows. The program enables the computation of water profiles, and therefore flow capacity, of channels that have slopes from zero to very steep gradients. It can deal with the complex changes in flow regime (subcritical, supercritical) that can occur in channels with lateral inflow.

An extensive laboratory program was carried out involving the determination of the flow capacity of kerb, grid and slot systems of various sizes, shapes (U-shape, "squarish", circular) and materials (concrete, resin concrete). The systems were

Summary continued

tested at full scale for lateral inflow rates ranging between 0.14 and 0.67 l/s per metre and slopes from zero to 1/67. The range of flow conditions and channel configurations were further extended by numerical simulations. A number of channel configurations involving series of flat and sloping inverts were investigated and their hydraulic capacity was determined. The tests also showed that locking devices for gratings or other elements that protrude into the flow can reduce the channel capacity significantly (to up to 60% of the unobstructed flow capacity). It is therefore necessary to define the design water depth so that the water level is just below the level of any obstructions.

A limited test program was also carried out to determine the minimum flow velocities required to initiate movement of deposited sediment. Typical conditions were chosen for the tests: channel slope of 1/1000, depth of sediment bed of 5% of the channel design depth, sediment size d_{50}= 1.35mm, lateral inflow rates between 0 and 0.67 l/s per metre. In general terms the tests showed that self-cleansing velocities appear to be about 0.4m/s. An investigation of where such velocities tend to occur along drainage systems revealed that, for the systems considered in this study, this was typically in the downstream half of the channel.

Design formulae were developed to determine the hydraulic capacity of drainage channels free from sediment (Equation 16). The capacity was found to depend primarily on the available cross-sectional area of the channel and on the channel slope. As previously found for roof gutters, the length of the channel in relation to its design depth was also found to affect the capacity and its effect depends also on the slope of the channel. The formulae are valid for channels at slopes not steeper than 1/30 and with length ratios (defined as the channel length divided by the design depth) not greater than 1000. Cases where channels would be used outside this range of applicability are considered to be very limited. For example, it is not recommended to install channels at very steep slopes as the flow is strongly affected by any manufacturing or installation imperfections and the collection efficiency of gratings, slots or entry holes can be very much reduced. Also very high length ratios would typically correspond to excessively long channels (above 150m to 300m long, respectively for small and large capacity channels) and outfall chambers would normally need to be constructed at smaller intervals.

From discussions with members of the relevant BSI sub-committee, it was concluded that inclusion of the study results in prEN 1433 would not be possible in the near future because the process of final approval was already underway. Also, prEN 1433 is a product standard rather than a design standard and therefore recommendations on design would be better included in another document. The best vehicle for rapid dissemination was identified to be European Standard BS EN 752 "Drain and sewer systems outside buildings – Part 4: Hydraulic design and environmental considerations". The study outcome was therefore submitted to BSI Committee B/505 for inclusion as a UK National Annex to BS EN 752.

The work was commissioned and partly funded by the Construction Directorate of the Department of the Environment, Transport and the Regions, and involved the collaboration and contributions of the following partners: HR Wallingford, ACO Technologies plc, Camas/Aggregate Industries, Marshalls Limited, TPS Consult, Wavin Plastics Limited and Whitby Bird & Partners.

Notation

A	Cross-sectional area of flow
A_c	Cross sectional area at the critical section
B	Surface width of flow
B_c	Surface width of the critical section
b	Coefficient in Equations (12) to (16)
Ch	Chezy roughness coefficient of channel or pipe
C_1, C_2	Coefficients in Equation (11)
C_3, C_4	Coefficients in Equation (12)
F_f	Frictional force
F_r	Froude number of flow $\left(F_r = \sqrt{\left(BQ^2/gA^3\right)}\right)$
g	Acceleration due to gravity
h	Design water depth of the channel
I	Rainfall intensity
J	Outlet spacing
K	Strickler roughness coefficient of channel or pipe
K_T	Factor by which the width of the trapezoidal cross-section increases with the vertical distance from the sole
k_s	Roughness length
L	Channel length
L_c	Critical length in Equation (7)
n	Manning roughness coefficient of channel or pipe
P	Wetted perimeter of channel
P_1	Pressure at the upstream end
P_2	Pressure at the downstream end
P_c	Wetted perimeter of the critical section
Q	Flow rate
q	Flow rate per unit length of channel
R	Hydraulic radius (=A/P)
Re	Reynolds number (Re = 4VR/ν, where ν is the kinematic viscosity of water)
S, S_o	Longitudinal gradient of channel
S_f	Friction gradient of flow
S_{oc}	Minimum slope for channels with only one singular section
S_w	Sole width of trapezoidal channel
V	Flow velocity
W	Road width
W_e	Weight of water body
x	Distance measured along the length of the channel in the direction of flow
y	Depth of flow normal to invert of channel
z	Depth of centroid of the flow area
β	Momentum coefficient for the effect of non-uniform velocity distribution in the flow
λ	Darcy-Weisbach roughness coefficient
θ	Angle of the channel slope
ρ	Water density
ω	Unit weight of water (= ρ g, where ρ is the water density)

Contents

Tables

Figures

Contents continued

Contents continued

1. INTRODUCTION

1.1 Drainage channel systems

A drainage channel or linear drainage system can be defined as a linear assembly that permits the collection and conveyance of surface water along its length for discharge at a suitable point. Drainage channels can be manufactured or constructed in situ and three main categories can be identified based on the type of channel cover: kerb units, grid units and slot units.

Drainage channels are increasingly being chosen as a means of disposing of surface water in a large number of applications: parking areas in retail and business parks, pedestrian areas, roads and airports, as well as inside commercial and industrial buildings. The use of drainage channels can produce significant savings, due essentially to lower installation costs, when compared with conventional gully and pipe systems. Furthermore, the increased use of large areas of paved surfaces in recent years both in the UK and world wide has made this option very popular with drainage engineers, architects and developers.

The popularity of drainage channels prompted the need to provide guidance, which is being addressed by the new European Standard prEN1433 "Drainage channels for vehicular and pedestrian areas", currently in draft form (prEN1433). However, although giving guidance on structural aspects, this document will not address the basic function of drainage channels, i.e. their hydraulic capacity. Because they receive flow continuously along their length, these channels are hydraulically very different from gully and pipe systems, which receive flow at specified points. The current limited knowledge of the hydraulic characteristics of drainage channels means that they may be over designed, which will result in excessive construction costs, or under designed, which will result in pavement flooding.

1.2 Scope of the study

Until now the choice and specification of the most satisfactory and cost effective types of drainage channel have been hampered by the following:

- Lack of design guidance in British or European Standards and other design documents on the hydraulic performance of the systems;
- Lack of sound and independent guidance to assist designers in selecting from the many products commercially available;
- Existing commercial design data, which in some cases are based on incorrect hydraulic principles.

The study described in this report was aimed at providing design engineers and manufacturers of drainage channels with accurate, and at the same time, simple means of estimating the hydraulic performance of the systems.

The detailed objectives of the study can be summarised as follows:

- To obtain data on the flow and self-cleansing capacity of drainage channels commercially available in the UK;
- To develop a general numerical method to predict the hydraulic capacity of drainage channels;
- To make recommendations on how the results of the study should be incorporated in relevant British or European standards.

The methodology adopted for the study relied essentially on a combination of laboratory work and numerical simulations of flows in channels with lateral inflow. This allowed the development of a general numerical method for the design or assessment of drainage channels used in paved areas and/or roads.

It should be noted that the guidance given in this report applies only to drainage channels formed from rigid materials, such as concrete, plastic or resins. Current trends towards sustainable drainage are increasingly placing more emphasis on options that include pervious, vegetative linings in channels (e.g. grass lined channels and swales). The hydraulic capacity of this type of channel is dominated by the resistance offered by the vegetation lining and therefore these options are outside the scope of this report.

The present report is the final output of a two-year long study commissioned by the Construction Directorate of the Department of the Environment, Transport and the Regions between April 1999 and March 2001. A Steering Group was formed for the project involving the manufacturers ACO Technologies plc, Camas/Aggregate Industries, Marshalls Limited, Wavin Plastics Limited, the engineering consultants TPS Consult and Whitby Bird & Partners and the Highways Agency.

This report is a technical description of the work carried out for the development of new hydraulic design formulae and is not intended as a design manual. It gives supporting information to the design document that will be available in the form of a National Annex to BS EN 752, as described in Chapter 7.

Following the Introduction in Chapter 1, a description of the theory behind linear drainage channels is given in Chapter 2. The numerical program that was developed for the spatially-varied flows that occur in drainage channels is described in Chapter 3, while Chapter 4 describes the test facility used for the experimental work. The laboratory testing and the numerical simulations carried out on representative systems are described in Chapter 5, and Chapter 6 presents the analysis of the data. The initiatives to incorporate the results into the appropriate normative document and the study conclusions can be found in Chapters 7 and 8, respectively.

2. THEORETICAL BACKGROUND AND PREVIOUS RESEARCH

2.1 Spatially-varied flow with increasing discharge

The flow in drainage channels (as in roof gutters or in channels receiving flow from a side weir) is very complex when compared with flow in pipes. The flow rate is not constant, gradually increasing as the run-off from the pavement enters the channel along its length. This type of flow is called spatially-varied flow with increasing discharge. The free surface in drainage channels receiving lateral inflow can be very disturbed. The slope of the channel, any discontinuities between each channel unit, the roughness of the channel material and the lateral inflow are all factors that can affect the free surface.

Theoretical and empirical studies have been carried out in the past to describe this type of flow and to provide designers of roof and road drainage systems with a basis for their calculations. Previous studies have concentrated on a fairly narrow range of conditions, such as certain cross-sectional shapes (rectangular or trapezoidal, which are common cross-sectional shapes used for roof gutters and road-edge concrete channels). The steepness of the channel slope is also a parameter that has not been studied in detail and the flow regime in steep channels is still an area requiring further investigation. Usually linear drainage channels in paved areas are installed almost level or have quite mild slopes. However, in some cases such as in roads, the slopes can be much steeper and the flow behaviour in the channel can change dramatically from that associated with mild slopes.

The parameters of interest to engineers are the required outlet spacing and the maximum discharge that a channel can drain. Three methods can be applied to compute these quantities: 1. experimental tests to measure directly the hydraulic capacity of the channels; 2. empirical equations developed from experimental data; and 3. numerical models based on hydraulic principles and, when possible, calibrated using data from laboratory tests.

2.2 Description of flow equation

A spatially-varied flow is a steady flow whose depth and flow vary gradually along the length of the channel. As the lateral inflow mixes with the flow already in the channel, there can be a significant loss of energy. However, assuming that the lateral inflow has no component in the general flow direction, momentum conservation principles can be applied. The general equation describing the flow is obtained by considering the balance between the forces acting on a control volume. The external forces acting on the fluid are: 1. the frictional force; 2. the weight of the element of fluid; and 3. the hydrostatic pressure. For steady state conditions these external forces must be balanced by the change in momentum flux entering and leaving the control volume:

$$\omega/g\,[QdV + (V+dV)dQ] = P_1 - P_2 + W_e\sin\theta - F_f \tag{1}$$

with

$P_1 = \omega\, z\, A$

$P_2 = \omega\,(z + dy)\, A + \omega/2\; dA\; dy$

$W_e\sin\theta = \omega\, S_o\, A\, dx$

$F_f = \omega\, S_f\, A\, dx$

In the above equation θ is the downward angle of the channel relative to the horizontal, ω is the unit weight of water (= ρg where ρ is the water density), F_f is the frictional resistance exerted by the boundaries of the channel, g is the acceleration due to gravity, P_1 is the pressure at the upstream end, P_2 is the pressure at the downstream end, Q is the flow discharge in the control volume, S_f is the friction slope, S_o is the channel slope, V is the velocity of the flow in the control volume, W_e is the weight of the body of water between the two sections, z is the depth of the centroid of the flow area A, x is the distance from the upstream section and y is the depth of flow measured normal to the invert of the channel.

Neglecting the term dVdQ and substituting the external forces defined above in Equation (1) gives:

$$dy = \frac{-1}{g}\left(VdV + \frac{V}{A}dQ\right) + \left(S_o - S_f\right)dx \tag{2}$$

If non-uniform velocity distribution in the channel section is considered, a momentum coefficient needs to be introduced in the momentum terms in Equation (1). Using the continuity principle, Equation (2) can be written in the form:

$$\frac{dy}{dx} = \frac{S_0 - S_f - \dfrac{2\beta qQ}{gA^2}}{1 - \dfrac{\beta BQ^2}{gA^3}} \tag{3}$$

where q is the flow rate per unit length of channel, B is the surface width of flow and β is the energy coefficient.

The friction slope may be evaluated from the Darcy-Weisbach equation as:

$$S_f = \frac{\lambda V^2}{8gR} = \frac{\lambda Q^2 P}{8gA^3} \tag{4}$$

where λ is the Darcy-Weisbach friction factor, P is the wetted perimeter of the flow and R is the hydraulic radius (defined as P/A).

It can be noted that if q is equal to zero, Equation (3) becomes the equation for gradually-varied flow of constant discharge.

2.3 Previous research

Beij (1934) carried out a theoretical analysis and a laboratory study which led to the development of an empirical equation for sizing level roof gutters. The gutters studied were of rectangular and semi-circular shape and discharged freely at the downstream end. The laboratory study involved the measurement of water depths along a roof gutter fed by run-off from an adjacent roof. The length and shape of the channel and the rate of lateral inflow were the only variables altered in the experiments. As expected, the measured water depths were higher than those predicted theoretically neglecting resistance effects. The differences were however not very significant, with an average of 8% difference between measured and predicted values.

The equation developed by Beij for rectangular channels was converted into metric units and re-arranged by the Transport and Road Research Laboratory, TRRL, in a study concerning the drainage of level, or nearly level, roads (Whiffin and Young, 1973). Trapezoidal channels are more appropriate to the drainage of roads than rectangular channels and Beij's equation was therefore modified to cope with trapezoidal shapes:

$$J = \frac{0.235\left(S_W + \frac{1}{2}K_T h\right)^{12/13} h^{16/13}}{(IW)^{10/13}} \qquad (5)$$

where J is the outlet spacing (m), S_W is the sole width of the trapezoidal channel (mm), K_T is the factor by which the width of the trapezoidal cross-section increases with increase of the vertical distance from the sole, h is the maximum water depth permitted in the channel (mm), I is the rainfall intensity (mm/h), W is the width of the road (m).

The corresponding maximum flow discharge, Q, in l/s can be obtained from Equation (5) and is given by:

$$Q = 6.5\text{x}10^{-5}\left(S_W + \frac{1}{2}K_T h\right)^{12/13} h^{16/13}(IW)^{3/13} \qquad (6)$$

where the various quantities have the meanings and units described above.

A numerical model developed by HR Wallingford, then Hydraulics Research Station, (HRS, 1971) was modified further by the TRRL team to estimate outfall spacings. The Wallingford model was designed for subcritical flow with slopes varying up to 0.002. The results of the model were found to agree well with Beij's experimental data and also with Beij's equation (within 5 %).

It is interesting to note that the channel slope does not figure in the above equations, which are valid for slopes up to 0.002 (or 1/500). Equation (6), known as the TRRL Report 605 formula has been used, along with Colebrook-White and Manning equations, by manufacturers and designers of drainage channels. Its obvious limitations with regard to proprietary drainage channels lie in the limited range of slopes for which it is valid (zero to 0.005) and its restriction to rectangular and trapezoidal cross-sectional shapes, which do not include some of the most common channel profiles such as U-shape.

In a comprehensive theoretical and experimental study of gutter capacity, May (1982) investigated the hydraulic behaviour of sloping gutters and analysed the transition between subcritical and supercritical flows. If the flow regime changes, the denominator of Equation (3) is equal to zero because the Froude number (defined as $Fr = \sqrt{\frac{BQ^2}{gA^3}}$) is equal to one. The numerator should also be equal to zero to avoid any discontinuities in the flow profile. May used the concept of critical length, L_c, defined as the distance between the section where the critical depth occurs and the upstream end of the gutter:

$$L_c = \frac{\frac{2A_c}{B_c}}{S_o - \frac{\lambda}{8}\frac{P_c}{B_c}} \qquad (7)$$

where λ is the Darcy-Weisbach friction factor, A_c is the cross sectional area at the critical section, B_c is the surface width of the critical section, P_c is the wetted perimeter of the critical section.

The analysis carried out by May identified the following three cases, which are illustrated in Appendix 1 (in the Figure of Appendix 1 the flow is from left to right, where the outlet is located):

- If the gutter has a mild slope ($8S_o/\lambda < 1$), the flow profile crosses the normal depth line and reaches a maximum depth upstream of the outlet - case (a);
- If the gutter has a steep slope ($8S_o/\lambda > 1$), the flow is supercritical at the outlet if the gutter is sufficiently long - case (b);
- If the gutter is shorter than in the case described above, the depth increases to a maximum upstream of the outlet and then decreases again - case (c).

In Equation (7), the bigger the friction in the channel (λ), the longer the distance will be between the critical section and the upstream end of the channel (L_c). It was found that if the length of the gutter is less than L_c the flow will be subcritical, otherwise it will become supercritical.

The work by May was the basis of the hydraulic design guidance in recent British and European Standards on roof drainage, as well as of the numerical program developed under the present study and described in Chapter 3.

3. DEVELOPMENT OF NUMERICAL PROGRAM FOR SPATIALLY- VARIED FLOWS

3.1 General

A program (LATIN, for LATeral INflow) was developed to model steady gradually-varied flows in channels. It computes the water profile along the channel by solving the spatially-varied flow equation which results from the balance between the forces acting on a control volume of fluid (see Equation (3) in Chapter 2). In this form the equation contains the following assumptions:

- The lateral inflow, q, initially has no component of momentum in the direction of flow in the channel;
- Pressures in the fluid are hydrostatic.

The input data needed to run LATIN are the characteristics of the channel and the flow conditions (lateral inflow rate and flow rate at the upstream end of the channel).

3.2 Capabilities and limitations of the program

LATIN was developed as a research tool in Fortran for two operating systems (Windows and Unix) and is therefore not commercially available.

The program allows the use of different friction laws (Strickler, Manning, Chezy, and Colebrook), which are presented in Appendix 2. Other friction laws can easily be added, if needed.

Different channel shapes can be computed (e.g. rectangular, trapezoidal, triangular, circular, U-shape, and irregular). There is a limitation with regard to irregular shapes as these must not differ much from a U shape or an elliptic shape (i.e. the program will not cope with two or more sub-channels inside the channel).

LATIN uses the Runge Kutta scheme of the 4^{th} order to solve Equation (3). The main aspect to solve in the numerical model is to determine the number and position of critical sections along the channel. At the upstream end of a channel, the flow is subcritical but in a steep channel, it can become supercritical due to the increase of flow along the channel length. The transition should be continuous because there is no sudden change of any parameters. Assuming that there is a smooth change between subcritical and supercritical conditions means that in Equation (3) the quantity dy/dx should remain continuous and finite. The denominator being equal to zero (Froude number equal to one, i.e. $\frac{\beta B Q^2}{gA^3} = 1$) then the numerator should also be equal to zero. This critical section is called in this report the "singular section".

3.3 Computation of the singular sections

The program starts by finding the number and the location of the singular sections. Knowing the flow rate at each section along the channel allows the determination of the critical depth. The numerator of Equation (3) is computed at each step along the channel. A change in the sign of the numerator indicates that the flow type (subcritical or supercritical) changes as well. The step length is then refined to give a more precise value for the location of the singular section. Having determined the number of singular sections and their location, the program can then compute the flow profile.

Several cases can occur and are described below:

a) No singular section

The flow is fully subcritical. A critical section will occur at the downstream end if there is a free exit. If the water depth is imposed at the downstream end, a simple backwater curve is computed. In the free exit case, the computation is more difficult because the denominator in Equation (3) is equal to zero and instead of solving Equation (3), its reverse is integrated numerically in order to find x as a function of y:

$$\frac{dx}{dy} = \frac{1 - \frac{\beta B Q^2}{gA^3}}{S_o - S_f - \frac{2\beta q Q}{gA^2}} \tag{8}$$

Instead of estimating the value of the depth for a point in the channel, now the increase in depth is given and the step increase in length corresponding to this depth is computed. However, at the upstream end, the profile could be flat and therefore the same problem of having the denominator almost equal to zero could occur. When a defined criterion is verified, Equation (3) is used again. The criterion is that if the value of dy/dx is smaller than the critical depth divided by the length of the channel, Equation (8) is used, otherwise Equation (3) is used.

b) One singular section

If there is one singular section along the channel the model starts to integrate the equation from that point, separately in both the upstream and downstream directions. The ratio dy/dx at the singular section is indeterminate but tends towards a finite value which can be found by applying a higher level of accuracy using the derivatives of the numerator and denominator:

$$\frac{dy}{dx} = \frac{G'(y)}{\left(1 - Fr^2(y)\right)'} \tag{9}$$

This equation has two solutions. An analytical solution of this equation is presented in Appendix 3.

At the singular section, the slope of the water depth is known. There are two choices for the slope at the section. The solution that should be considered is the one that transforms a subcritical flow into a supercritical flow. This method is used for two steps or even more if the Froude number remains equal to one. From this new depth, Equation (3) is used to compute the profile upstream and downstream.

If a second singular section occurs at the downstream end, both the numerator and the denominator are known. Since the Froude number has a value of unity and the discharge at the downstream end is known, the corresponding water depth can be computed. Knowing the water depth (and the corresponding values of A and R), it is then possible to calculate the slope S_{oc} that will produce the second singular section at the outlet:

$$S_{oc} = \frac{n^2 Q^2}{A^2 R^{4/3}} + \frac{2qQ}{gA^2} \tag{10}$$

with A, R, Q computed at the downstream end (critical depth).

For slopes steeper than S_{oc}, there will be only one singular section in the channel.

c) Two singular sections

Consider the channel subdivided into three parts separated by singular sections. From the upstream end to the first singular section, the flow is subcritical. The slope of the water profile is computed at the singular section, as described in item b) above, and a new water depth upstream is computed. When the corresponding Froude number is slightly different from unity then a backwater curve is computed (see item a) above). The new water depth is the starting point for the integration of the equation. If the Froude number is still equal to unity, the slope procedure is repeated. From the first singular section to the second singular section, the flow is fully supercritical. The slope at the first singular section gives a new water depth downstream. If the Froude number at this point is almost equal to unity then the slope procedure is used again. When the Froude number is slightly different from unity, Equation (3) is numerically integrated up to the second singular section. At the downstream end of the channel, between the second singular section and the exit, the flow is subcritical again. A simple backwater curve is computed from the downstream end to the second singular. At the outlet, there can be a free exit or the water depth can be imposed.

3.4 Effect of the channel slope on water profiles

The channel slope has a very important effect on the number of singular sections. For a flat channel, the water depth decreases all the way along the channel. The flow is fully subcritical. When the slope becomes slightly steeper, the water depth increases and then decreases towards the downstream end. The flow regime could be either fully subcritical or have two singular sections (and three flow types: subcritical, supercritical and subcritical again). For a steep channel, the water depth increases towards the downstream end and the flow is subcritical at the upstream end of the channel and then supercritical (one singular section). The various cases are summarised in Table 1.

Illustrations of the variation of the water profile with the channel slope are presented in Appendix 4.

3.5 Calibration

This program was also used to find the friction coefficient associated with the experimental data (see tests described in Section 5.3.2). The laboratory tests provided information on the water depths along the various channels tested. For each experimental profile, several values of the friction coefficient were tested until the theoretical profile matched the experimental profile.

3.6 Running LATIN

The program is easy to run and the computational time is short. The user can either use an input text file or enter the data directly into the program. Using an input file is very convenient if the user wants to repeat almost the same test (just altering some values). Entering the data directly in the program is more suitable if the user has to set up a new model.

The number of computational steps to define along a channel is an important issue especially for steep gradients when the flow becomes supercritical in a short distance from the upstream end. If the step is too large the model cannot accurately describe the change of flow regime which can lead to inaccurate results for the flow profile. The user has also the ability to calibrate the model if needed, provided that a profile from experimental data is available. It is worth noting that during calibration (see Section 3.5) several friction coefficients are tested and the water depth may be predicted to reach beyond the maximum permissible water depth in the channel. For the case of a circular channel (i.e. a pipe), the concept of Froude number no longer applies when it becomes full. The calibration will not provide valid results in this case. In order to overcome this problem, the user can define a very narrow slot at the top of the pipe; the conveyance of the pipe will not be affected by the very small flow in the virtual slot.

4. EXPERIMENTAL SET-UP

4.1 Requirements

Many of the requirements of the test rig were assessed through discussions with the manufacturers of linear drainage systems, from which it was decided that:

- The tests would be carried out under steady state conditions;
- A small crossfall would be introduced on the pavement adjacent to the channel units;
- All types of drainage channel (i.e. kerb, grid and slot units) would be tested with lateral flow from one side only;
- The flows simulated in the test facility would be representative of typical catchment areas and rainfalls;
- The full capacity of a system would be considered to be reached when the water level inside the unit was just at the underside of gratings or bottom of slots;

- The channel units would be installed in the test facility to form a 10m long channel;

- The test facility would reproduce longitudinal slopes representative of those found in roads and paved areas drained by linear drainage systems.

Further requirements identified for the test facility were:

- Flexibility to allow installation and testing of drainage units with very different characteristics in terms of weight, size, length and slope;
- Accessibility for installation of the drainage units;
- Sufficient strength to take the weight of the heavier kerb units.

Based on the above requirements, calculations were carried out to roughly estimate the flow capacity of the larger units as well as to determine the limiting flow conditions associated with the simulation of the smaller rainfall intensities. This showed that the range of flow rates necessary for the testing (maximum flows of about 100 l/s) could be provided by an existing test facility, a 2.44m wide tilting flume.

Although the existing test facility satisfied the requirements in general terms, several modifications were necessary for the present tests and these are described in the section below.

4.2 Adaptation of test facility

The existing test rig is a 2.44m wide flume that can be tilted to slopes from zero to 1/40. The flume length is approximately 25m and the flow is supplied to an upstream tank by two equal pumps with total capacity of 152 l/s. British Standard-compliant orifice plates inserted in the pumps' pipework were used to measure the flow rates in conjunction with a manometer board. A third pump of 28 l/s capacity was also available for use. Figure 1 shows a schematic layout of the test rig.

Flow from the upstream tank of the test rig (2.44m wide) needed to be contracted gradually to the considerably smaller width of the channel drainage units (typically 100 to 300mm). This was achieved by reducing the flume width to 1.2m and then creating a gradual contraction to 0.6m wide. A further smooth contraction was made at the entry to the most upstream drainage unit. The flow from the drainage channels was discharged into a tank where water levels were controlled by a tailgate.

For the present study the smaller pump (28 l/s capacity) was connected to a pipe manifold suspended above the flume. The flow rate from the pump was measured by means of an electromagnetic flow meter with a voltmeter display. The pipe manifold was designed to convey the lateral inflow into the linear drainage units (see Figures 1 and 2). It consisted of a 10m long plastic pipe of 150mm diameter with 20 equally spaced ports fitted with valves. These valves were connected to flexible transparent tubes approximately 1.3m long, which discharged smoothly onto the wooden platforms that reproduced the carriageway. In order to avoid pneumatic effects inside the pipe, air bleed valves were installed at either end of the manifold. The manifold was suspended above the test section from steel portal structures which were fixed to the floor of the laboratory so that the tilting of the flume would not affect the simulation of the lateral inflow. Plates 1a and 1b illustrate the work carried out on the test rig.

Flow depths inside the drainage channels were measured using electronic point gauges fitted with additional acoustic devices that emitted a sound when the point of the gauge established contact with the water surface. This feature was found to be indispensable particularly for the testing of slotted channels where no visual observation of the water surface was possible.

5. TESTING PROGRAMME

As mentioned in Section 1.2, the study methodology comprised experimental tests on various channel types as well as the development of a computer program which allowed numerical simulations to be carried out on an additional number of channel configurations. The availability of the computer program was particularly useful for the analysis of channel configurations comprising sequences of flat and sloping inverts, which would have been very impractical to test in the laboratory.

5.1 Selection of units to test

The first stage of the testing programme involved the selection of suitable channels to test from among the many options offered by the industrial partners. The main criterion for selection was the need to cover a representative range of channel types (kerb, grid and slot units), cross-sectional shapes and sizes as well as different materials.

During the first Steering Group meeting, it was agreed that the testing programme should include channels that incorporate kerbs for drainage at the edge of pavements, as well as systems used across paved areas. This influenced the choice of units to test, giving more emphasis to kerb units than originally envisaged.

The various systems tested were:

- System A

The first system to be tested was a kerb drainage system manufactured by Marshalls, with the trade name Beany Blocks (see Figure 3 for a schematic representation of this drainage channel). This system was formed by concrete channels of large cross-sectional area, formed by separate base and top units with side holes for flow entry (one hole in the top unit). The internal shape of the cross-section was approximately rectangular, with rounded corners. The approximate relevant dimensions were measured and are listed below:

Overall height of the unit = 570mm
Internal height (from invert to soffit) = 375mm
Internal height to external invert level of side holes (design height, taken to road/pavement level) = 340mm
Overall base width = 430mm
Maximum internal width = 284mm.

Other characteristics:
Length of each unit = 0.5m
Weight of each unit = 152kg (72kg base block and 80kg top block).

- System B

The second system to be tested was a kerb drainage system manufactured by ACO Technologies plc, with the trade name KerbDrain 305 (see Figure 4 for a schematic representation of this drainage channel). This system was formed by one-piece resin concrete channels with two side holes per unit for flow entry. The internal shape of the cross-section included half-circles at the base and top connected by straight vertical walls. The approximate relevant dimensions were measured and are listed below:

Overall height of the unit = 305mm
Internal height (from invert to soffit) = 200mm
Internal height to external level of side holes (design height, taken to road/pavement level) = 150mm
Overall width = 150mm
Maximum internal width = 100mm.

Other characteristics:
Length of each unit = 0.5m

Weight of each unit = 25kg.

- System C

System C was a kerb system manufactured by Camas - Aggregate Industries, with the trade name of Safeticurb (see Figure 5 for a schematic representation of this drainage channel). This system was formed by concrete kerb units incorporating a circular void for the conveyance of the flow collected through a slot at pavement level. The approximate relevant dimensions were measured and are listed below:

Overall height of the unit = 350mm (including 100mm high kerb)
Internal height (from invert to slot level) = 185mm
Internal height to soffit (design height) = 125mm
Overall base width = 250mm
Maximum internal width = 125mm.

Other characteristics:
Length of each unit = 0.915m
Weight of each unit = 100kg.

- System D

System D was a linear drainage system manufactured by Wavin Plastics Limited, with the trade name Wavin PolyChannel NW100 SK021 (see Figure 6 for a schematic representation of this drainage channel). This system was formed by resin concrete channel units that collected the flow continuously along their length through gratings of various different geometries and materials. The cross-section included a half-circle at the base and straight vertical walls above the rounded base, thus forming a U shape. The top of each unit was reinforced with a steel edge and the gratings sat on longitudinal ledges 10mm wide. Other features of this system were a locking device that is used to secure the gratings in position in about 60% of the systems that are installed. This locking device was formed by a transverse metal bar at about 90mm above the channel invert and a vertical bolt to fix the gratings. Two of these devices were placed in each of the 1m long units. The approximate relevant dimensions were measured and are listed below:

Overall height of the unit = 140mm
Internal height (from invert to top edge) = 123mm
Internal height to underside of gratings (design height) = 103mm
Overall width = 130mm
Maximum internal width = 100mm.

Other characteristics:
Length of each unit = 1m
Weight of each unit = 14kg.

Systems A to D described above were tested in the laboratory. Three more systems were evaluated using the numerical model and their descriptions are presented in Section 5.4.

5.2 Installation of the units in the test rig

The systems were placed in the test flume according to the manufacturers' guidelines so as to reproduce, in the laboratory, conditions as close as possible to those encountered in site installations. In most cases the manufacturers were directly involved in the installation and provided valuable information on the jointing of the units and relative levels of the edge of the units and the adjacent pavement. All four systems were quite different in their requirements for installation as the weight, size and shape of the units were very varied.

System A's base units were first lifted by gantry onto the test flume and silicon sealant was used to join them. The top units were then also lifted by gantry, and placed over the base units that had received a

layer of cement mortar at the longitudinal joints between the base and top blocks. Care was taken at each unit to ensure that neither the silicon sealant nor the mortar protruded into the inside of the blocks so that they would not adversely affect the internal flow. Relatively high seepage through the mortar joints was noticed during the tests, due to the lack of the concrete backing that is usually found I
n site installations (the units were free standing on the test flume, only bedded on concrete at the base). The seepage was however soon controlled by painting the outside of the channels with bitumen sealant. It was also important to ensure that uniform flow conditions were produced at the upstream end of the 10m long test section. For this purpose a gradual transition, including a ramp on the floor of the flume, was formed in concrete between the rectangular 0.6m wide channel and the rounded shape of the blocks.

System B was assembled in the test rig using silicon sealant in the joints between the units and also occasionally on the external walls in order to limit some seepage through the concrete that was observed during the tests. As for the previous system, the seepage was noticeable because of the lack of concrete backing. A gradual transition was built at the upstream end of the test section to ensure uniform flow entry into the test section. Since the units of System B were considerably smaller in cross-section than the width of the channel that conveyed the flow from the upstream tank of the test rig, the transition had to be made much longer than for System A. As before, the definition of the transition length was determined by gradually reducing the width in a 1W/3L relationship (where W is the width and L is the length). The connection to the most upstream system unit was smoothed carefully to minimise the formation of flow disturbances that would otherwise affect the hydraulic capacity of the channels, particularly at steep longitudinal slopes. Some inspection units, which featured lifting lids, were introduced to allow measurements of the water depth along the test channel.

System C was installed in a similar way to System A, i.e. by using the gantry to place the units in the flume on a mortar bed. Plastic jointing rings provided with the system were used to connect the units around the circular void, and silicon sealant was also used at each joint to minimise leakages. Care was taken at each unit to ensure that the silicon sealant did not protrude into the inside of the blocks and affect the internal flow. In order to ensure that uniform flow conditions were produced at the upstream end of the 10m long test section, a gradual transition, including a ramp on the floor of the flume, was formed in concrete between the rectangular 0.6m wide channel and the circular void of the blocks.

System D was installed in the test rig using silicon sealant in the joints between the units, which were fixed to the floor of the test flume on a mortar bed. As a preventative measure, some sealant was used on the outside of the units at the connections between the steel edge and the resin concrete channels and also around the plastic features embedded within the channels that were used to allow fixing of the gratings into position. Since the cross-sectional area and shape of these channels were similar to those of System B (which was tested immediately before system D), only small modifications were necessary to the upstream transition.

All the units were accurately installed in the test rig with a flat invert using an engineering level. Once the units were in place, a 10m long wooden platform simulating the pavement was fixed to the wall of the flume and to the drainage units. This platform was installed with a cross-fall of approximately 1in 40 to simulate typical pavement cross-falls at the edge of surface drainage systems. The tubes used to supply flow to simulate run-off (see Section 4.2) were attached at regular intervals along the pavement to produce uniform distribution of inflow.

5.3 Experimental tests

Following a number of preliminary tests, carried out to get familiarisation with the test rig and measuring equipment, three types of test were carried out for each drainage system: 1. tests to determine the roughness of the channel without lateral inflow (base roughness), 2. tests to determine the hydraulic capacity of the systems with lateral inflow and 3. limited tests using sediment to determine each system's self-cleansing velocity.

5.3.1 Test procedures

Base roughness tests

In order to be able to compare the effect of lateral inflow into the drainage channels with longitudinal flow in the channels, it was decided first to determine their base roughness without lateral inflow. This was carried out for various longitudinal slopes and generally for two values of flow rate: one corresponding to the channel practically full and a smaller flow rate, with the channel approximately half full.

Hydraulic capacity tests with lateral inflow

Prior to the start of the tests, the range of flow conditions to be tested was discussed with the manufacturers of the drainage systems to determine typical catchment areas, longitudinal slopes and rainfall intensities. The information on each of the systems was then extended into a wider range of flow conditions to cover the conditions under which linear drainage systems are likely to be required to perform. The computer program that was developed to deal with spatially-varied flow (see Chapter 3) was then used for each of the systems to give an estimation of their capacity under the various flow conditions, assuming an estimated value of Manning's roughness coefficient (see Equation A2.2 in Appendix 2).

This first estimation was necessary to determine the length of pavement that could in principle be drained by the different systems. In most cases, this length was different from the 10m of channel available in the test rig, and this affected the way the tests were performed, as described next:

- For drainage lengths greater than 10m
  The tests started by simulating the last 10m of channel, with an inflow from upstream corresponding to the total length minus the flow along the last 10m long section. The upstream flow depth measured was used to set the level of the tailgate at the downstream end of the test section, which determined the downstream flow depth for the next 10m long section. This "piecing-together" procedure was repeated until the capacity of the channel was reached. Since the estimation of flow capacity (and drainage length) was based on an assumption of the channel roughness, the above procedure sometimes led to the maximum water depth being less or greater than the design depth. Therefore, the whole set of part-tests had to be repeated until the overall channel capacity was found. It should be noted that the maximum flow depth in a drainage channel can occur at any point in the channel (and not just at the upstream end as in the case of flat slopes). The tests therefore not only allowed the determination of the flow capacity but also determined where the maximum flow depth occurred in the channel. For the very large capacity channels, such as System A when set at steep slopes, the drainage length could exceed 300m. In this case the above test method was too time consuming and a different approach was followed. Values of Manning's n were obtained by setting up flow conditions that would encompass the range of flow depths that would be encountered in the channels for a range of inflow rates. This data was then used in the numerical model to determine the channel's overall drainage capacity.

- For drainage lengths equal to 10m
  These tests were straightforward, with rainfall simulation over the 10m length.

- For drainage lengths smaller than 10m
  In this case, the rainfall simulation device (see Figure 2) could be adjusted to produce rainfall over only the required length. This was done by closing some of the valves of the manifold suspended above the test channel.

Sediment tests

The tests on the self-cleansing capacity of the systems were intended to provide a very general guideline on the minimum flow velocities that are likely to be required to remove deposited sediments from the invert of drainage channels. The size of the sediment used was representative of sediments found in run-off from urban pavements and highways. This sediment was a fairly uniform sand which was analysed in HR's Sedimentation Laboratory to determine its grading curve. The analysis revealed a mean sediment size of d_{50}=1.35mm (see Figure 7). The sediment was introduced in the channels as a deposited bed with a depth corresponding to 5% of the channel's available depth. The sediment bed was placed only over the last downstream one or two metres of channel. This length was dictated by the kerb units, where access for sediment introduction and measurements was very restricted. The test procedure was as follows: the flat deposited bed was reproduced, then water was slowly introduced at the downstream end of the flume through a separate hose to produce a "cushion" of water controlled by the tailgate. This was necessary to prevent the movement of sediment at the start of the test, before the test flow conditions (including rainfall simulation) had reached a steady state. Once these were reached, the tailgate level was then gradually lowered until the sediment showed signs of movement at threshold conditions. The flow rate and water depth were measured, which then allowed the determination of the limiting flow velocity.

In all the above types of test, the slope of the flume was set to the required value and the pump(s) were started to supply the required flow rate to the test rig. Sufficient time was allowed for the flow to reach steady-state conditions. Measurements were then taken of the following quantities: the flow rate using the orifice plates in the pump pipeline with the associated manometer board; the lateral inflow rate using the electromagnetic flowmeter; and water depth at four sections along the channels using the electronic point gauges.

5.3.2 Hydraulic test results

The data collected during the tests consisted of flow rates and water depths at four locations along the channels for various combinations of slope and lateral inflow. A larger number of tests was carried out for System A than for the other systems, which was principally due to the fact that this was the first system to be tested and it was necessary to establish the importance of the various parameters. Due to its larger capacity and therefore longer drainage lengths, this system also required a more complex test procedure (see Section 5.3.1).

Plates 2 to 9 illustrate the tests carried out on the four systems. Photographic shots (Plates 3, 5, 7 and 9) taken from the free outfall at the downstream end of the test section show the flow conditions inside the channels. For example, in Plate 5, it is possible to observe the lateral flow (q= 0.28 l/s per metre) entering this kerb system and wave formation inside the channel, which was set at 1/1000 slope. It should be noted, however, that these waves were not observed further upstream for this slope and were a product of the flow acceleration at the outfall (drawdown). At steep gradients, waves and series of hydraulic jumps were observed for all the systems.

Not all the test results were directly used in the analysis described later in Section 6 as some revealed that the flow surface was too disturbed to allow reliable results. Among the causes of these disturbances were the discontinuities at the joints between channel units and the formation of cross waves due to the high velocity of the flow. Following a preliminary analysis, the test data that was considered to be sufficiently accurate was identified and is summarised in Tables 2 and 3 (tests with no lateral inflow and with lateral inflow, respectively).

The tests carried out with no lateral inflow provided information on the "base roughness" of the channels, i.e. the values of Manning's roughness coefficient n for open channel flow (see Table 2). Manning's n is a measure of the roughness of the channel material (concrete, resin concrete, plastic, etc) but also, and sometimes more importantly, of the flow resistance caused by the joints (type and number) between the channel units. Longer channel units will have fewer joints per unit length and will therefore be hydraulically smoother than equivalent channels of smaller unit length. The n values in Table 2 were obtained by using the numerical program LATIN with the test data (water depths along the channel and channel slope). It can be seen in Table 2 that the values of Manning's n were generally fairly constant for each system, ranging between 0.007 and 0.012 for all the systems tested. On average, Systems B and D were found to be hydraulically smoother, as expected because of the nature of the channel material (resin concrete as opposed to concrete).

For tests with lateral inflow LATIN was run with the test data (water depths, lateral inflow rate and channel slope) and with different values of n until there was a good agreement between the numerical simulations and the experimental water profiles.

System D featured a locking system for the gratings whereby they were fixed by a vertical bolt connected to a bar across the upper part of the channel (see Plates 8 and 9). Several types of grating of various loading classes can be used with System D. The present tests were not aimed at determining the flow efficiency of the gratings but the locking system was found to have an effect on the capacity of the channels. In order to investigate this issue, tests were carried out with the following arrangements: 1. no gratings or locking devices; 2. with thin gratings (i.e. gratings with flat underside); 3. with gratings of Class E with bowed underside. The test results showed that locking systems such as in System D or gratings with bowed underside can reduce the capacity of the channels if the design depth is taken up to the level at which the gratings rest on the channel. The reduction in flow capacity is greater the steeper the channel slope because the energy loss caused by protruding elements depends strongly on the flow velocity. Figure 8 shows this effect. Reductions in capacity to about 60% of the channel capacity without protruding elements were measured for slopes of 1/67. It can be concluded therefore, that it is necessary to define the design height of the channel at a level just below the level of any locking cross-bars or the underside of bowed gratings. In the present study the test results for System D used in the data analysis were those corresponding to this lower level (see Table 3).

5.3.3 Self-cleansing test results

Being a fairly restricted test programme, it was decided to carry out the tests at a single slope (1/1000), with a single sediment size, and to use a deposited bed of sand with a d_{50}=1.35mm and formed to a depth equal to 5% of the design depth of the channels (see Section 5.3.1 for description of test procedure). The tests were performed with various flow depths inside the channels; the conditions at the downstream end, where the flow accelerated towards the free exit, were not considered for the identification of threshold velocities.

Illustrative examples of these tests are given in Plates 10 to 12. Plate 10 shows the sediment bed after a test in System A. Two eroded areas can be seen in this plate: 1. a large area in the foreground created by the drawdown of the flow at the free exit from the channel; and 2. a smaller area created by the flow entering the side holes of this kerb channel. Plates 10 to 12 also show the erosion near the downstream end caused by flow acceleration. In Plate 12, which was taken following a test with lateral inflow q = 0.42 l/s per metre, most of the uneroded sediment bed is concentrated on the left hand side of the channel (when viewing towards downstream). This behaviour is likely to result from the fact that the lateral inflow was introduced in the test channel from one side only, whereas in many applications the flow would be entering the channel from both sides. This difference is however believed not to affect significantly the value of velocity at which the sediment will start moving.

Table 4 summarises the results obtained at the threshold of movement, i.e. for conditions at which the sediment just started moving. As can be seen, tests were carried out both with no lateral inflow and with lateral inflow at various rates but the results did not show significant differences between the two types of test. A slightly lower velocity can however be noted for tests with lateral inflow, as might be expected due to the additional turbulence created by the flow entering the channel (compare for example tests A1S and A4S or D2S and D4S for flow depths close to the design depth). In general terms the test data indicated that velocities of the order of 0.4m/s may be required to start moving deposited sediment in drainage channels. It should be noted that the tests were carried out for a non-cohesive sediment without a significant percentage of fines. In practice sediment entering drainage channels may become cemented if regular maintenance is not carried out and the above findings may therefore underestimate the velocity required in practice to erode sediment beds.

5.4 Numerical tests

At the request of the channel manufacturers supporting the present research, the capacity of channels consisting of a series of flat and sloping inverts was also investigated. In view of the many different configurations possible, the most effective way to conduct such a study was to use the numerical program LATIN (see Chapter 3), after calibration with experimentally determined values of Manning's roughness coefficient, n. The numerical tests calculated the drainage length of the channels as well as the water surface profile for three different channel systems in several configurations, which are described below.

It should be noted that the results of these simulations did not always correspond to the limiting capacities of the channels because they were intended to provide manufacturers with information about their systems. Although these simulations provided useful information with regard to the behaviour of channels with in-built slopes and stepped inverts, they were specific to the configurations tested and were therefore not used for the development of general design equations.

5.4.1 System E

System E was the system manufactured by Marshalls with the trade name Birco 150 (see Figure 9 for a schematic cross-section). The concrete channels had a U-shaped cross-section and could be covered by a range of different gratings. Units with in-built falls as well as flat base units were available in this system. The approximate relevant dimensions are listed below:

Overall height of the unit ≥ 230mm
Internal height (from invert to top edge) ≥ 180mm
Internal height to underside of gratings (design height) ≥ 150mm
Overall width = 250mm
Maximum internal width =150mm.

Other characteristics:
Length of each unit = 1m

The four configurations tested are illustrated in Figure 10. The manufacturer supplied details of the configurations (channel cross-sectional sizes and lengths, invert slopes) as well as the catchment widths and rainfall intensities to use in the simulations. Graphs showing the water profile along the channels are given in Figures 11 to 18.

5.4.2 System F

System F was manufactured by Camas - Aggregate Industries with the trade name Waterway (see Figure 19 for a schematic cross-section). These concrete channels had a U-shaped cross-section and could be covered by a variety of grating types. Units with in-built falls as well as flat base units were available in this system. The approximate relevant dimensions are listed below:

Overall height of the unit ≥ 151mm
Internal height (from invert to top edge) ≥ 130mm
Internal height to underside of gratings (design height) ≥ 100mm
Overall width = 158mm
Maximum internal width =100mm.

Other characteristics:
Length of each unit = 1m

The five configurations tested are illustrated in Figure 20. The manufacturer supplied details of the configurations (channel cross-sectional sizes and lengths, invert slopes) as well as the catchment widths and rainfall intensities to use in the simulations. Graphs showing the water profile along the channels are given in Figures 21 to 30.

5.4.3 System G

The shape and configuration of System G were suggested by Wavin Plastics Limited (see Figure 31 for a schematic cross-section). These channels were assumed to have the following characteristics: be made of concrete resin; have a U-shaped cross-section; and be covered by a variety of gratings. Units with in-built falls as well as flat base units were assumed to be available in this system. The approximate relevant dimensions available are listed below:

Internal height (from invert to top edge) $\geq$ 170mm
Internal height to underside of gratings (design height) $\geq$ 150mm
Maximum internal width = 200mm.

Other characteristics:
Length of each unit = 1m

The three configurations tested are illustrated in Figure 32. The manufacturer supplied details of the configurations (channel cross-sectional sizes and lengths, invert slopes) as well as the catchment widths and rainfall intensities to use in the simulations. Graphs showing the water profile along the channels are given in Figures 33 to 38. The computed water profiles in Figures 37 and 38 show discontinuities at the step in the channel invert. These discontinuities are a result of the lack of a point-energy loss term in the equation for spatially-varied flow.

6. ANALYSIS

6.1 Data analysis

The objective of the data analysis was to develop formulae for predicting the flow capacity of drainage channels based on the experimental data and supported by numerical simulations using the computer program (LATIN) specifically written to deal with lateral inflow.

The analysis began by identifying the main parameters that influence the flow capacity of the channels. Knowing that the channel slope would be one of the major variables, several parameters were defined involving other quantities such as the flow rate, Q, the channel cross-sectional area, A, the hydraulic radius, R, the water depth, h, and the acceleration due to gravity, g. Values of these parameters obtained from the experimental results (Tables 2 and 3) were plotted against the slope. A very marked power relationship, was found between the non-dimensional parameter $Q/(g^{0.5}A^{1.25})$ and the channel slope (Figure 39). It can be seen in Figure 39 that the experimental scatter is quite small and that data corresponding to very different channel shapes and sizes all follow the same power law. At zero slopes the average value of the parameter $Q/(g^{0.5}A^{1.25})$ was calculated as 0.4. If no other variables are of importance, the flow capacity can be written as:

$$\frac{Q}{g^{0.5}A^{1.25}} = C_1 S^{C_2} + 0.4 \qquad (11)$$

where C_1 and C_2 are coefficients in the power law term. Although the general pattern of the data could be represented by the above equation, further refinements can be made to try to reduce the existing scatter in the data. Work previously carried out by HR Wallingford on flow in roof gutters (see for example May, 1996) indicated that if gutters are shallow in relation to their length, the flow capacity can be affected by the flow resistance. A similar behaviour would be expected in drainage channels and the effect of the channel length was therefore also investigated. Having identified the parameter $Q/(g^{0.5}A^{1.25})$ as the basis of the analysis, this parameter was plotted against the ratio L/h, where L is the channel length and h is the design water depth (Figure 40). This suggested that the variation of the discharge parameter with the slope and the relative length of the channel could be described by an equation of the form:

$$\frac{Q}{g^{0.5}A^{1.25}} = C_3 S^{C_4} + 0.4 + b\frac{L}{h} \tag{12}$$

where the coefficient b is also a function of the channel slope.

It is interesting to note in the graph of Figure 40 that, for a certain cross-sectional area, the length ratio has different effects on the flow depending on the slope: for flatter slopes, as the length ratio increases the flow capacity decreases; for steeper slopes, as the length ratio increases the flow capacity also increases. The trendlines in Figure 40 illustrate this finding, which is also confirmed numerically. The Figure in Appendix 5 was produced using LATIN for a channel such as that of System A and it shows the same behaviour found for the experimental data. The reasons are implicit in the form of the spatially-varied flow equation (Equation 3) and are due to the complex interaction between the three terms in the numerator of the equation. However, similar sets of curves to those shown in Appendix 5 have been obtained theoretically and experimentally by other researchers and were used to develop guidance in the European Standard on roof drainage (BS EN 12056).

Linear regression analysis was carried out to determine the intercepts and gradients of the various lines defined in Figure 40. The dependency of the gradients on the channel slope was investigated for the experimental data as shown in Figure 41, and numerical simulations were also carried out to extend the range of points and thereby define the curve for steeper slopes. The analysis revealed that the gradient, b, increased linearly with slope up to a certain value of the slope and remained approximately constant from then onward. Two lines were therefore defined by linear regression and by simple average, respectively:

$$b = 0.132\,S - 0.00022 \tag{13}$$

for $S \leq 1/200$

$$b = 0.00044 \tag{14}$$

for $1/200 < S \leq 1/30$

6.2 Hydraulic capacity equations

The analysis described in Section 6.1 led to the following best-fit equation, which is valid for slopes not steeper than 1/30 and for channels with length ratios $L/h \leq 1000$:

$$Q = g^{0.5}\,A^{1.25}\,(\,6.74\,S^{0.7} + 0.4 + \frac{L}{h}\,b) \tag{15}$$

with

$b = 0.132\,S - 0.00022$

for $S \leq 1/200$

$b = 0.00044$

for $1/200 < S \leq 1/30$

where

Q is the flow rate, g is the acceleration due to gravity, A is the channel cross-sectional area, S is the channel slope, L is the channel length, and h is the design water depth.

A comparison between measurements and predictions using Equation (15) can be seen in Figure 42, where the 1 to 1 line is also depicted. As can be seen, the agreement between the experimental data and predictions is very good and gives confidence in the use of the derived equation. In order to check the suitability of Equation (15) for values outside the experimental range, numerical simulations carried out for System A were plotted in Figure 43, together with all the experimental values. The numerical values corresponded to flow rates up to about 250 l/s (and values of $L/h \leq 1000$), i.e. much above the values measured experimentally (<100 l/s). Even for large capacity channels Equation (15) still produces results that are quite close to the numerical predictions (see 1 to 1 solid line in the graph), although the agreement is not as good as for the experimental data. This is an expected finding as the term b(L/h) in Equation (15) may not remain linear for very large values of L/h.

6.3 Design formulae

The formulae recommended for design should provide a safe estimate of the flow capacity in drainage channels. However, it was decided by the project partners that a safety factor would not be necessary in view of the fact that an exceedance of the flow capacity would not generally present a large economic or safety risk. The dashed line marked in Figure (43) is an envelope of all the data (experimental and numerical) within the range of application of the present study. This line can be obtained by applying a reduction factor of 0.85 to Equation (15):

$$Q = 2.66\, A^{1.25}\, \left(6.74\, S^{0.7} + 0.4 + \frac{L}{h}\, b \right) \qquad (16)$$

with

$b = 0.132\, S - 0.00022$

for $S \leq 1/200$

$b = 0.00044$

for $1/200 < S \leq 1/30$

where

Q is the flow rate in m^3/s, A is the channel cross-sectional area in m^2, S is the channel slope, L is the channel length in metres, and h is the design water depth in metres. This equation is valid for slopes not steeper than 1/30 and channels with length ratios, L/h, not greater than 1000. The equation applies to channels with continuous invert, i.e. not formed by series of flats and in-built slopes.

6.4 Comparison with guidance for roof gutters

As mentioned earlier, the hydraulic behaviour of roof gutters is similar to that of drainage channels installed at ground level since in both types of channel the flow increases steadily from the zero-flow point to the point of discharge. British Standard BS 6367 and the new European Standard BS EN12056 "Gravity drainage systems inside buildings – Part 3: Roof drainage, layout and calculation" that has superseded BS 6367, give guidance on the hydraulic design of roof gutters. The design formulae were based on experimental and theoretical work on commonly used shapes and sizes of gutter, and materials. Gutters are defined hydraulically as either short (if the effects due to flow resistance can be neglected), or long (if ratios of gutter length to gutter design depth are above 50) when a factor is applied to correct the hydraulic capacity accordingly. Values of this correction factor are given in BS EN 12056 in a table that was derived from theoretical calculations of gutter capacity.

In order to compare the results of the present study with the guidance in BS EN 12056, use was first made of the experimental study carried out for Systems A, B and D (note that System C had a circular cross-section, which is not covered by the Standard). The flow capacity for the above systems at flat slopes was calculated using the HR Wallingford equation in its two forms: the best-fit equation and the design equation (Equations 15 and 16, respectively). These values were plotted against the values given by BS

EN 12056, with and without the safety factor of 0.9 recommended by the Standard (Figure 44). The agreement is very close. Another comparison was carried out (see Figure 45) with synthetic data that was created to extend the range of conditions covered in Figure 44. A channel 0.15m by 0.15m in cross-section was used for the comparisons. Slopes from flat to 1/100 and ratios of channel length to channel design depth (L/h) between 50 and 500 were considered. For smaller flow rates, which correspond to the flatter slopes, the agreement between the two methods is very good, but differences become more apparent for the larger flow rates associated with steeper slopes. This results essentially from the application of different correction factors for the effect of the channel length in the two methods.

6.5 Self-cleansing velocities

Experimental tests to investigate the self-cleansing characteristics of drainage channels indicated that flow velocities above approximately 0.4m/s would be required to initiate sediment movement along the invert of the channels (Section 5.3.3). Since the flow rate is not constant along a channel, i.e. it increases gradually from the upstream end of the channel to the downstream end, the flow velocities are not constant either. The location at which velocities exceed 0.4m/s will be dependent on a number of factors, such as the rate of inflow, the channel slope and its cross-sectional shape and size. Further analysis was carried out to investigate where this limiting value of velocity would typically be exceeded along channels.

Use was made of numerical simulations carried out on the configurations studied for Systems E and G (see Section 5.4) and also on another commercially available drainage channel which has a narrow trapezoidal cross-sectional shape. Although the study was not comprehensive, it was possible to conclude that velocities of 0.4m/s and higher usually tended to occur in the downstream half of the channel and occasionally in the second quarter. In none of the 15 simulations carried out was the velocity of 0.4m/s found in the first quarter of the channel, even for configurations with series of flat and sloping inverts. Self-cleansing velocities cannot occur along the whole length of drainage channels and adequate provision for regular maintenance is therefore very important.

6.6 Channels with sloping or stepped inverts

For various reasons, including topographical constraints and landscaping requirements in paved areas, drainage channel systems are often installed on level ground and are designed to incorporate invert slopes to increase their drainage capacity. The invert slope can be achieved in a number of ways: by using channel units with in-built slopes; by placing flat invert units in between units with in-built slopes; or by placing flat invert units of increasing depths thus creating a series of steps. Because of the flow disturbance that these steps generate, this third option is less effective and will not be discussed further.

Within each proprietary drainage system, a large number of combinations can be envisaged to achieve the drainage requirements of a particular paved area. Manufacturers usually have their own design methods that are based on experience and also make the best use of the sizes of unit available. The design of channels with stepped inverts formed by a series of flats and slopes therefore depends on a mixture of commercial and technical factors, and lies outside the scope of the present study. However, some analysis was carried out to give guidance on the design of these systems in the absence of specific experimental or numerical data.

During the numerical tests described in Section 5.4, considerable information was obtained on the water profiles for typical applications of sloping and stepped inverts. Although not covering the whole range of possible applications, this information provided a good representation of common configurations. In all cases the maximum water depth occurred in the second half of the channels, and in many cases close to the downstream end. At these locations the channel depth generally exceeds by a large amount the required water depth. In all cases studied the maximum water level was found to occur at the upstream end of the channel.

Application of the proposed equations using the average slope of the channel showed that the cross-sectional area required for the most upstream channel unit would be on the conservative side of the cross-sectional area necessary to ensure the required drainage capacity. It should be noted that this conclusion was based on the configurations tested and may therefore not be valid for other configurations or for slopes or flow conditions outside those investigated. For this reason experimental testing or numerical modelling of these systems is generally recommended.

7. INCORPORATION OF RESULTS INTO STANDARD

One of the objectives of the study was to make recommendations on how the results should be incorporated in a British or European Standard. From discussions with members of the relevant BSI sub-committee, it was concluded that inclusion of the study results in prEN 1433 would not be possible in the near future because the process of final approval was already underway. Also, prEN 1433 is a product standard rather than a design standard and therefore recommendations on design would be better included in another document. The best vehicle for rapid dissemination was identified to be European Standard BS EN 752 "Drain and sewer systems outside buildings – Part 4: Hydraulic design and environmental considerations". The results of the study will be used to revise the National Annex NE of EN752, which deals with the drainage of paved areas.

8. CONCLUSIONS

A comprehensive experimental and numerical study was carried out to develop simple-to-use design formulae for calculating the hydraulic flow capacity of drainage channels. Laboratory tests were performed on a number of drainage channels commercially available in the UK (kerb, grid and slot units) to determine their flow capacity and to investigate self-cleansing conditions. The main stages of the study and the conclusions reached are summarised below:

- Numerical program for spatially varied flows
  A numerical program was developed to model steady spatially-varied flows in channels of various cross-sectional shapes, hydraulic roughnesses, and set at slopes ranging from flat to steep. This program is able to compute complex water profiles for a wide range of slopes and identifies subtle changes in flow types (subcritical, supercritical) that can occur in channels with lateral inflow. This new tool is not confined to channels used to drain paved areas and roads - other applications include for example roof gutters and channels receiving flows from side weirs.

- Hydraulic capacity
  Design formulae
  Based on a combination of experimental and numerical data, simple formulae were developed to determine the hydraulic capacity of drainage channels. For design it is recommended to use the following formulae:

$$Q = 2.66\, A^{1.25}\, \left(6.74\, S^{0.7} + 0.4 + \frac{L}{h}\, b \right) \qquad (16)$$

  with
  $b = 0.132\, S - 0.00022$
  for $S \leq 1/200$

  $b = 0.00044$
  for $1/200 < S \leq 1/30$

where
Q is the flow rate in m^3/s, A is the channel cross-sectional area in m^2, S is the channel slope, L is the channel length in metres, and h is the design water depth in metres. The design water depth is defined as the difference between the channel invert level and the maximum level of unobstructed flow, i.e. just below the level of any grating locking devices or the underside of gratings. This equation is valid for clean channels at slopes not steeper than 1/30 and channels with length ratios L/h not greater than 1000. The equation applies to channels with continuous inverts, i.e. not formed by series of flats and in-built slopes (see following item on channels formed by series of flats and stepped inverts below).

For channels with ratios of channel length to design water depth above 1000, which are outside the applicability of the above equations, it is recommended to determine their capacity by laboratory testing or a combination of laboratory and numerical simulations. However, situations where channel lengths corresponding to such high ratios will be used are considered to be quite unusual (typically, lengths of the order of 300 or 400m for large capacity channels and above 150m for smaller capacity channels). Designers would normally need to incorporate outfall chambers at more regular intervals for reasons other than those purely related to the hydraulic capacity.

Steep slopes
It should also be noted that, although the above formulae are in principle valid for channels at slopes up to 1/30, at such steep slopes any manufacturing and/or installation imperfections are likely to produce significant disturbances in the flow. At higher slopes series of hydraulic jumps were observed inside the channels. Also, the collection efficiency of grids, slots and kerb entry holes reduces as the velocity of the run-off increases, thereby increasing the by-pass flow, which will need to be collected downstream.

Effect of protruding elements into the channels
In systems that use grating locking devices or gratings with bowed undersides that protrude into the flow inside the channel, significant disturbance to the flow was observed during the experimental work if the water level exceeded the level of the protruding elements. The percentage reduction in flow capacity in relation to undisturbed conditions increases with the channel slope as the flow velocity increases (reductions to about 60% of the unobstructed flow capacity were observed). It is therefore important to define the design water depth as the difference between the channel invert level and the maximum level of unobstructed flow, i.e. just below the level of any grating locking devices or the underside of gratings.

- Self-cleansing velocities
  Limited tests were carried out to measure the flow velocities required to initiate movement in a sediment bed with a deposited depth corresponding to 5% of the channel design depth. The results indicated that sediment movement is not likely to occur for flow velocities below about 0.4m/s. In drainage channels, where the flow gradually increases towards the discharge point, velocities of 0.4m/s or above will typically be produced in the downstream half of the channel length. Therefore, unless demonstrated by experimental evidence, self-cleansing conditions cannot be guaranteed along the whole length of the channels. This supports the need for regular maintenance to try to keep the channels clean from sediment and the grids/slots and side entry holes unblocked.

- Channels formed by series of flats and sloped inverts
  The hydraulic formulae presented in this report were developed for channels that follow the ground slope and have constant depth. In many situations, however, drainage channels are designed as a series of flat invert units and units with in-built slopes (typically at 0.6%). Because a wide variety of configurations is possible, the design of these channels is necessarily quite specific. However, an approximate estimate (on the conservative side) of the channel capacity can be obtained if the average slope of the channel is used in the proposed equations and the effective cross-sectional area of the channel is taken as that of the most upstream channel unit.

Tables

- Incorporation of results into Standards
  A formal request has been made to the relevant BSI Committee (B/505) to revise National Annex NE to BS EN 752 "Drain and sewer systems outside buildings - Part 4: Hydraulic design and environmental considerations" (EN752). National Annex NE, which deals with the drainage of paved areas, will be amended to incorporate the results of the present study.

9. ACKNOWLEDGEMENTS

The project was part funded by DETR with contributions from HR Wallingford, ACO Technologies plc, Camas/Aggregate Industries, Marshalls Limited, TPS Consult, Wavin Plastics Limited and Whitby Bird & Partners. The authors are very grateful for the excellent co-operation given by all the members of the Steering Group formed by the organisations listed above and also including the Highways Agency. Special thanks are due to the drainage manufacturers for providing technical support and channels for testing. A list of the Steering Group members is presented below:

ACO Technologies plc: Mr Walter McIntyre
Camas/Aggregate Industries: Messrs Tim Blower and Steve Blurton
Marshalls Limited: Messrs David A Morrell, Matt Dolan and N Beanland
TPS Consult: Mr D Wilbraham
Wavin Plastics Limited: Mr Neil Cooper; and Mr Graham Martin-Loat (in the first stages of the work)
Whitby Bird & Partners: Mr Nick J Price
Highways Agency: Mr Santi Santhalingam.

10. REFERENCES

BELJ KH (1934). "Flow in roof gutters". J. Res., US Nat. Bur. Stand., Vol 12, Res. Paper 644.

BS EN 752 "Drain and sewer systems outside buildings - Part 4: Hydraulic design and environmental considerations", 1998, BSI, ISBN 0 580 29361 0.

BS EN 12056 "Gravity drainage systems inside buildings – Part 3: Roof drainage, layout and calculation", 2000, BSI, ISBN 0 580 36486 0.

HRS (1971). "Trapezoidal drains for motorways". Hydraulics Research Station Report No. DE.2, 1971.

MAY, RWP (1982). "Design of gutters and gutter outlets. Theory and experiments". Hydraulic Research Station, Report No. IT 205, April 1982.

MAY RWP (1996). "Manual for the hydraulic design of roof drainage systems. A guide to the use of British Standard BS 6367:1983". HR Wallingford Report SR 485, October 1996.

prEN 1433 "Drainage channels for vehicular and pedestrian areas" (draft).

WHIFFIN AC and YOUNG CP (1973). "Drainage of level or nearly level roads". TRRL, Report 602.

Table 1 Effect of channel slope on water profiles in spatially-varied flows: Critical sections

Slope	Number of sections	Regime	Water depth	Comments
$S_0 = 0$	No singular section	Subcritical	↘	Flat channel
$S_1 > S_0$	No singular section	Subcritical	↘	
$S_2 > S_1$	No singular section	Subcritical	↗ ↘	
$S_3 > S_2$	Double singular section	Subcritical	↗ ↘	The two singular sections are at the same location
$S_4 > S_3$	Two distinct singular sections	Subcritical Supercritical Subcritical	↗ ↘	The first section moves to the upstream end whereas the second moves towards the downstream end
$S_5 > S_4$	Two singular sections. The second section is at the downstream end	Subcritical Supercritical	↗	The second section reaches the downstream end
$S_6 > S_5$	One singular section	Subcritical Supercritical	↗	Only one section remains in the channel very close to the upstream end

*The arrows represent the behaviour of the flow profile from the upstream end to the downstream end.

Table 2 Tests with no lateral inflow: Results

Test	Slope	Q l/s	Max. water depth measured m	Manning's n
System A				
A1	0	11.8	0.111	0.012
A2	0	18.1	0.136	
A3	0	31.2	0.193	
A4	0	44.3	0.224	
A5	0.001	11.8	0.105	0.012
A6	0.001	53.6	0.223	
A7	0.0033	11.8	0.0763	0.012
A8	0.0033	53.6	0.203	
A9	0.01	11.8	0.0631	0.012
A10	0.01	31.2	0.111	
A11	0.01	53.6	0.154	
System B				
B1	0	3.37	0.0961	0.009
B2	0	6.57	0.150	0.012
B3	0.001	3.37	0.0842	0.008
B4	0.001	6.57	0.138	0.009
B5	0.002	3.37	0.0784	0.010
B6	0.002	6.57	0.134	0.012
B7	0.005	3.37	0.0770	0.012
B8	0.005	6.57	0.121	0.012
B9	0.005	8.31	0.140	0.010
B10	0.01	3.37	0.0542	0.007
B11	0.01	8.31	0.110	0.009
B12	0.01	10.2	0.124	0.008
System C				
C1	0	3.37	0.0916	0.012
C2	0	5.13	0.117	
C3	0	5.81	0.123	
C4	0.001	3.89	0.0909	0.012
C5	0.001	6.71	0.126	
C6	0.002	7.73	0.124	0.011
C7	0.005	Series of hydraulic jumps		--
C8	0.01			
System D*				
D1	0	2.96	0.0936	0.011
D2	0	3.64	0.104	0.011
D3	0.001	4.12	0.106	0.012
D4	0.002	2.76	0.0678	0.009
D5	0.002	8.31	0.105	0.010
D6	0.006	3.37	0.0670	0.012
D7	0.006	6.98	0.0980	0.010
D8	0.01	3.37	0.0548	0.011
D9	0.01	8.64	0.101	0.010
D10	0.015	4.76	0.0598	0.010
D11	0.015	10.1	0.0989	0.010

* without gratings or locking devices

Table 3 Tests with lateral inflow: Results

Test	Slope	Lateral inflow q l/s per metre	Total flow (d/s) Q l/s	At section of maximum water depth		
				Water depth m	Area m^2	Hydraulic radius m
System A						
A1L	0	0.28	44.2	0.340	0.08576	0.09533
A2L	0	0.67	53.6	0.340	0.08576	0.09533
A3L	0.001	0.28	59.6	0.340	0.08576	0.09533
A4L	0.001	0.67	67.0	0.340	0.08576	0.09533
A5L	0.002	0.28	74.2	0.340	0.08576	0.09533
A6L	0.002	0.67	76.4	0.340	0.08576	0.09533
A7L	0.0033	0.28	87.6	0.340	0.08576	0.09533
A8L	0.0033	0.67	87.1	0.340	0.08576	0.09533
System B						
B1L	0	0.56	5.60	0.144	0.01332	0.03862
B2L	0	0.67	6.70	0.162	0.01511	0.03963
B3L	0	0.58	5.78	0.151	0.01402	0.03906
B4L	0	0.28	5.60	0.150	0.01392	0.03900
B5L	0.001	0.56	7.60	0.161	0.01501	0.03959
B6L	0.001	0.67	6.70	0.152	0.01412	0.03912
B7L	0.001	0.28	7.00	0.152	0.01412	0.03912
B8L	0.001	0.14	5.60	0.139	0.01282	0.03828
B9L	0.002	0.67	8.38	0.161	0.01501	0.03959
B10L	0.002	0.56	8.40	0.162	0.01511	0.03963
B11L	0.002	0.28	7.56	0.151	0.01402	0.03906
B12L	0.005	0.67	8.66	0.152	0.01412	0.03912
B13L	0.005	0.56	9.52	0.155	0.01442	0.03929
B14L	0.005	0.28	8.96	0.153	0.01422	0.03918
B15L	0.01	0.67	10.1	0.151	0.01402	0.03906
B16L	0.01	0.56	11.2	0.154	0.01432	0.03923
B17L	0.01	0.28	11.2	0.142	0.01312	0.03848
B18L	0.015	0.67	12.1	0.151	0.01402	0.03906
System C						
C1L	0	0.28	5.04	0.121	0.01215	0.03495
C2L	0	0.42	5.46	0.124	0.01226	0.03310
C3L	0	0.67	5.56	0.123	0.01223	0.03388
C4L	0.001	0.28	5.60	0.115	0.01181	0.03680
C5L	0.001	0.42	6.09	0.125	0.01227	0.03125
C6L	0.001	0.67	6.03	0.123	0.01223	0.03388
C7L	0.002	0.28	6.72	0.124	0.01226	0.03310
C8L	0.002	0.42	6.51	0.125	0.01227	0.03125
C9L	0.002	0.67	6.03	0.118	0.01200	0.03604
C10L	0.005	0.28	8.40	0.119	0.01206	0.03572
C11L	0.005	0.42	8.32	0.123	0.01223	0.03388
C12L	0.01	0.42	10.1	0.122	0.01220	0.03447
C13L	0.01	0.67	9.46	0.122	0.01220	0.03447

Table 3 Tests with lateral inflow: Results (Continued)

Test	Slope	Lateral inflow q l/s per metre	Total flow (d/s) Q l/s	At section of maximum water depth		
				Water depth m	Area m^2	Hydraulic radius m
System D*						
D1L	0	0.28	2.80	0.097	0.00862	0.03436
D2L	0	0.42	3.36	0.105	0.00942	0.03529
D3L	0.001	0.28	4.20	0.112	0.01012	0.03603
D4L	0.001	0.42	3.78	0.104	0.00932	0.03518
D5L	0.002	0.42	4.20	0.107	0.00962	0.03551
D6L	0.006	0.28	5.60	0.100	0.00892	0.03472
D7L	0.01	0.28	7.00	0.108	0.00972	0.03562
D8L	0.01	0.42	6.90	0.107	0.00962	0.03551
D9L	0.015	0.28	8.12	0.105	0.00942	0.03529
D10L	0.015	0.42	8.20	0.108	0.00972	0.03562

* without gratings or locking devices

Table 4 Assessment of self-cleansing capacity: Test results

All tests with slope 1/1000 and sand with d_{50} =1.35mm

Test	q l/s per metre	$Q_{u/s}$ l/s	Water depth m	Threshold velocity m/s
System A				
A1S	0	29.3	0.279	0.40
A2S	0	10.5	0.129	0.33
				Average = 0.36
A3S	0.28	21.8	0.212	0.39
A4S	0.67	10.5	0.339	0.34
A5S	0.67	16.0	0.396	0.40
				Average = 0.38
System B				
B1S	0	3.30	0.100	0.40
B2S	0	5.10	0.139	0.40
				Average = 0.40
B3S	0.28	2.20	0.147	0.37
B4S	0.14	3.67	0.132	0.37
				Average = 0.37
System C				
Due to uncertainties associated with the observation of sand movement inside this slotted system no tests were performed.				
System D				
D1S	0	2.00	0.064	0.38
D2S	0	3.89	0.104	0.42
				Average = 0.40
D3S	0.28	0	0.008	0.32
D4S	0.42	0	0.009	0.33
				Average = 0.33

Notes:

q Lateral inflow rate

$Q_{u/s}$ Flow rate from catchment upstream of 10m long test section

Figures

Figure 1 Test rig – schematic layout

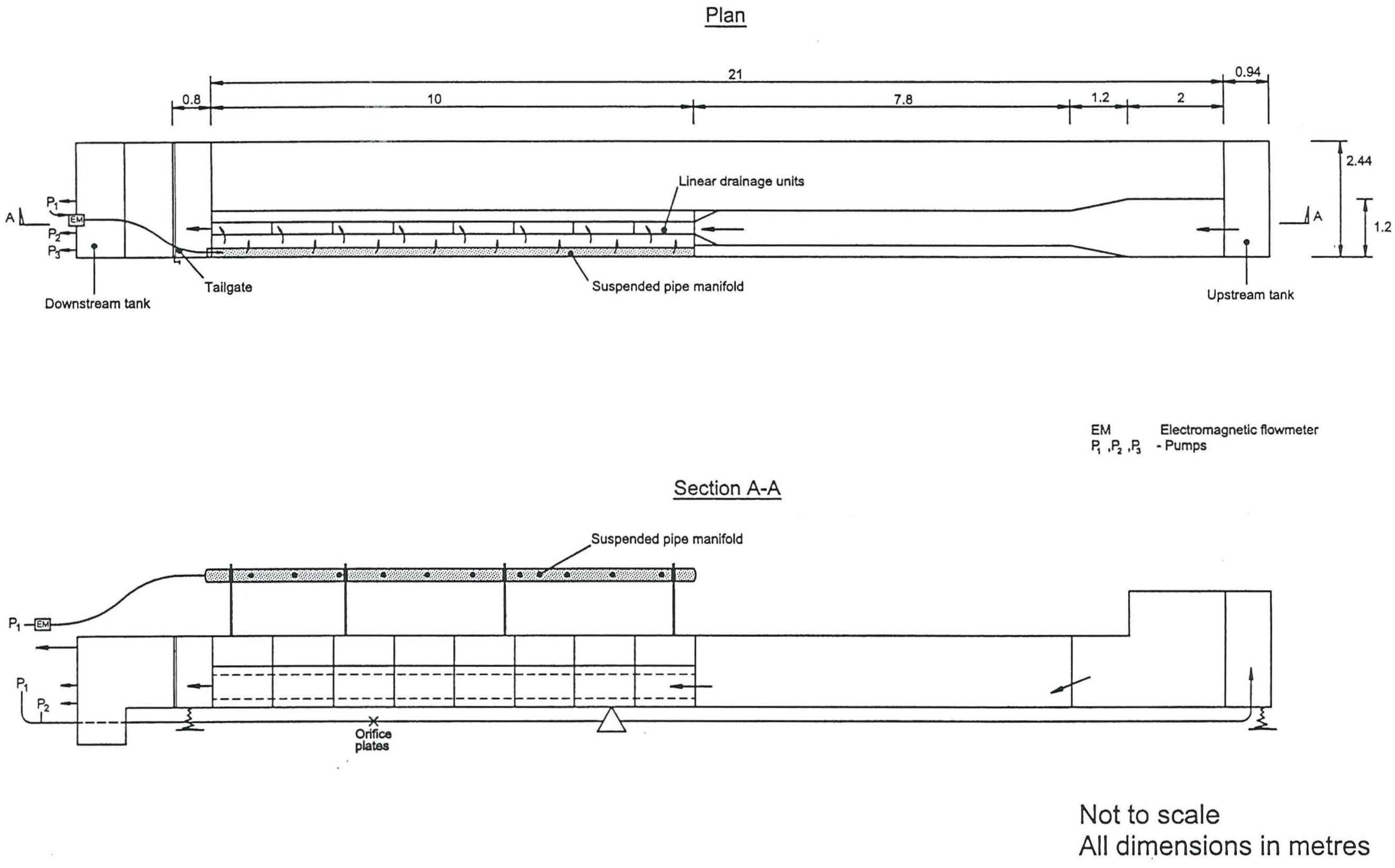

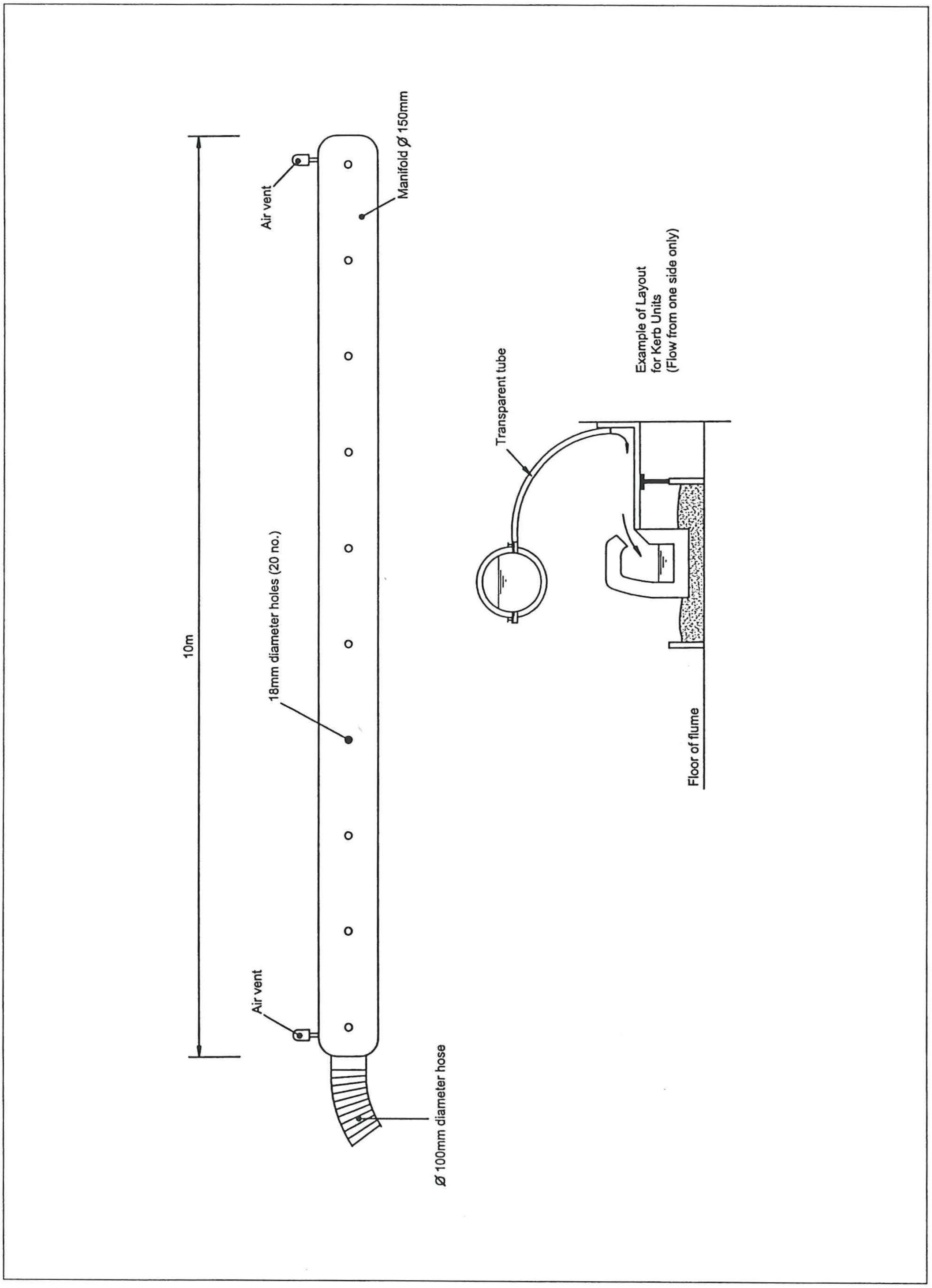

Figure 2 Pipe manifold used for rainfall simulation

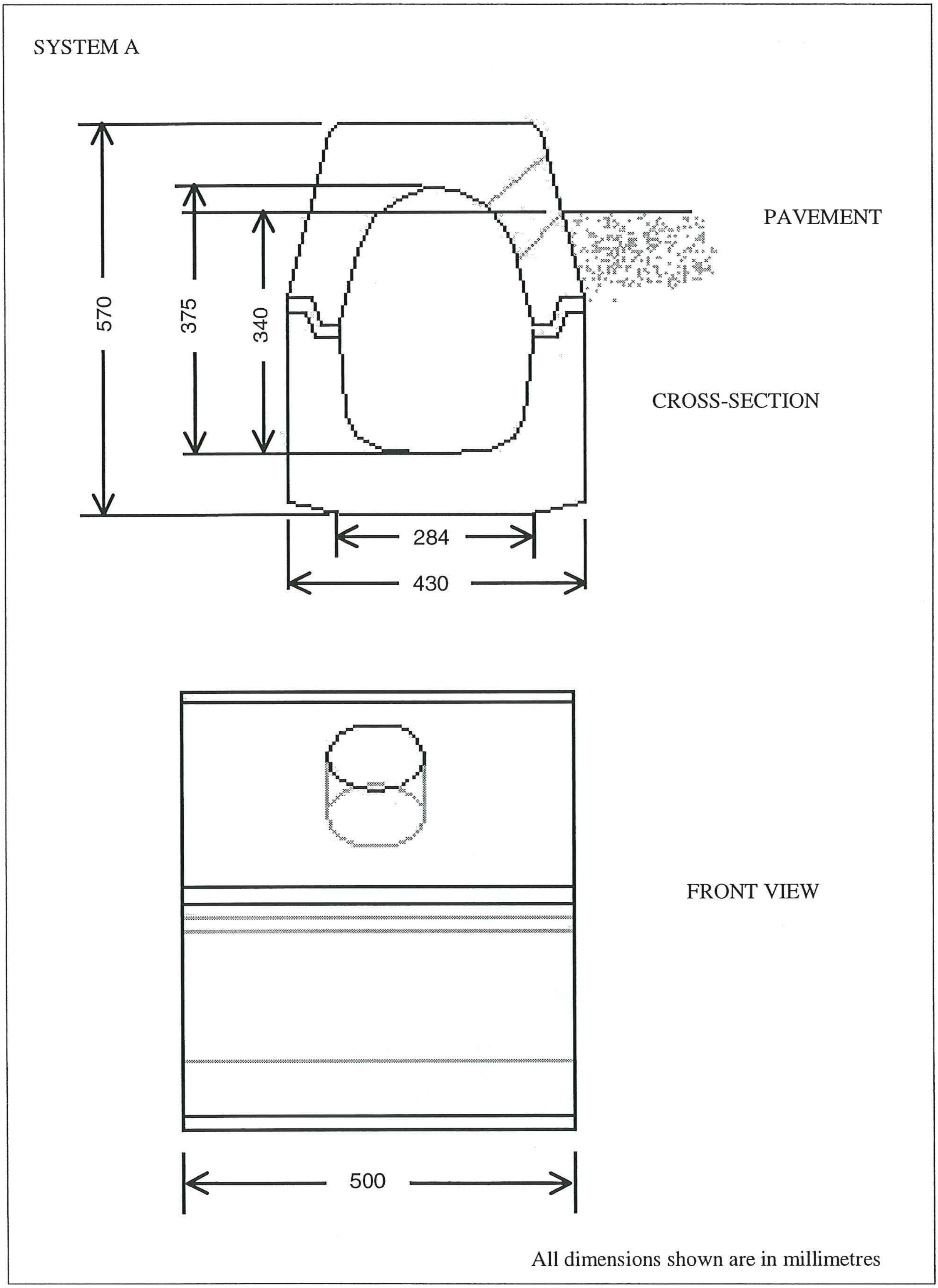

Figure 3 Schematic diagram of System A units

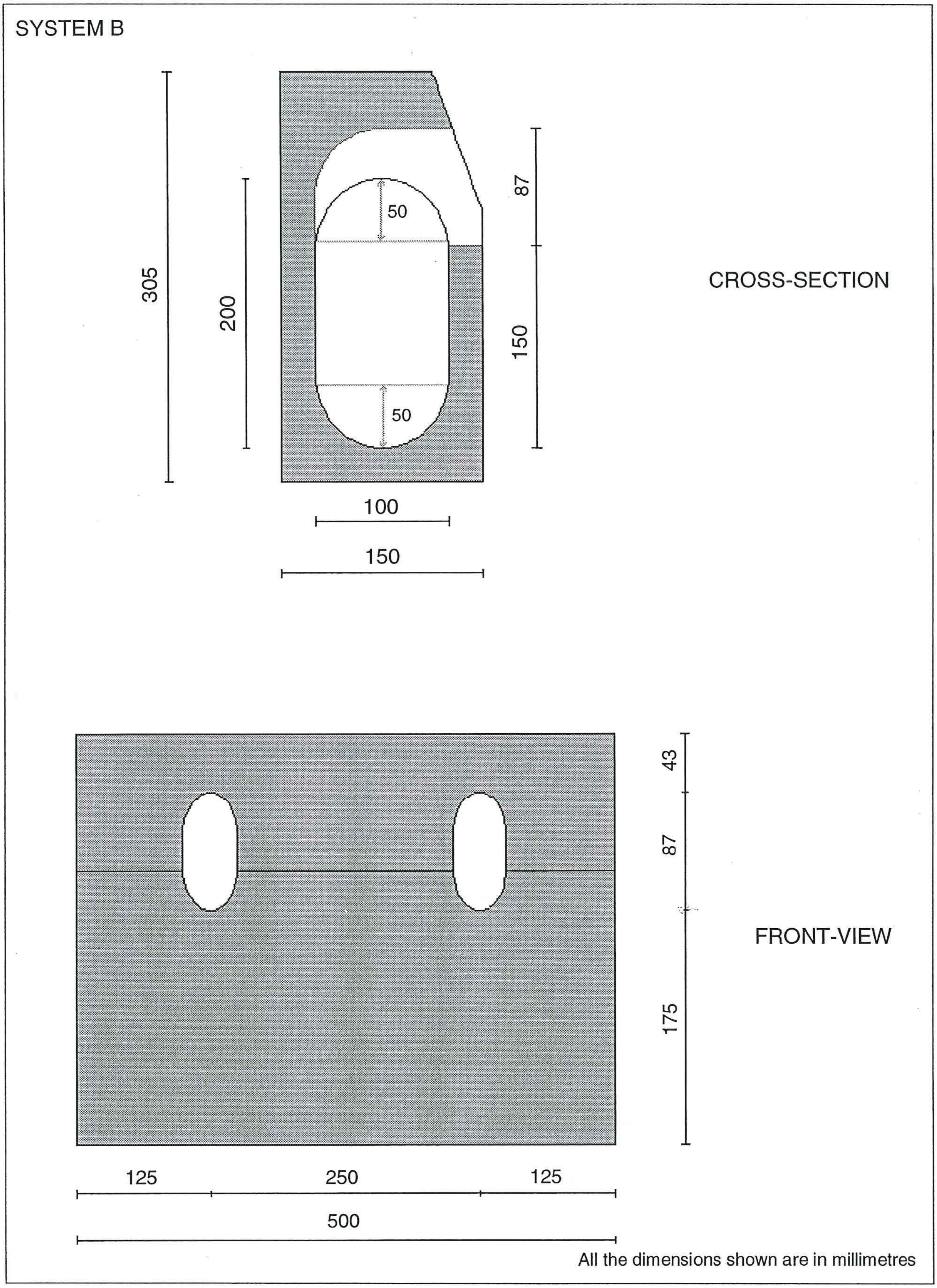

Figure 4 Schematic diagram of System B units

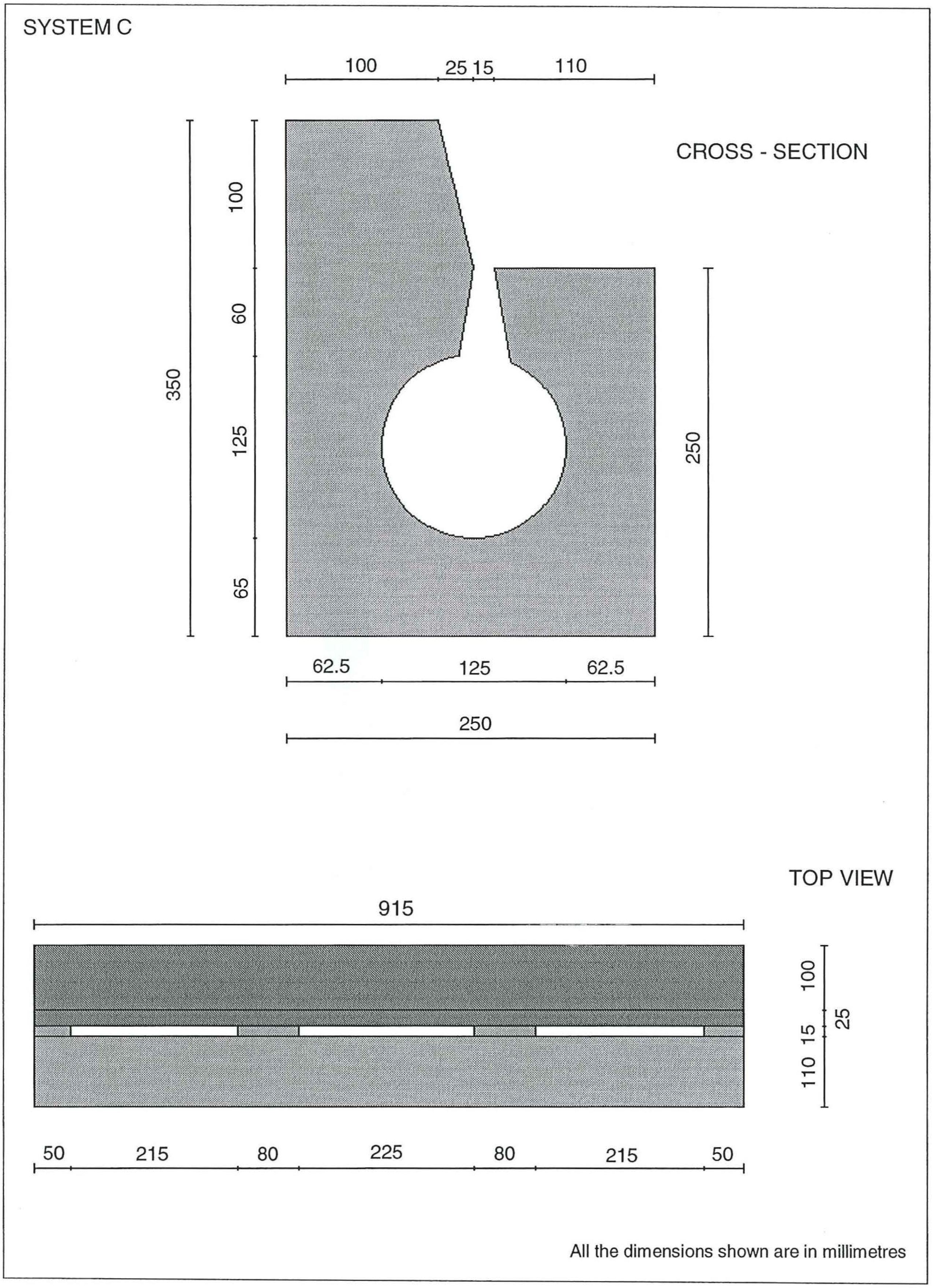

Figure 5 Schematic diagram of System C units

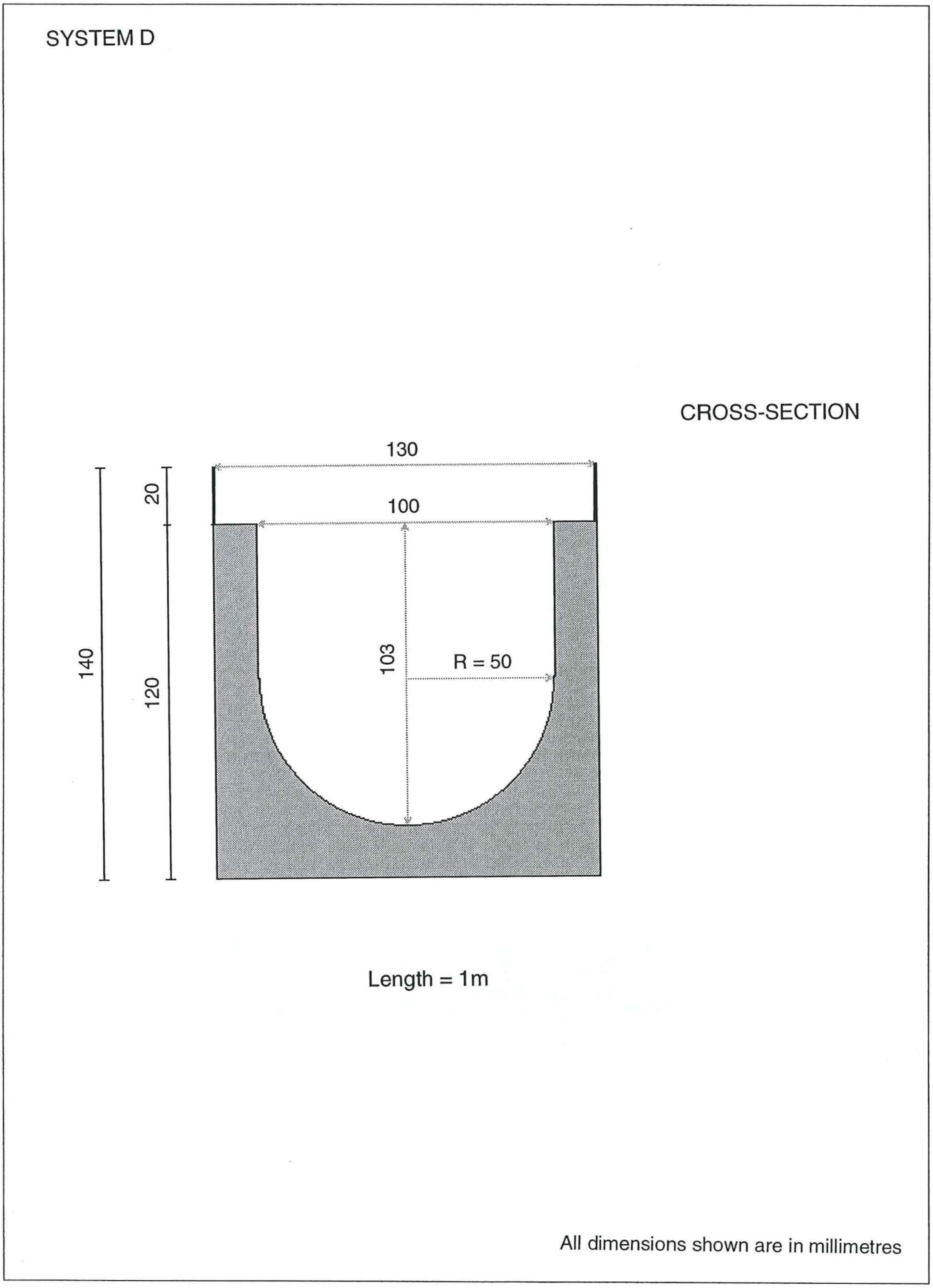

Figure 6 Schematic diagram of System D units

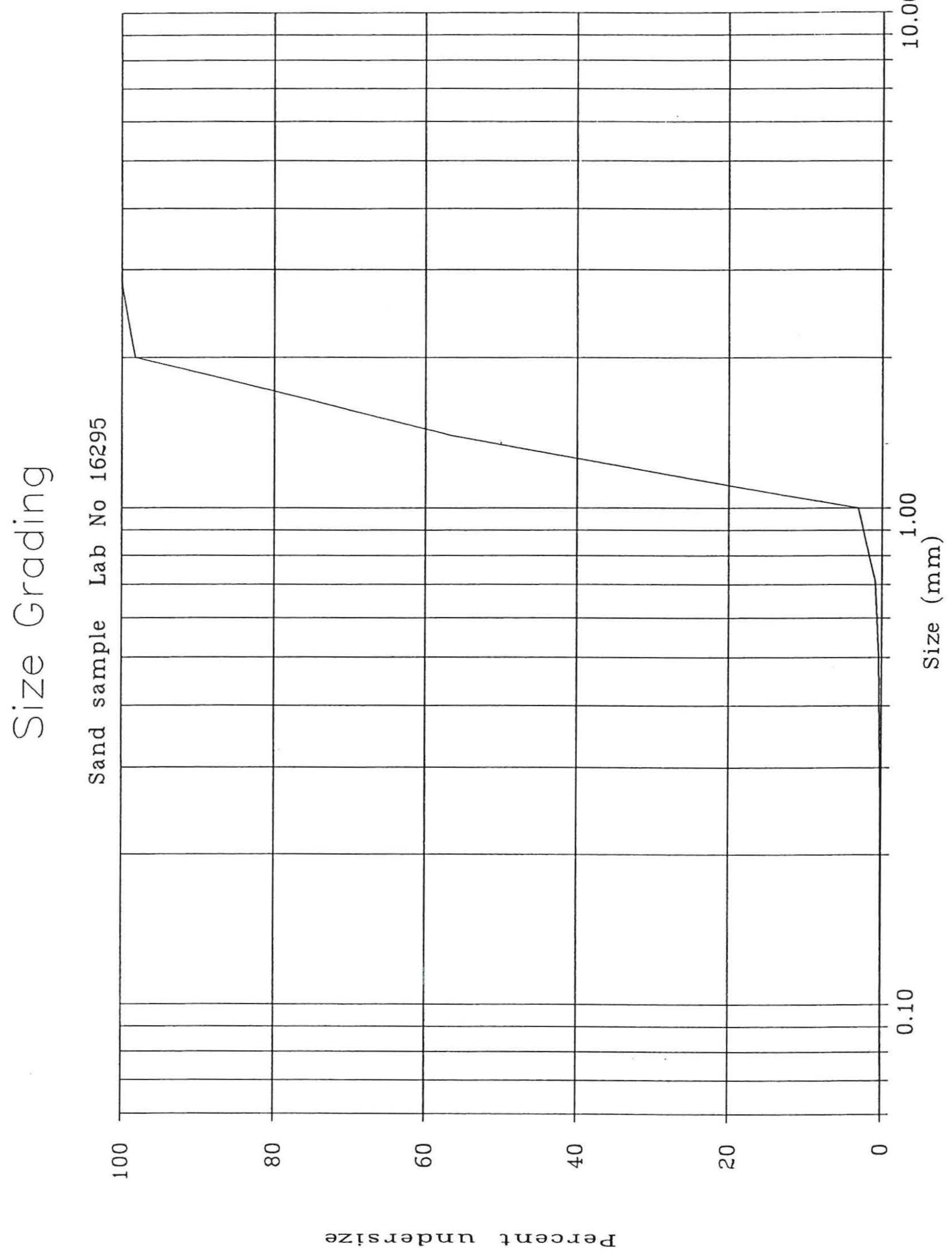

Figure 7 Grading curve of sediment used in self-cleansing tests

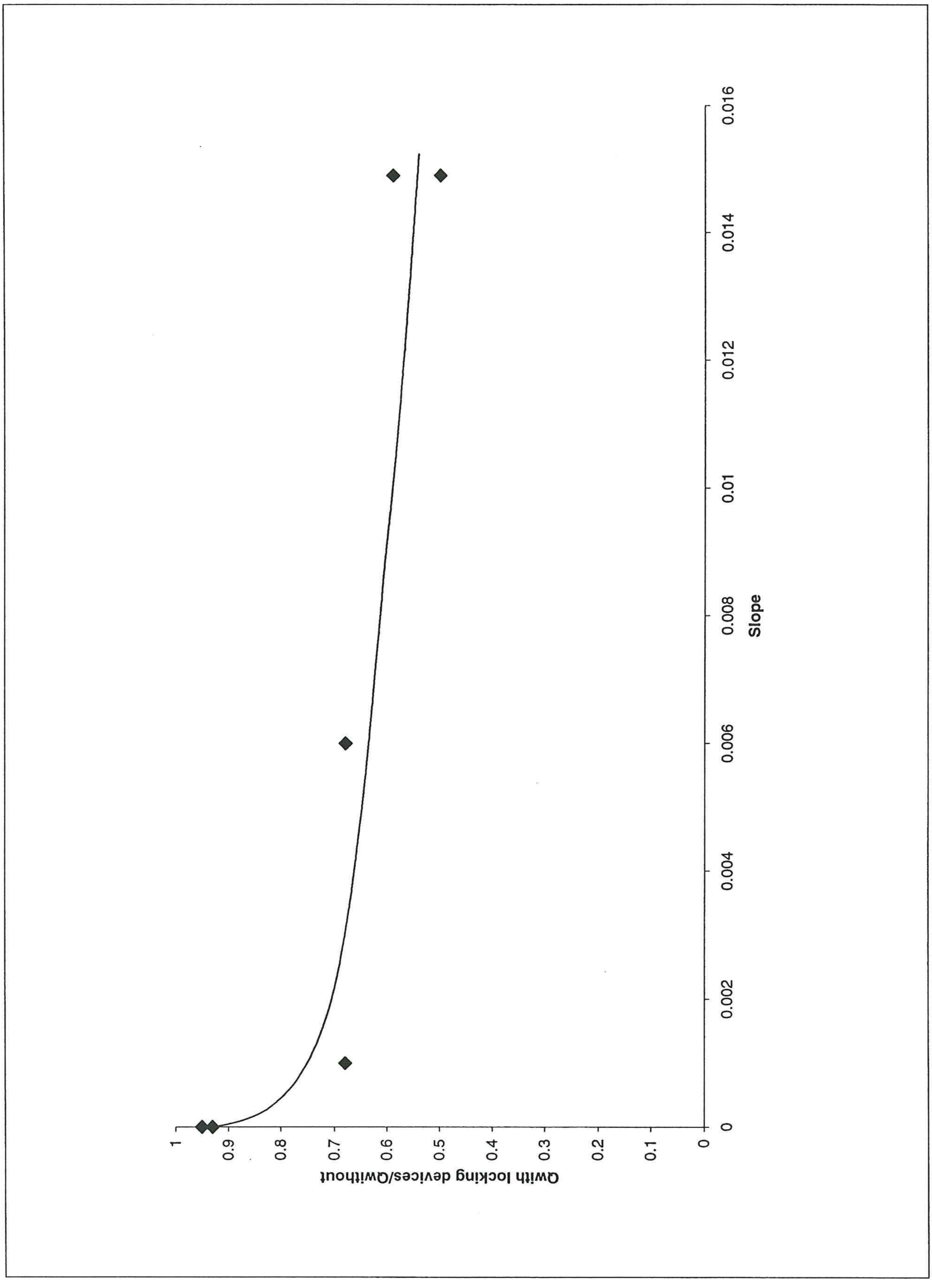

Figure 8 **Effect on flow capacity of protruding elements such as grating locking devices**

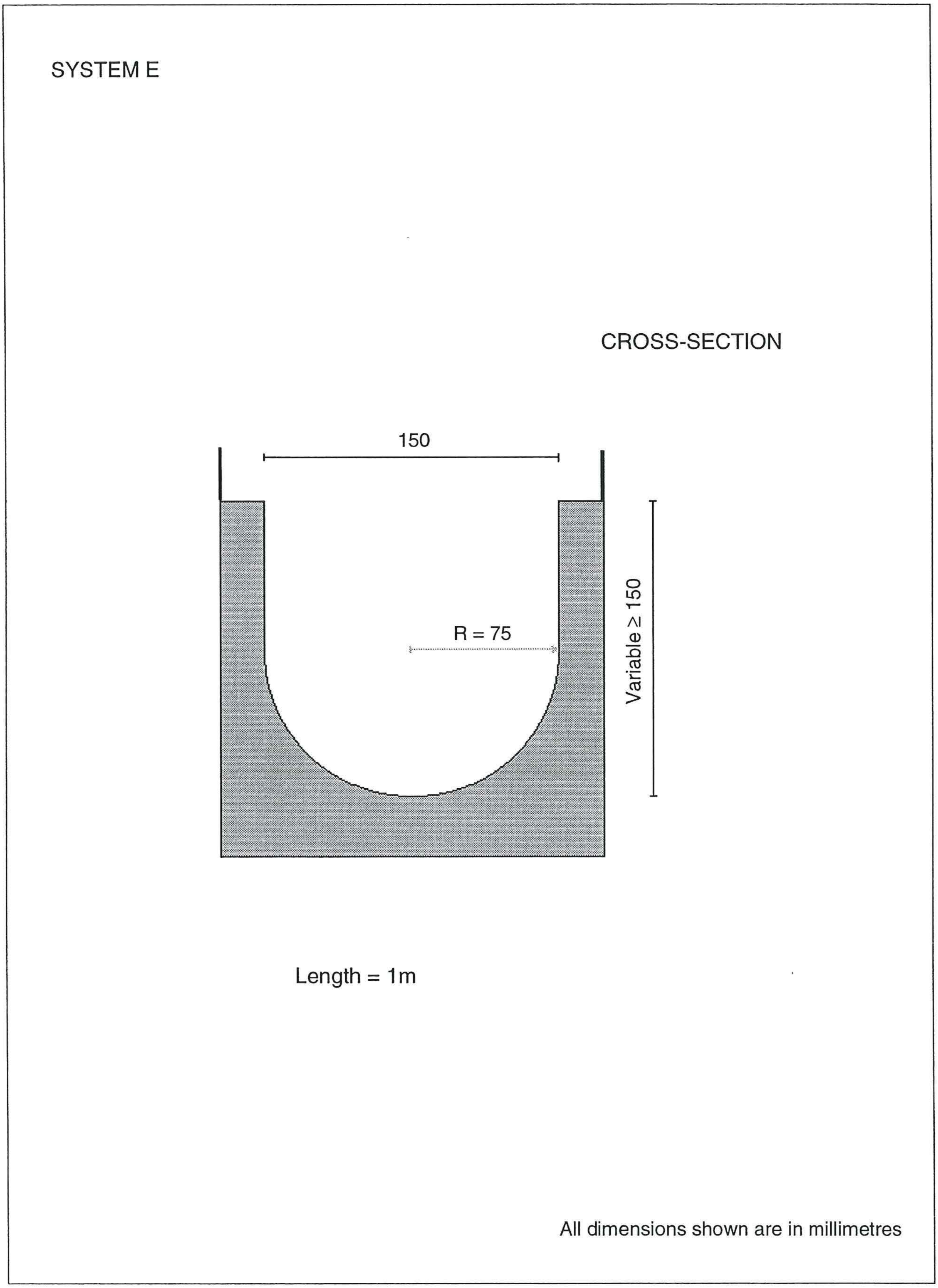

Figure 9 Cross-section of System E channels

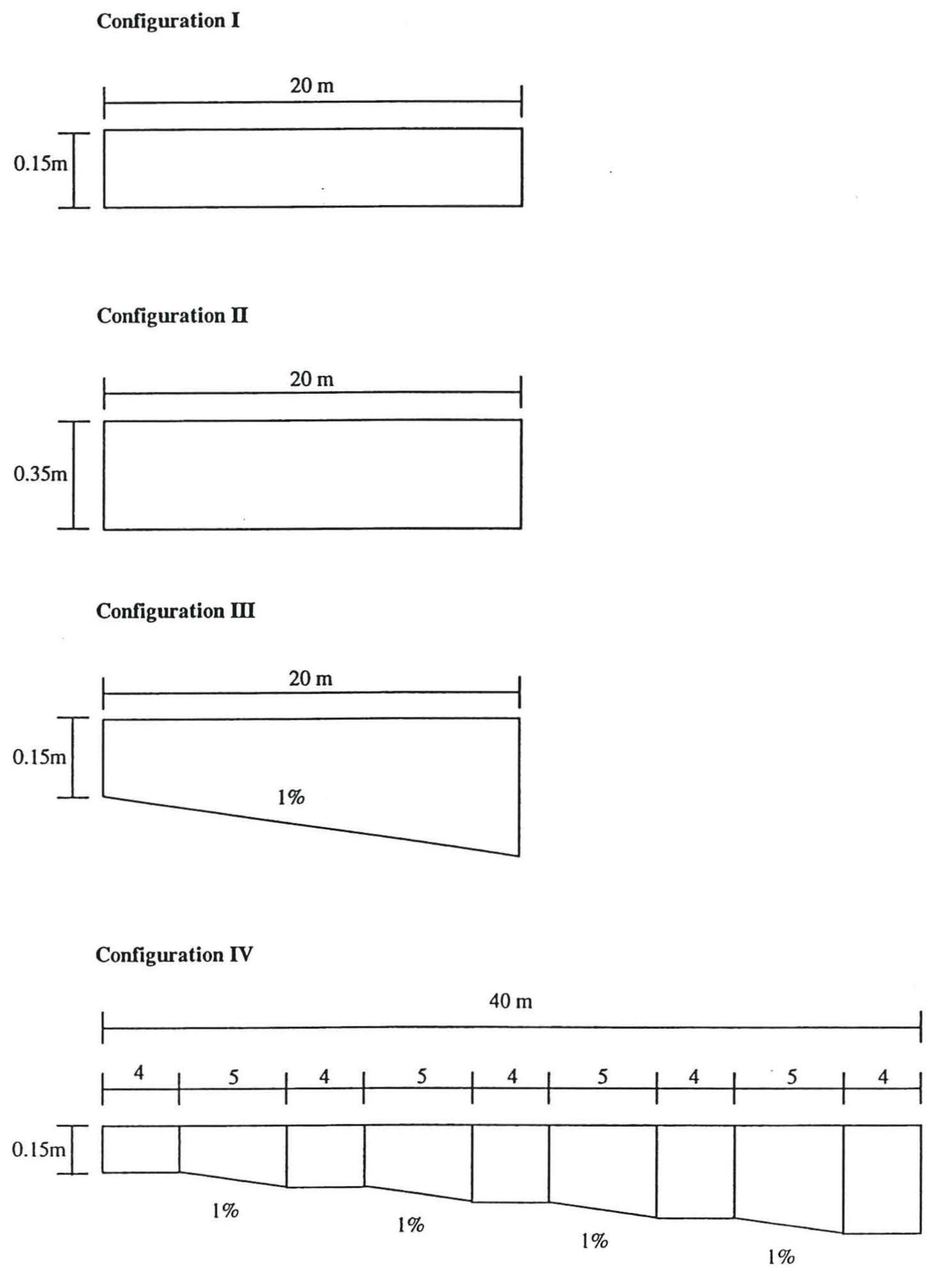

Figure 10 Configurations simulated numerically for System E

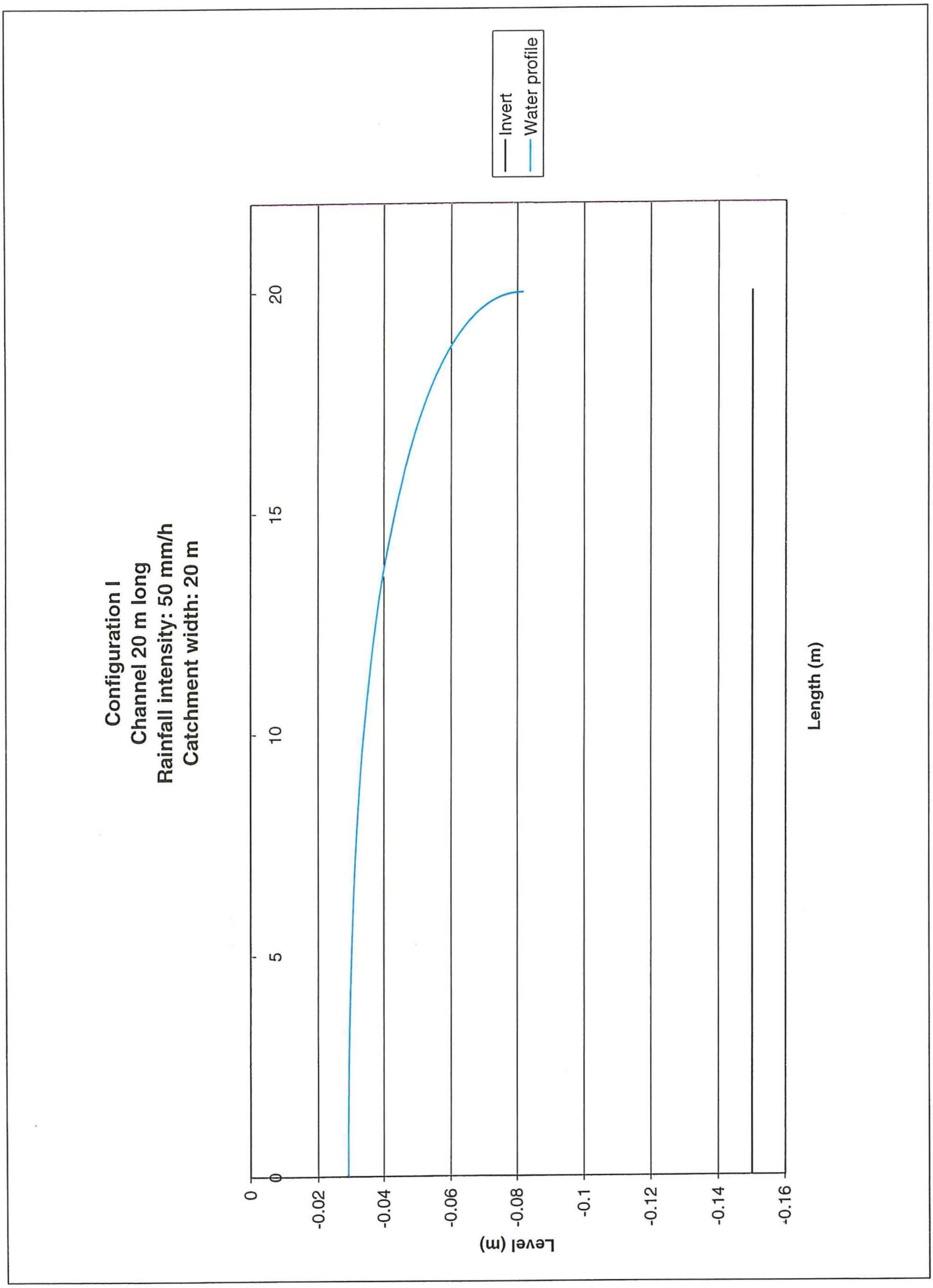

Figure 11 Numerical simulation of water profile. System E; Conf. I; catchment width 20m

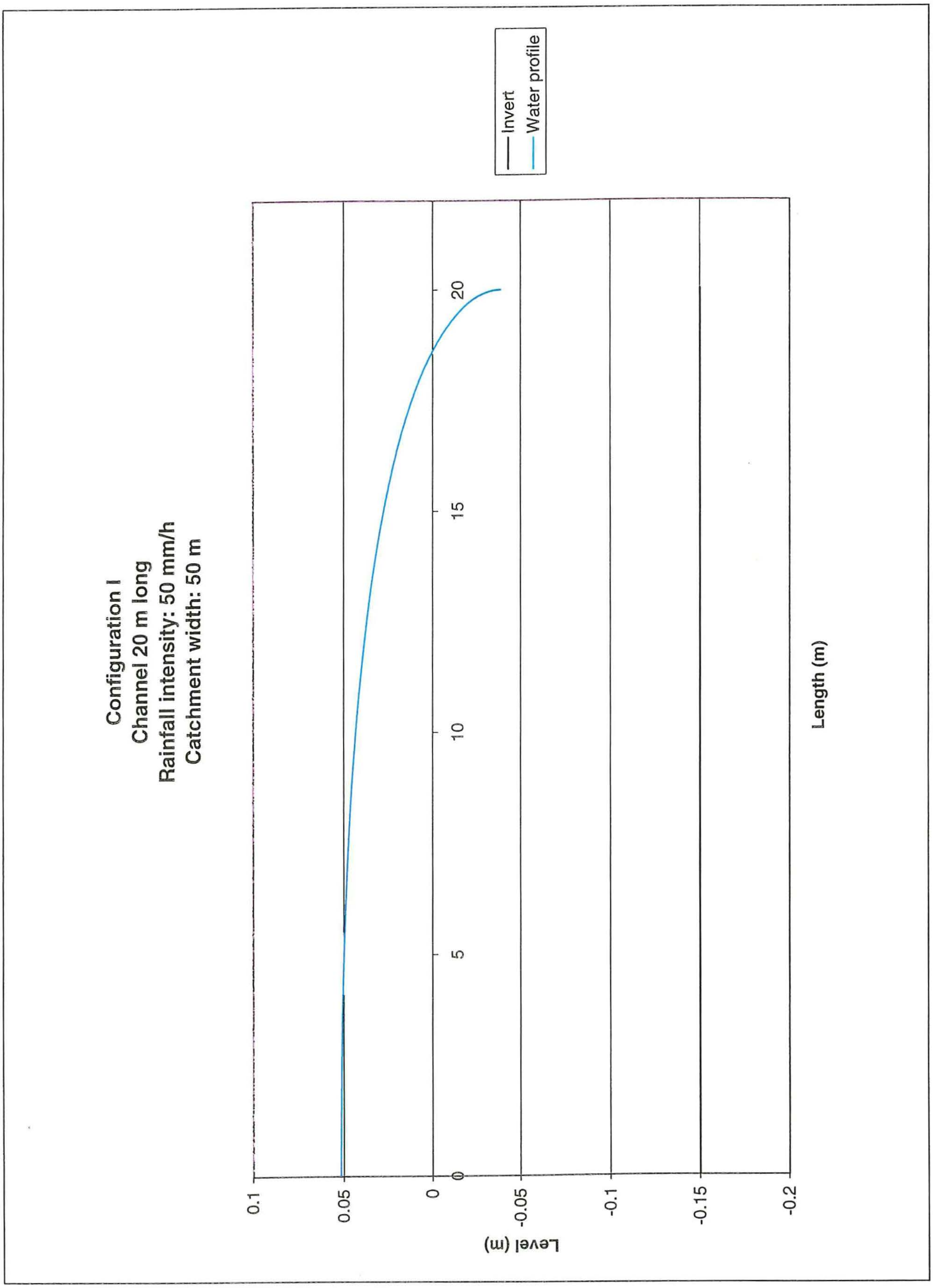

**Figure 12 Numerical simulation of water profile.
System E; Conf. I; catchment width 50m**

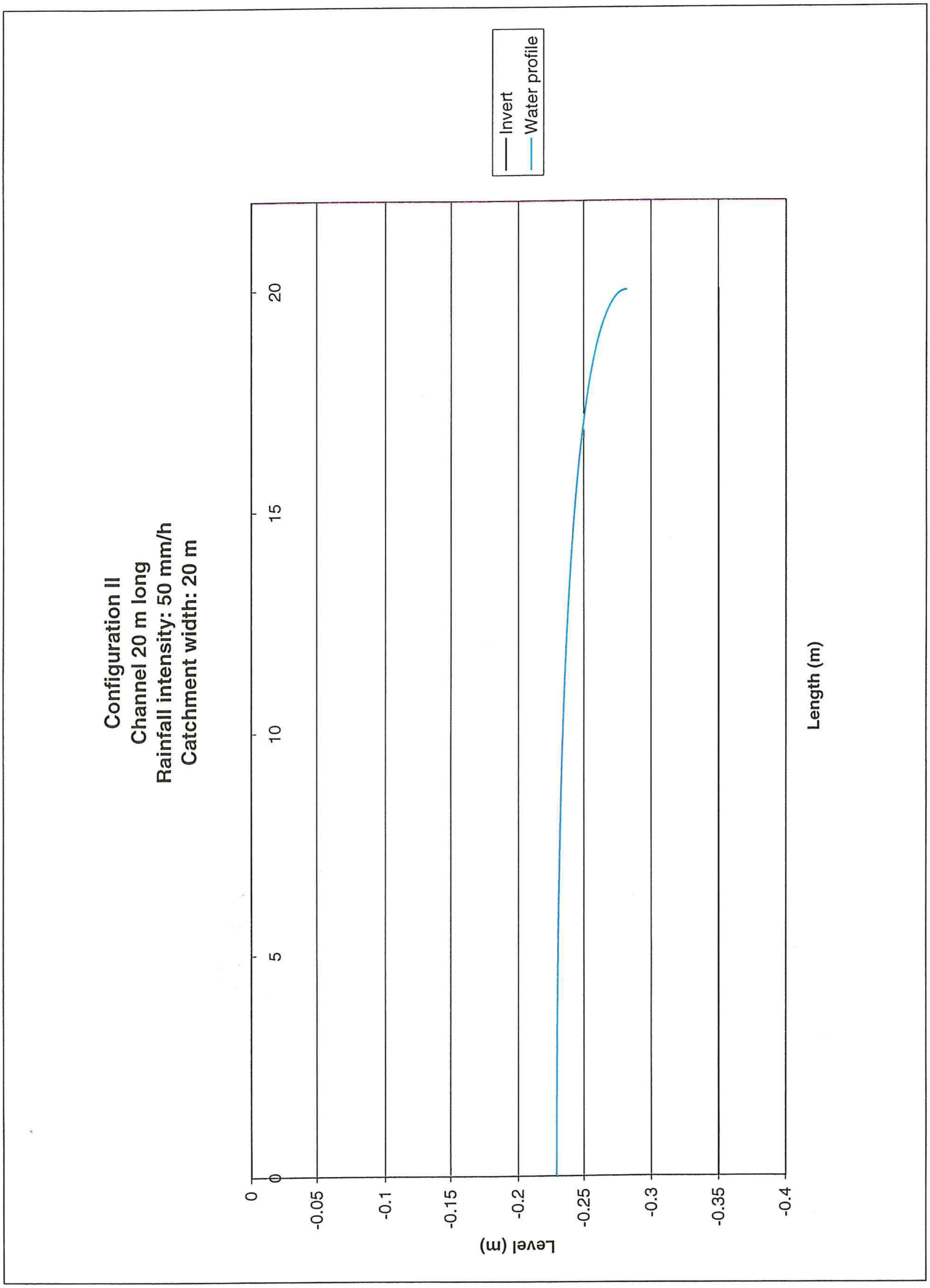

**Figure 13 Numerical simulation of water profile.
System E; Conf. II; catchment width 20m**

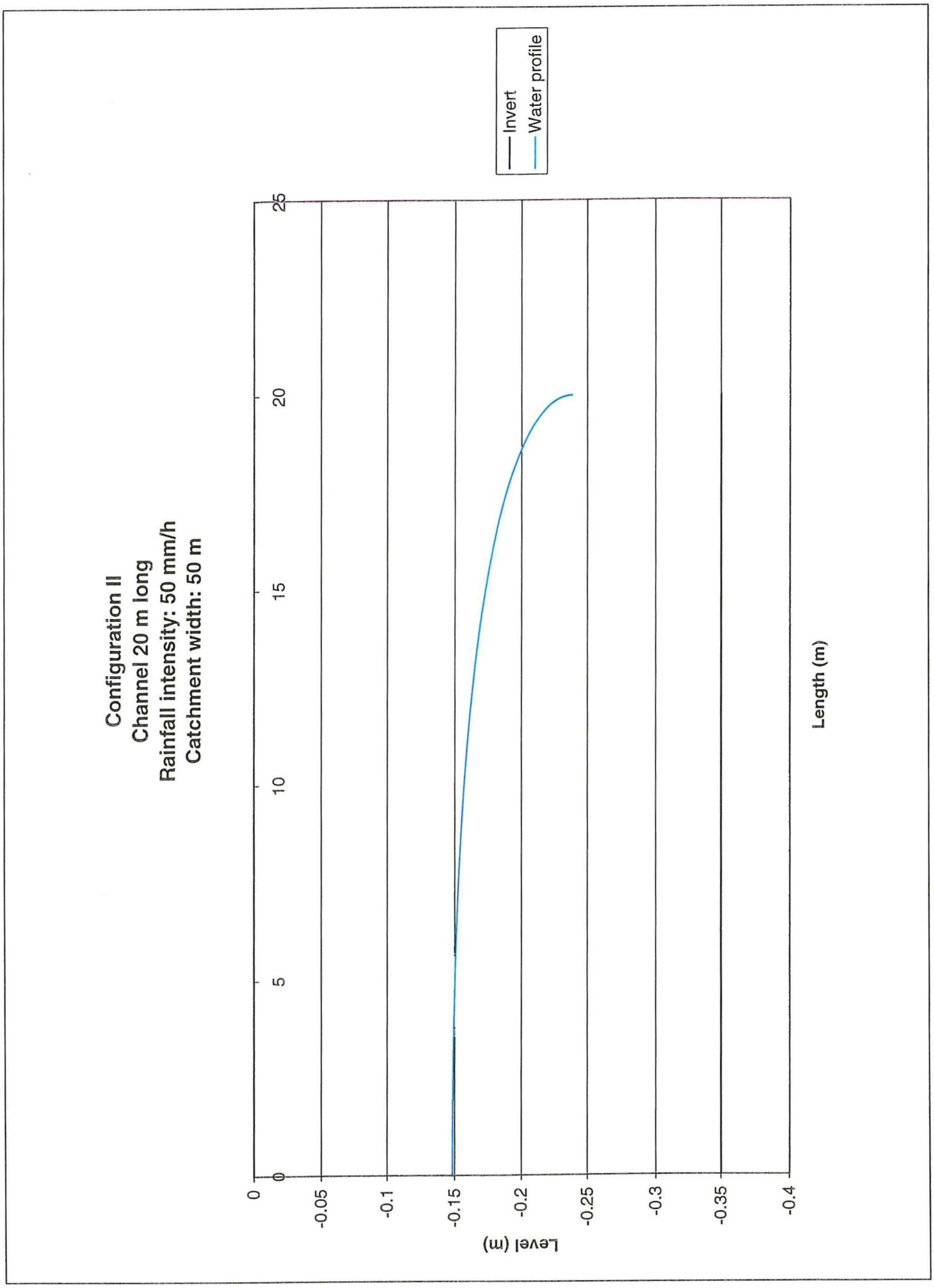

**Figure 14 Numerical simulation of water profile.
System E; Conf. II; catchment width 50m**

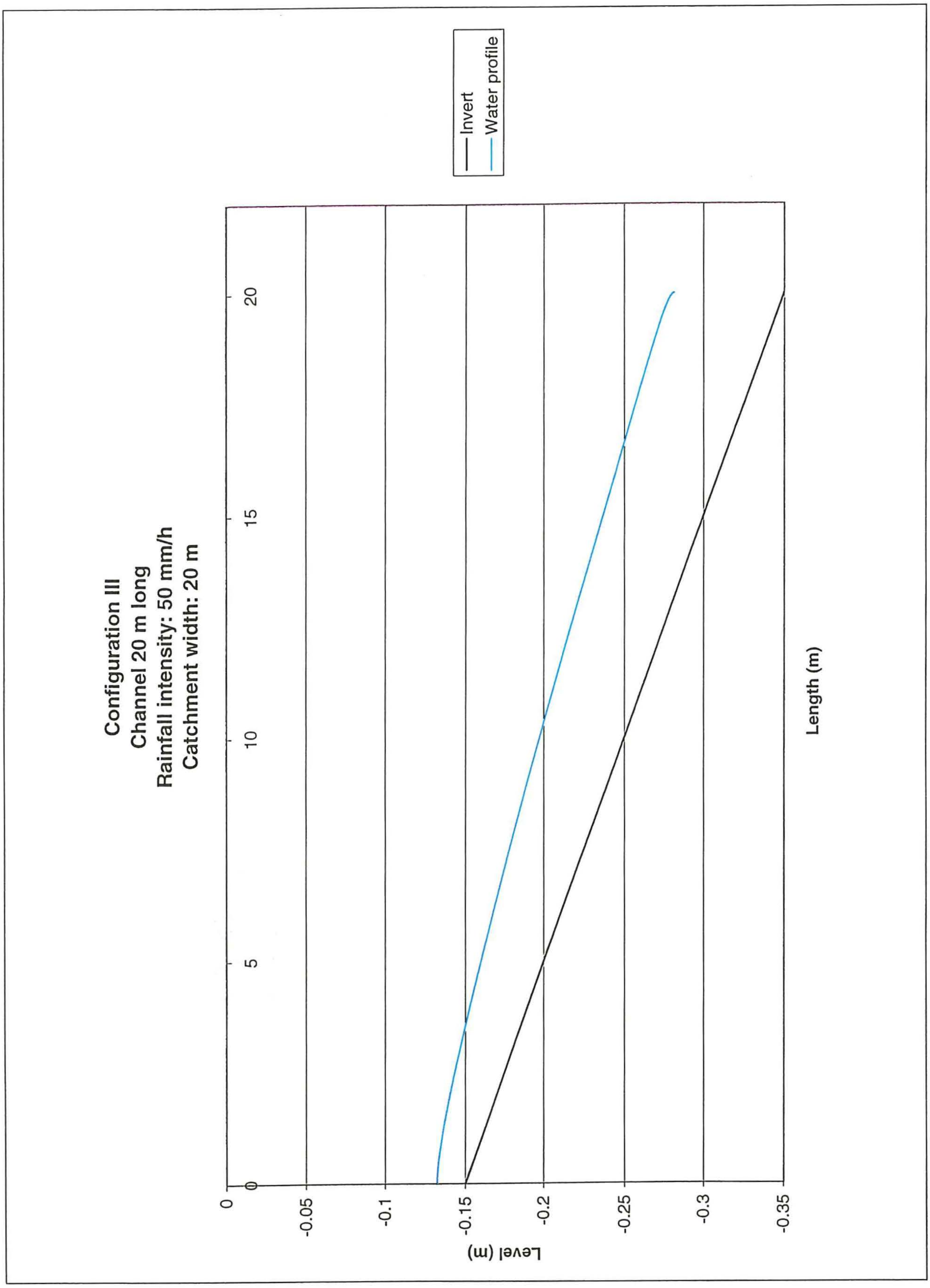

**Figure 15 Numerical simulation of water profile.
System E; Conf. III; catchment width 20m**

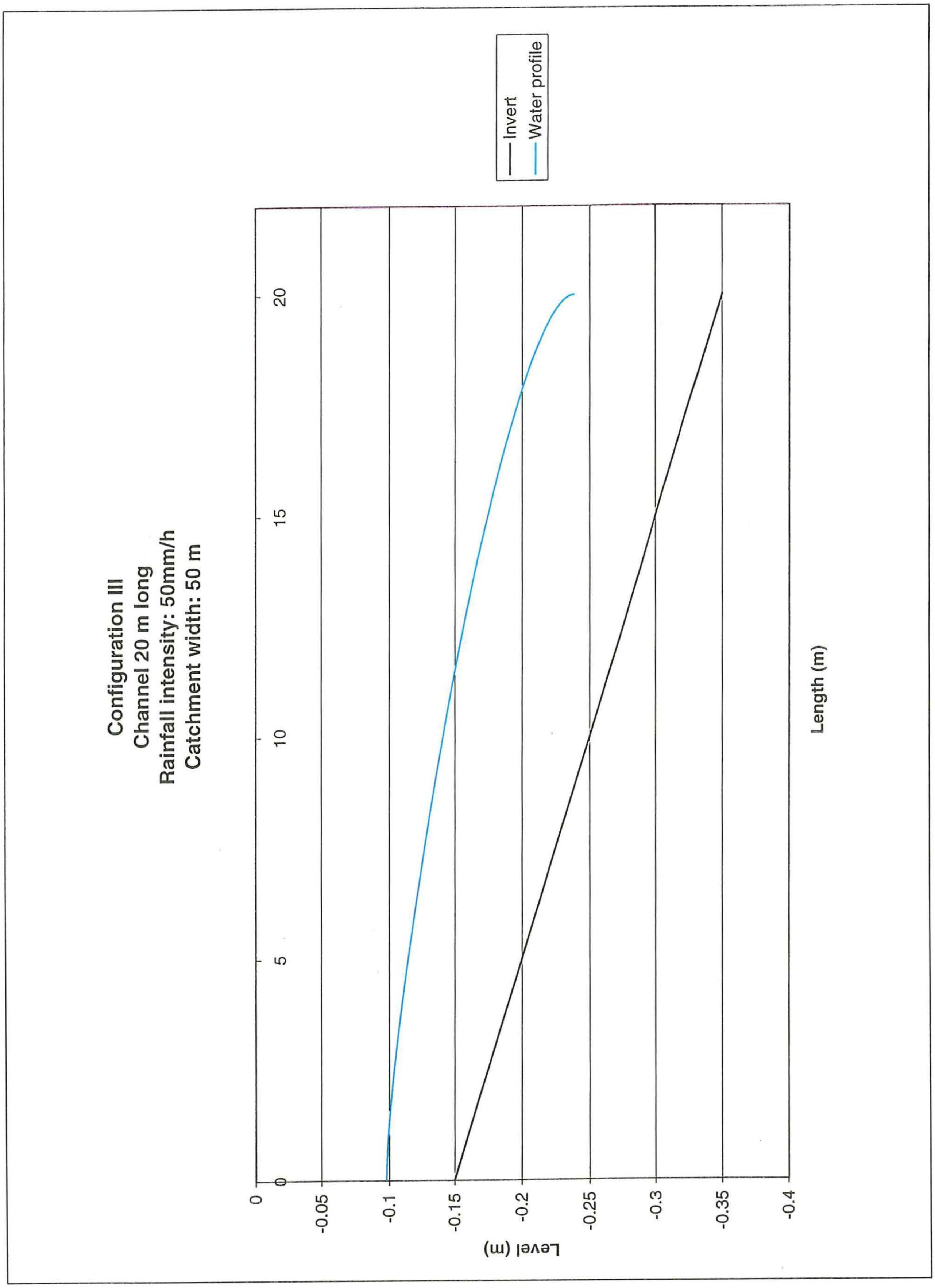

**Figure 16 Numerical simulation of water profile.
System E; Conf. III; catchment width 50m**

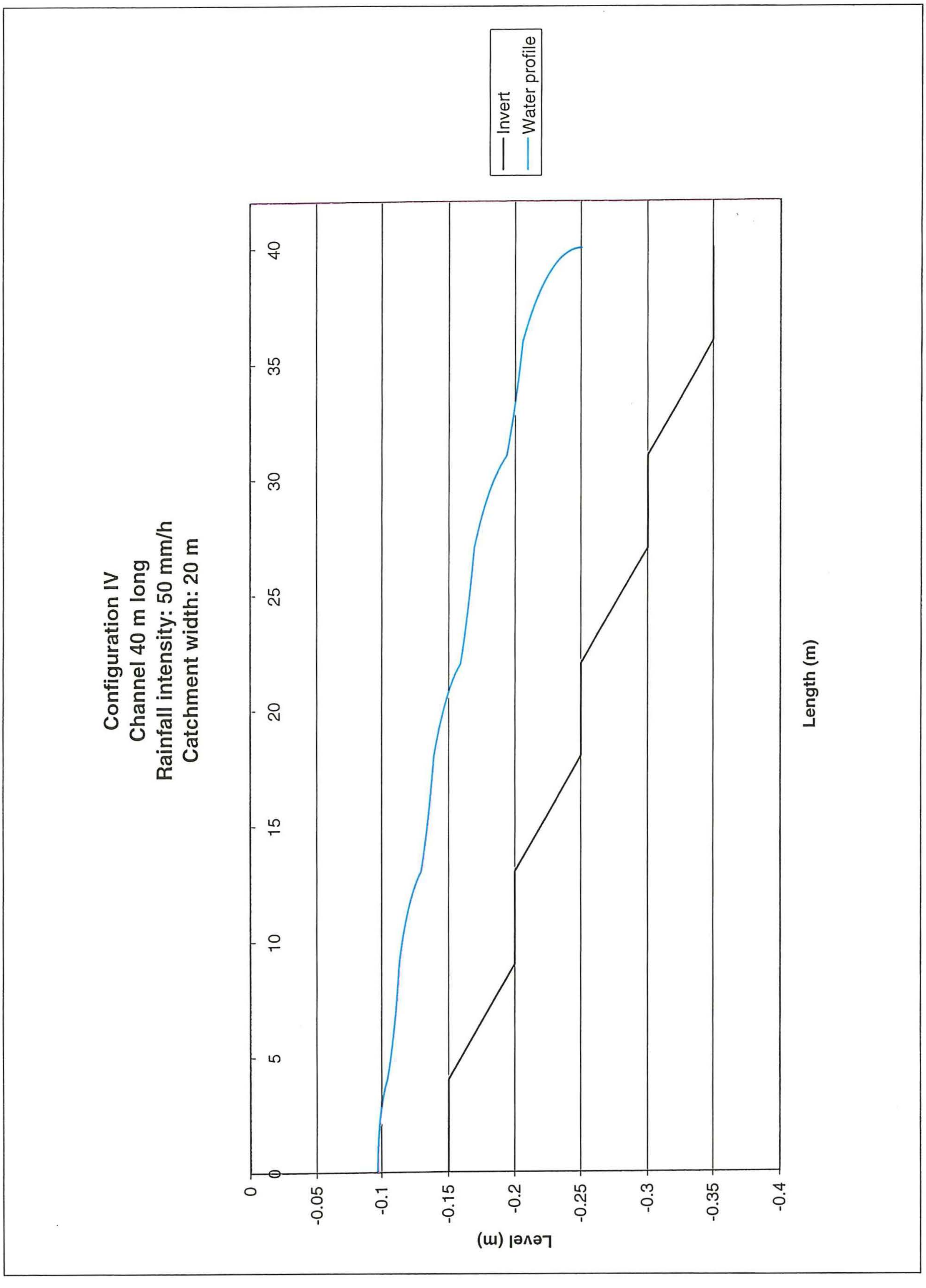

Figure 17 **Numerical simulation of water profile.**
System E; Conf. IV; catchment width 20m

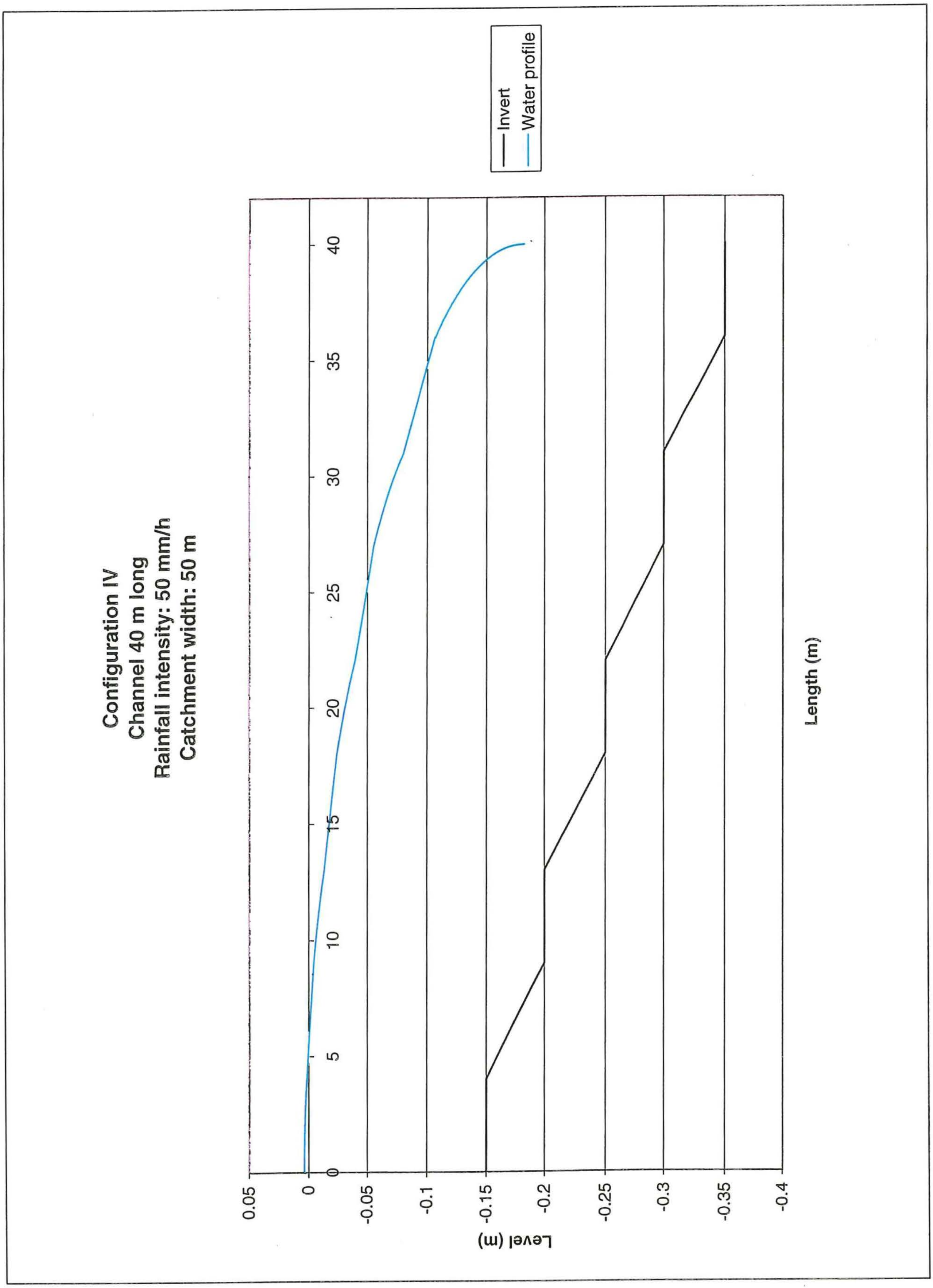

Figure 18 Numerical simulation of water profile.
System E; Conf. IV; catchment width 50m

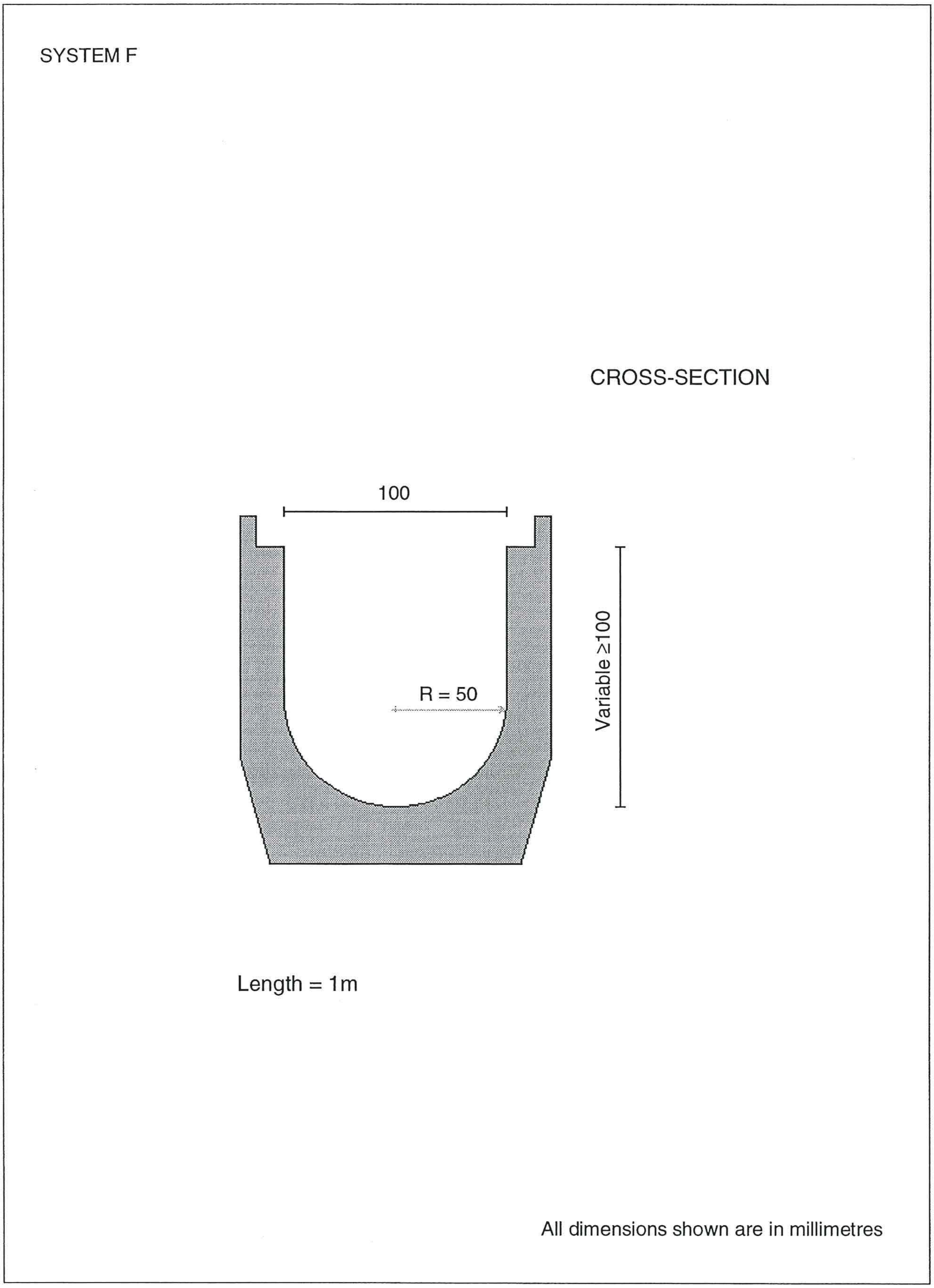

Figure 19 Cross-section of System F channels

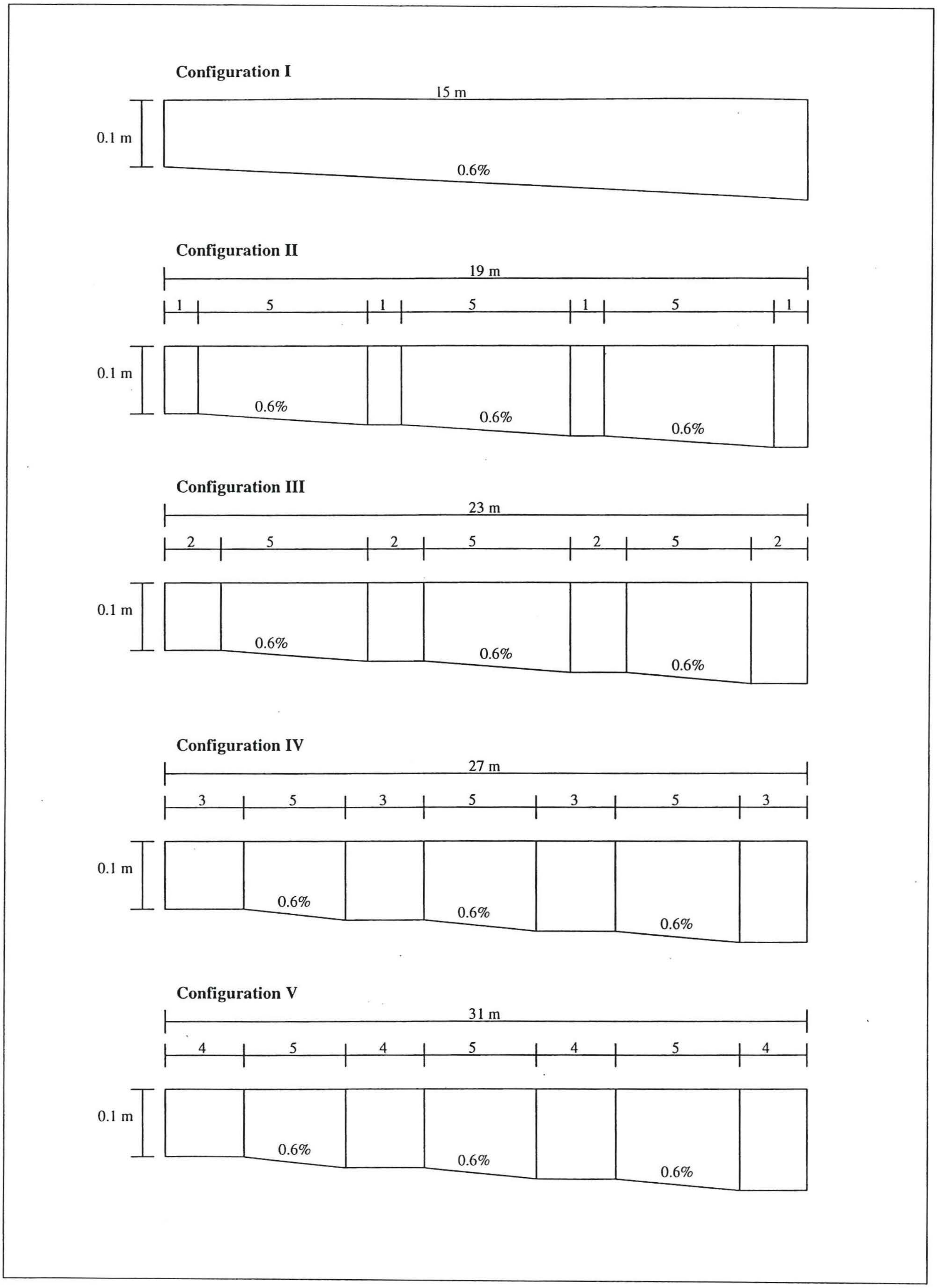

Figure 20 Configurations simulated numerically for System F

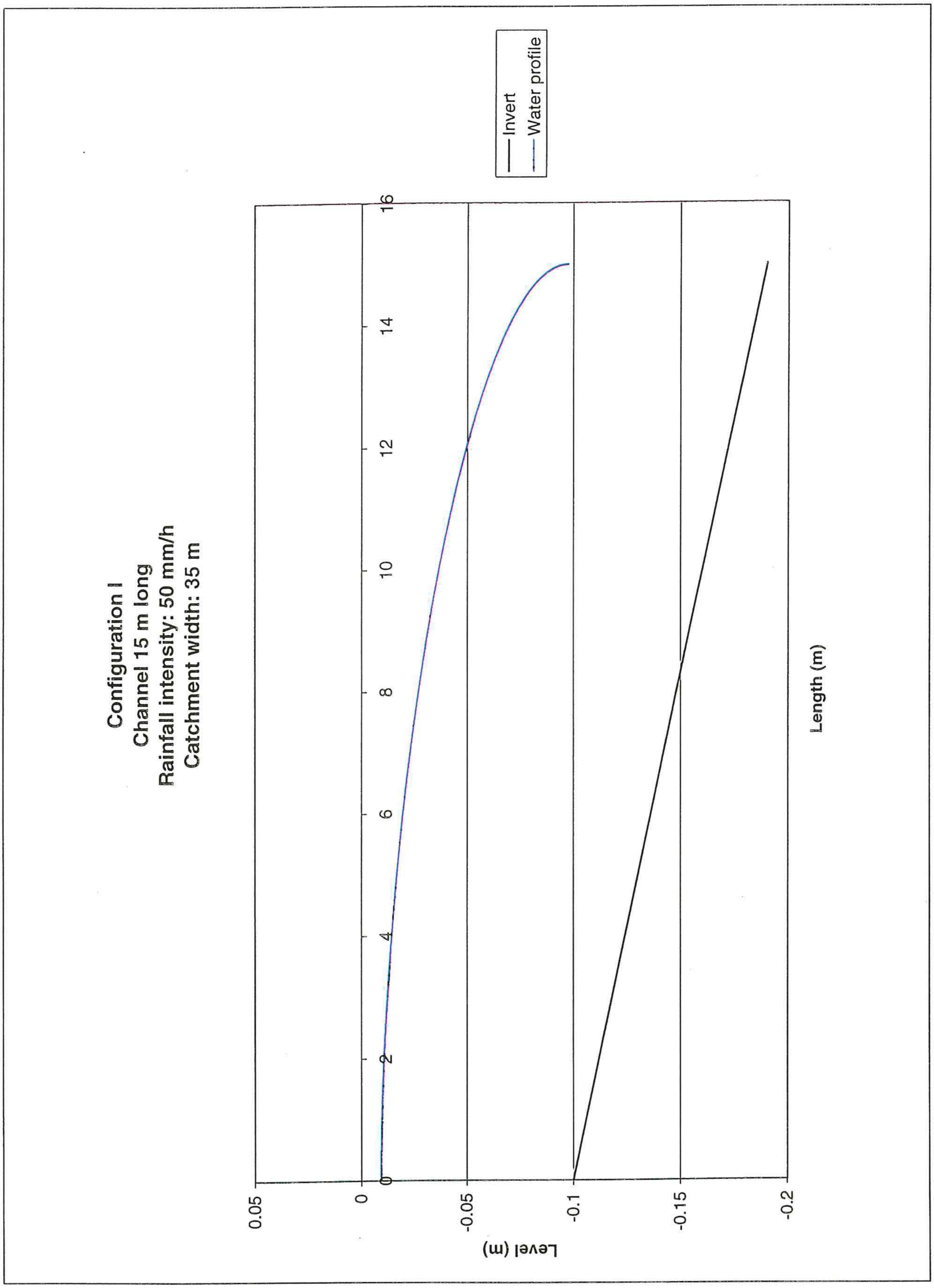

Figure 21 Numerical simulation of water profile. System F; Conf. I; catchment width 35m

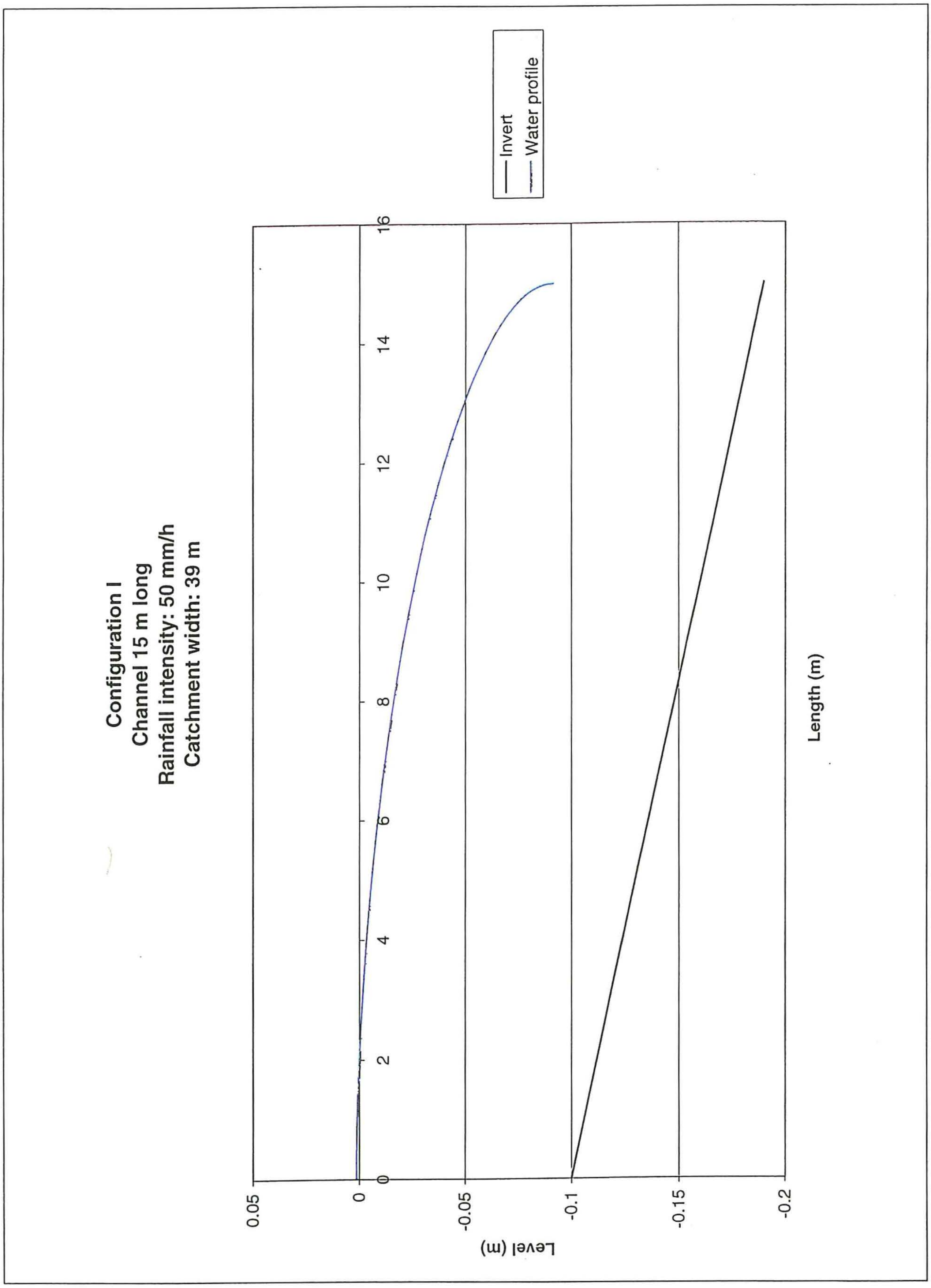

Figure 22 Numerical simulation of water profile. System F; Conf. I; catchment width 39m

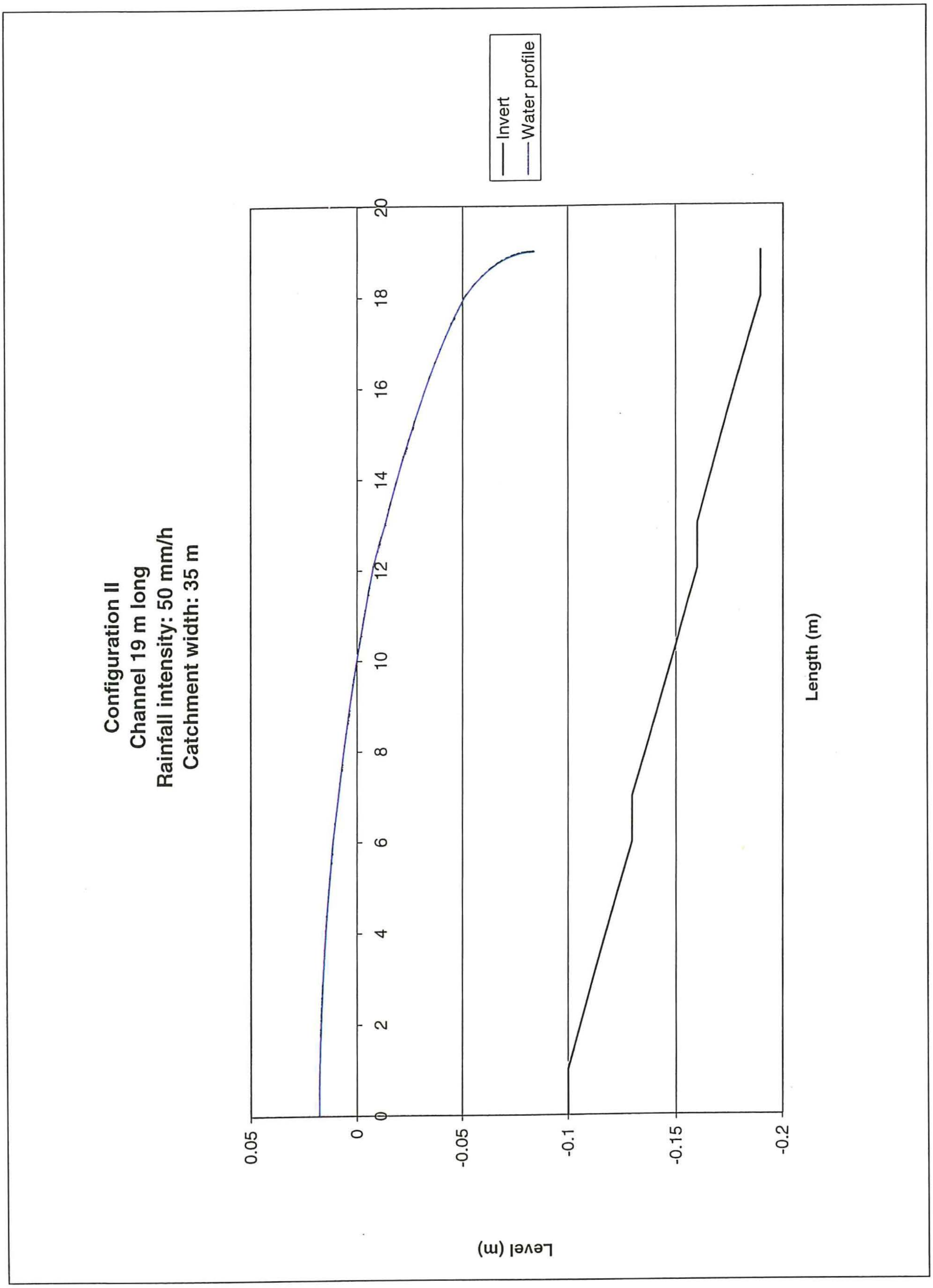

Figure 23 Numerical simulation of water profile.
System F; Conf. II; catchment width 35m

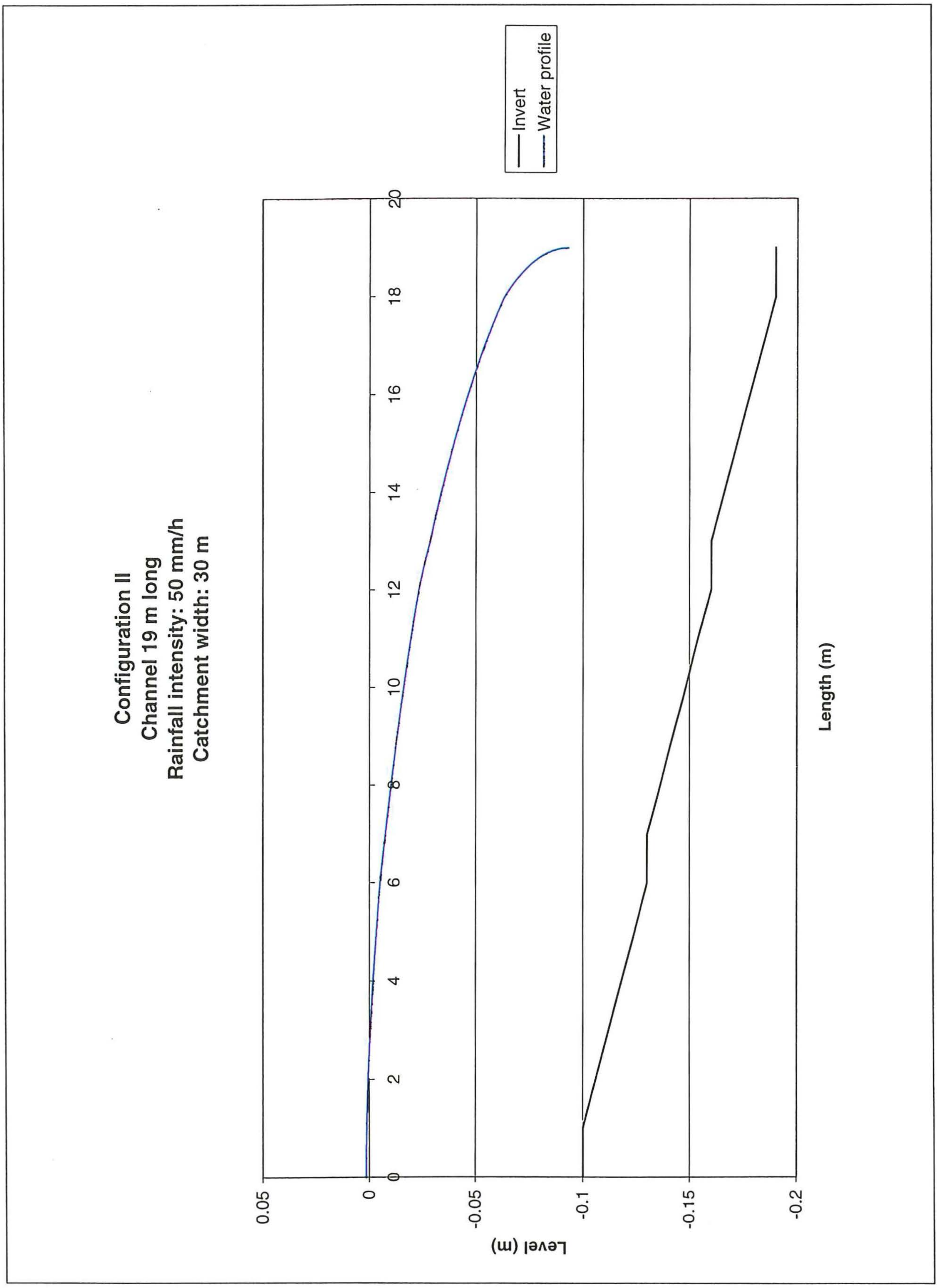

**Figure 24 Numerical simulation of water profile.
System F; Conf. II; catchment width 30m**

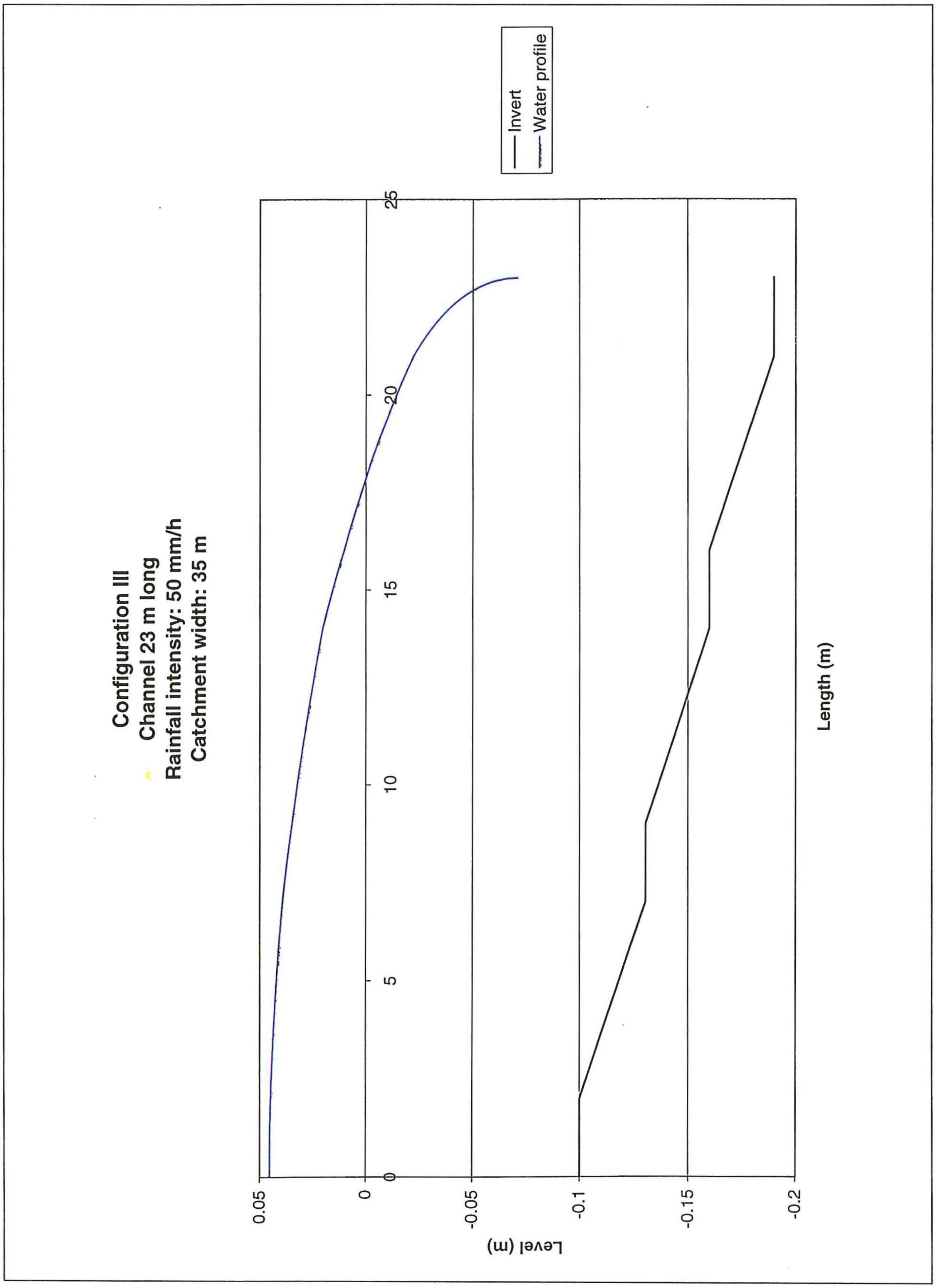

Figure 25 Numerical simulation of water profile. System F; Conf. III; catchment width 35m

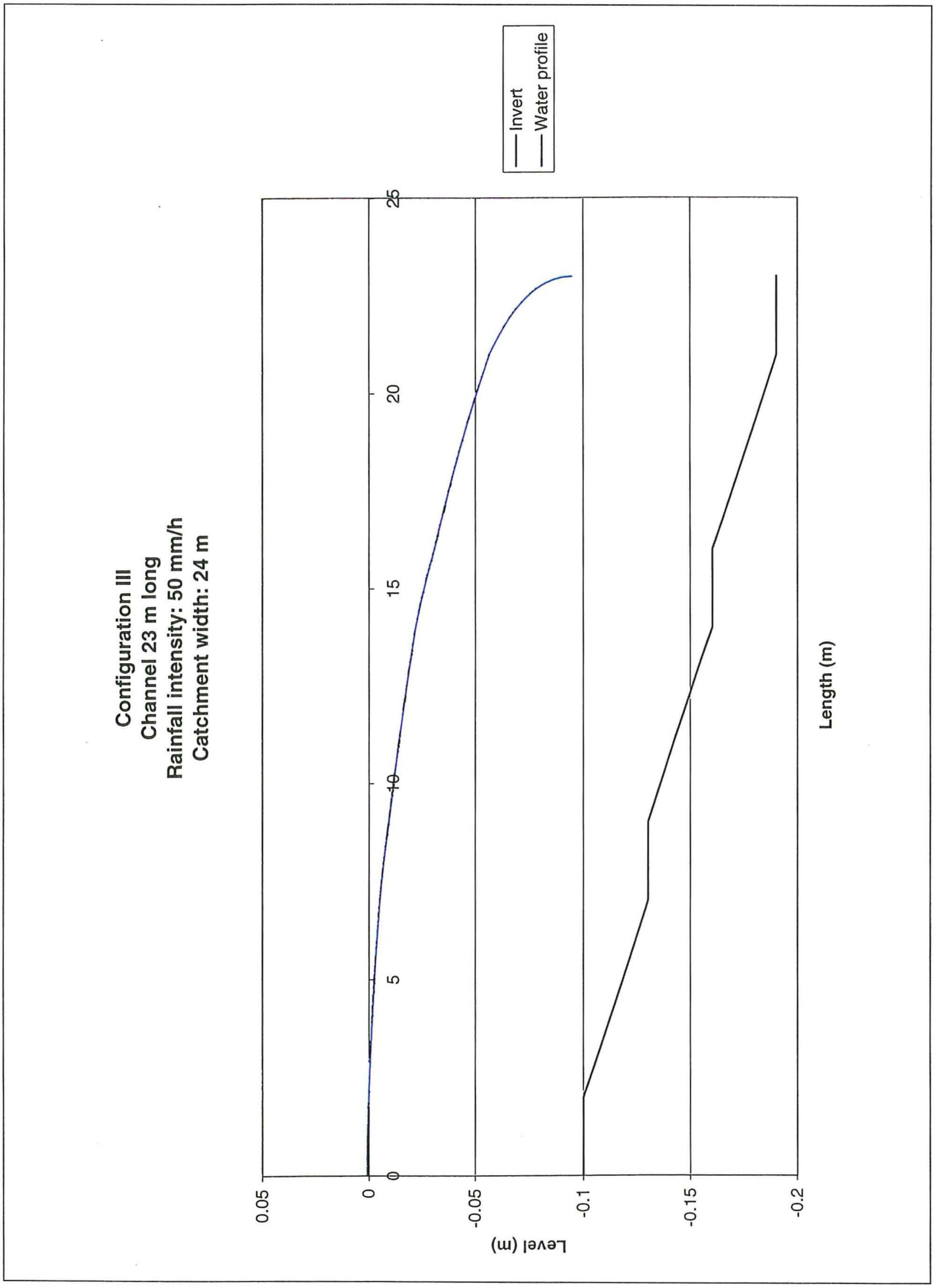

Figure 26 Numerical simulation of water profile. System F; Conf. III; catchment width 24m

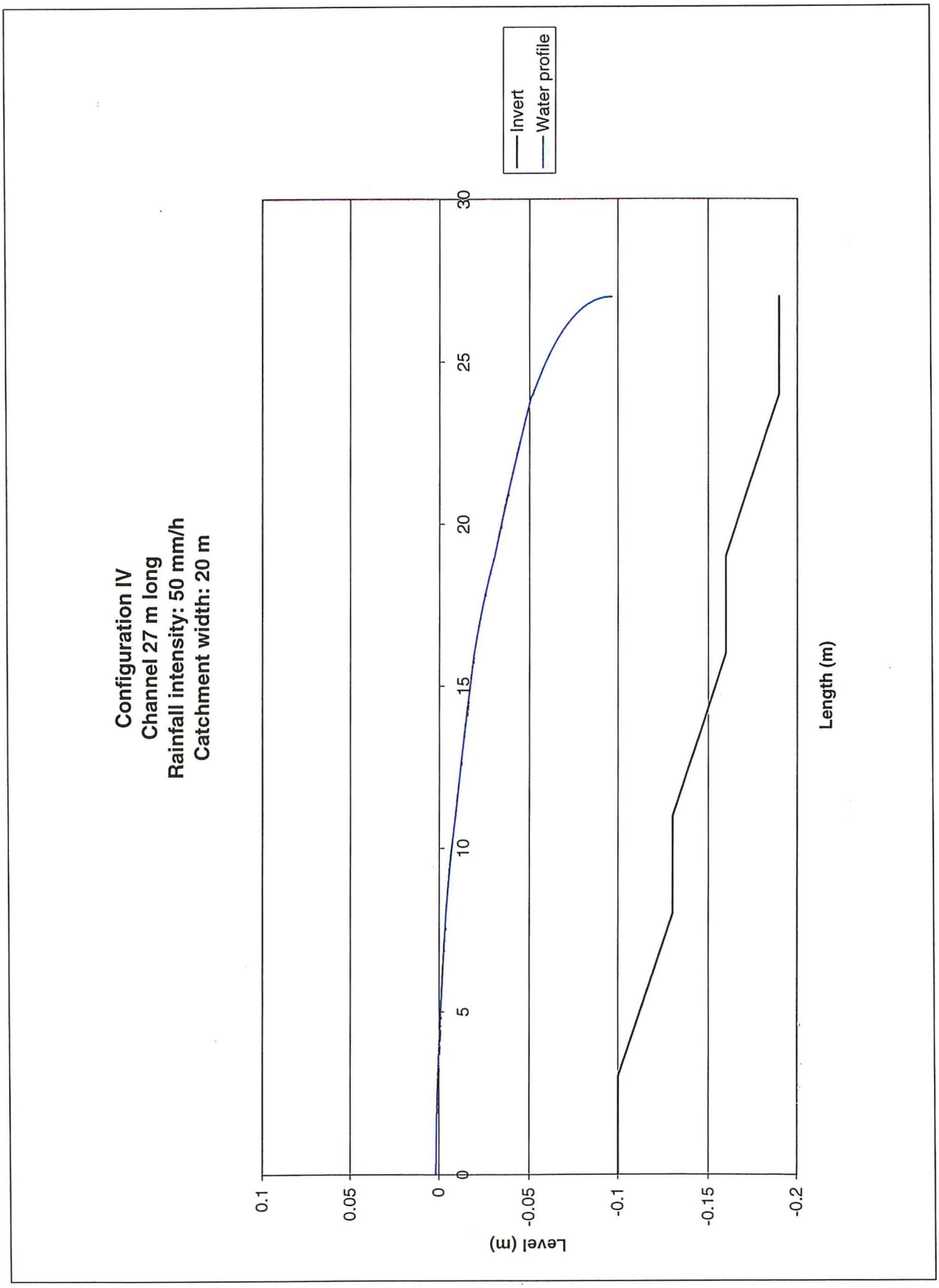

Figure 27 Numerical simulation of water profile. System F; Conf. IV; catchment width 20m

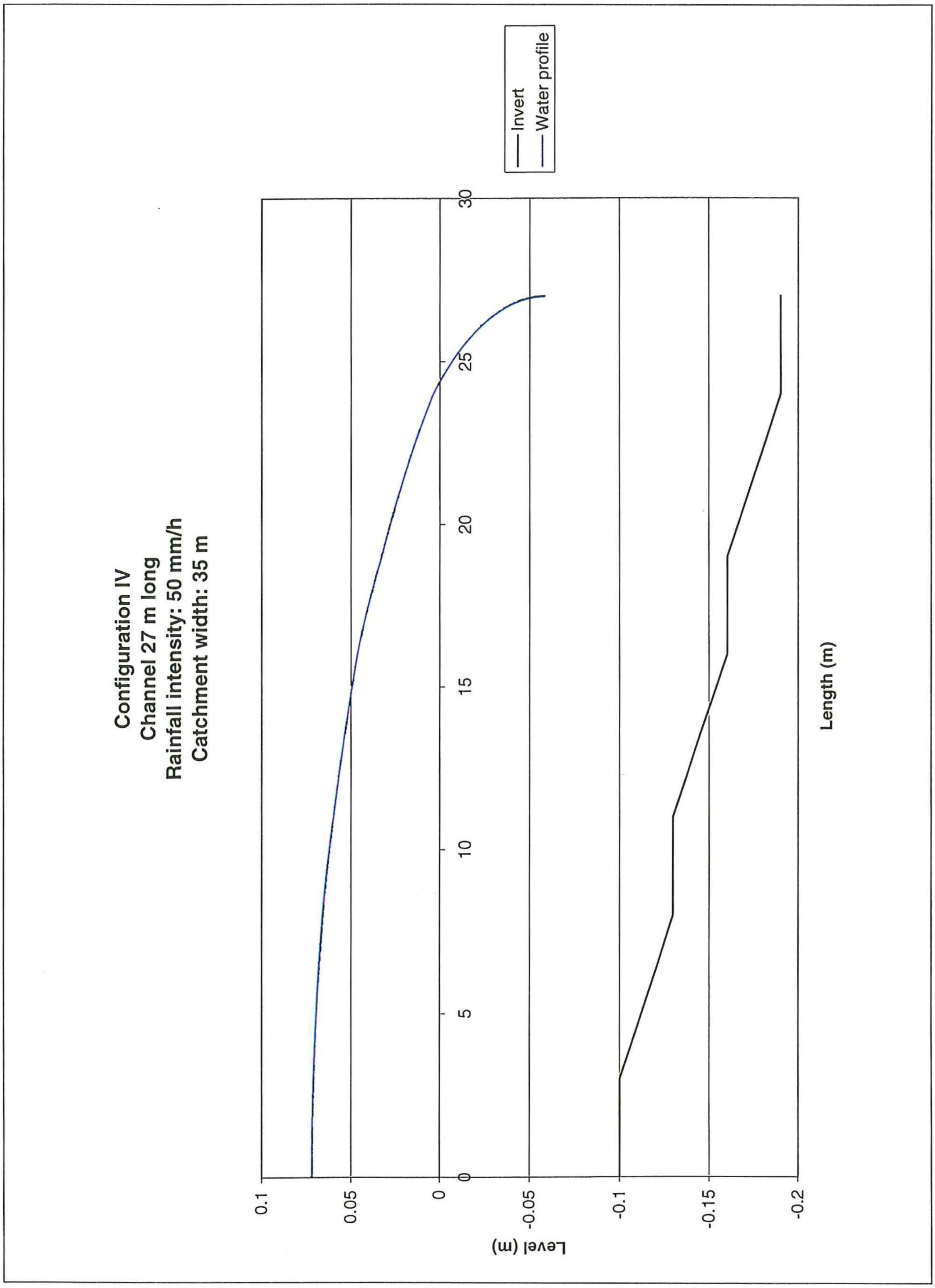

Figure 28 Numerical simulation of water profile. System F; Conf. IV; catchment width 35m

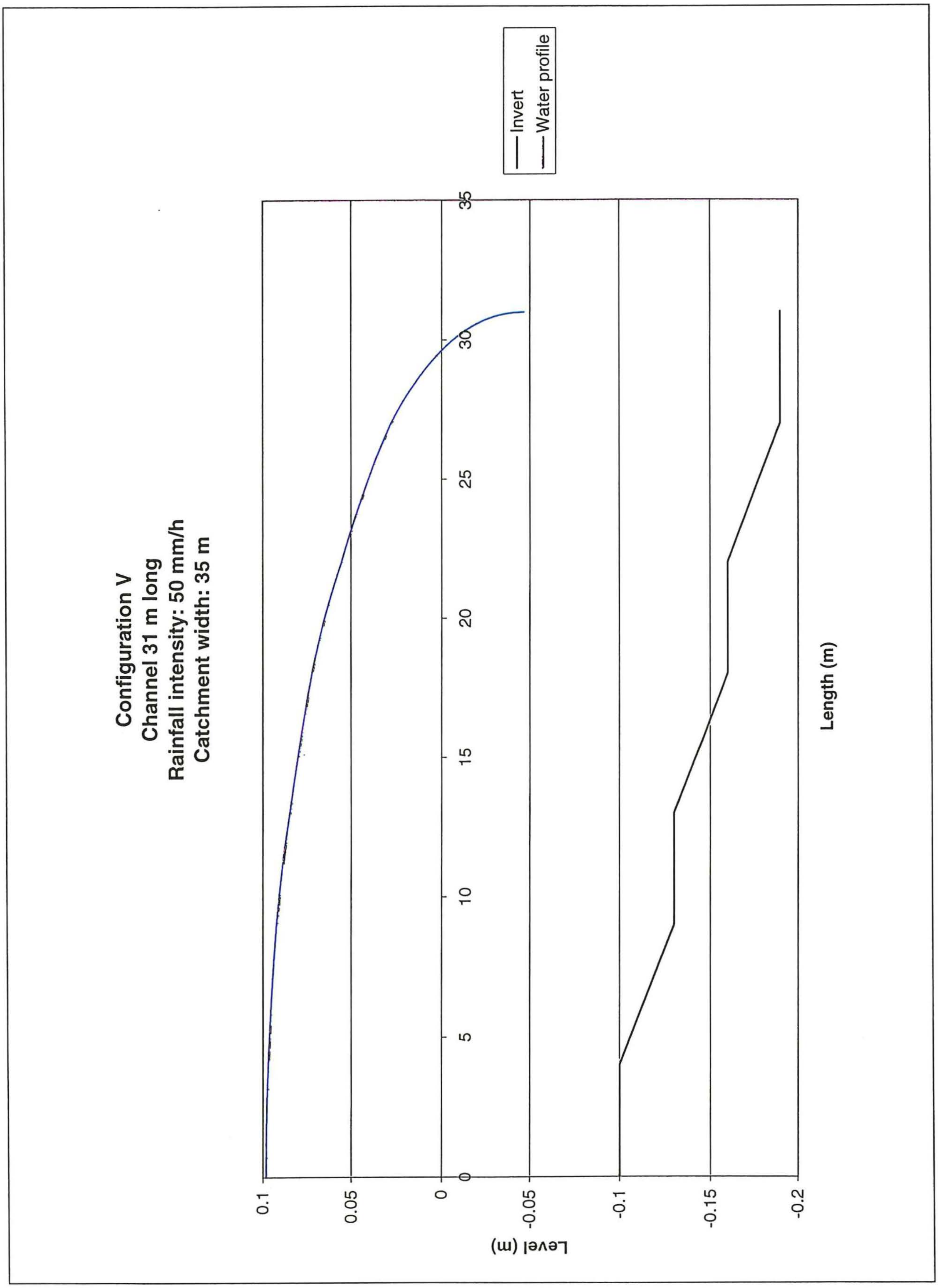

Figure 29 Numerical simulation of water profile.
System F; Conf. V; catchment width 35m

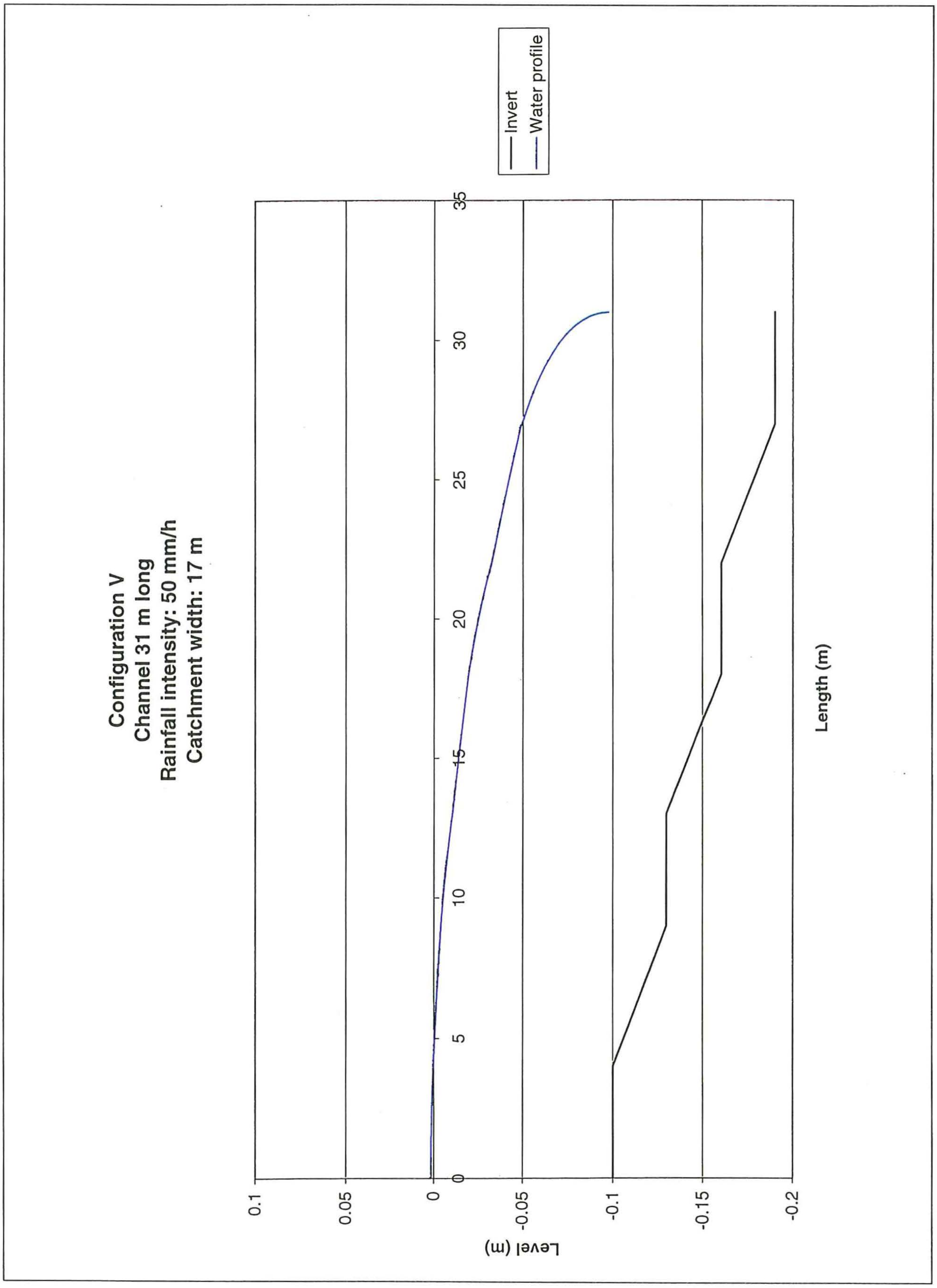

Figure 30 Numerical simulation of water profile.
System F; Conf. V; catchment width 17m

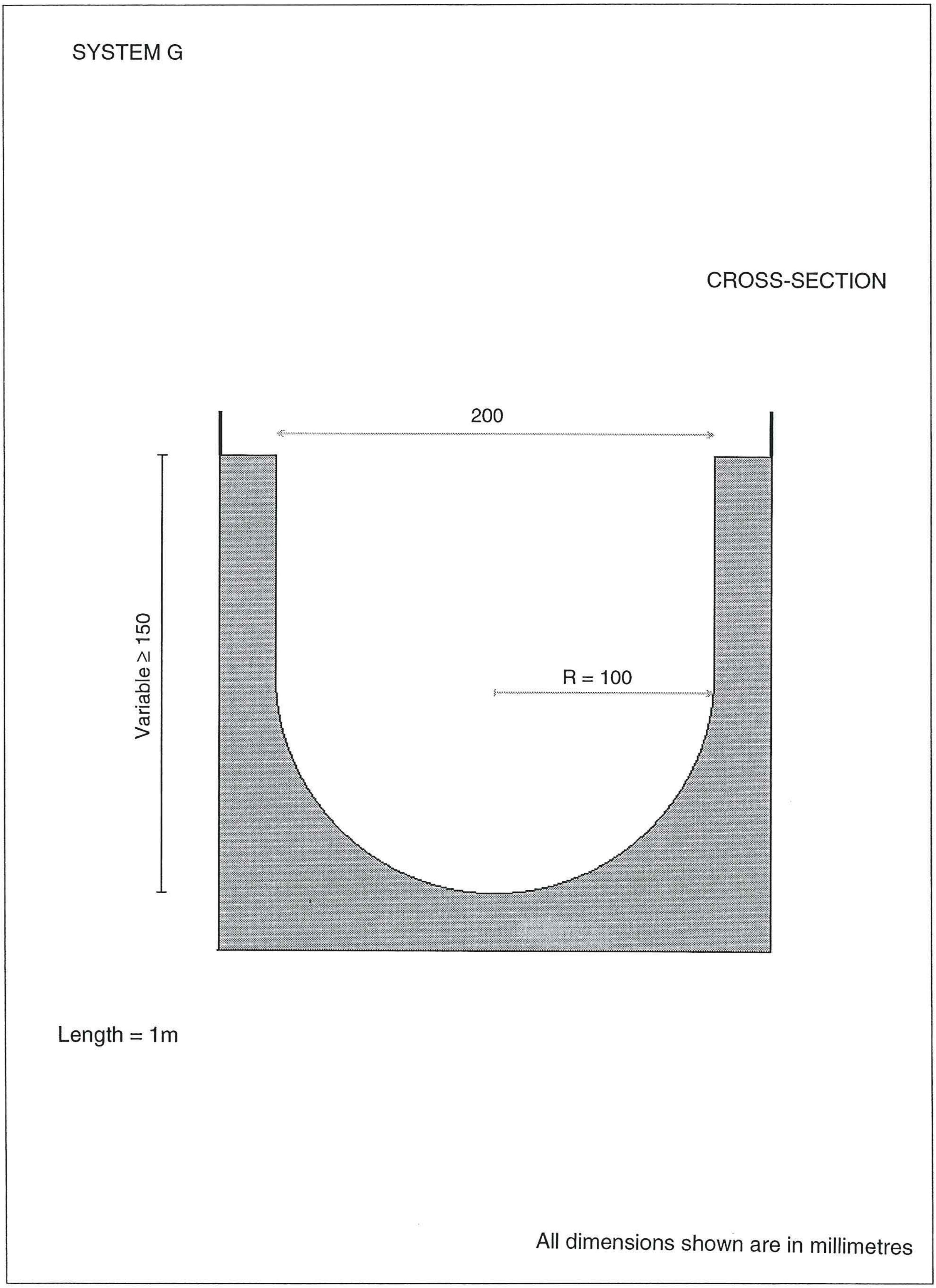

Figure 31 Cross section of System G channels

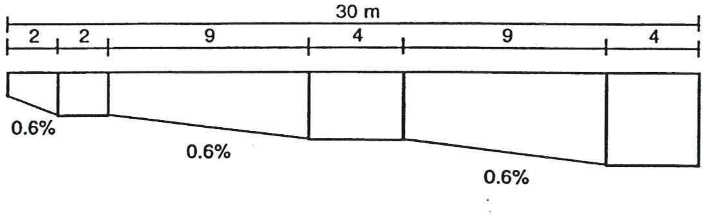

Configuration I

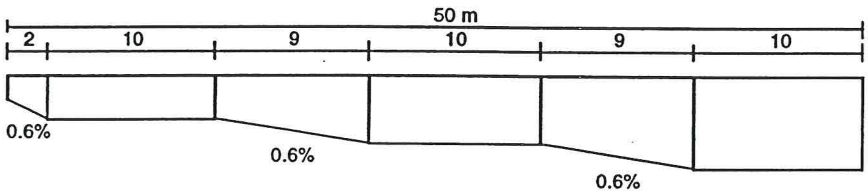

Configuration II

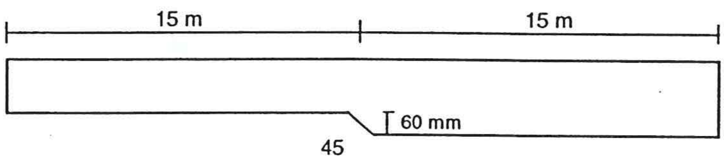

Configuration III

Cross-section: 200mm wide with half round base (100mm radius)

Figure 32 Configurations simulated numerically for System G

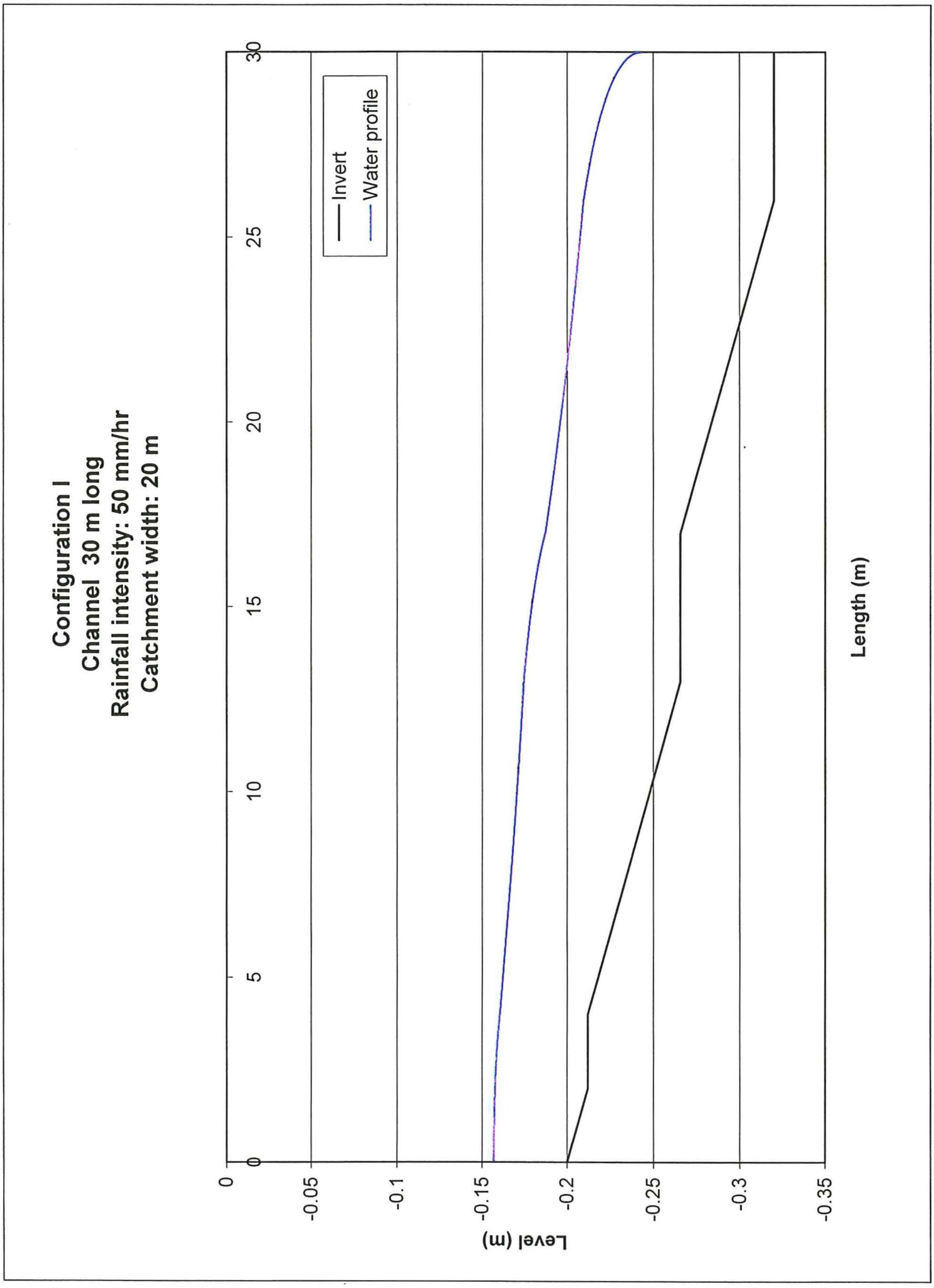

**Figure 33 Numerical simulation of water profile.
System G; Conf. I; rainfall intensity 50mm/hr**

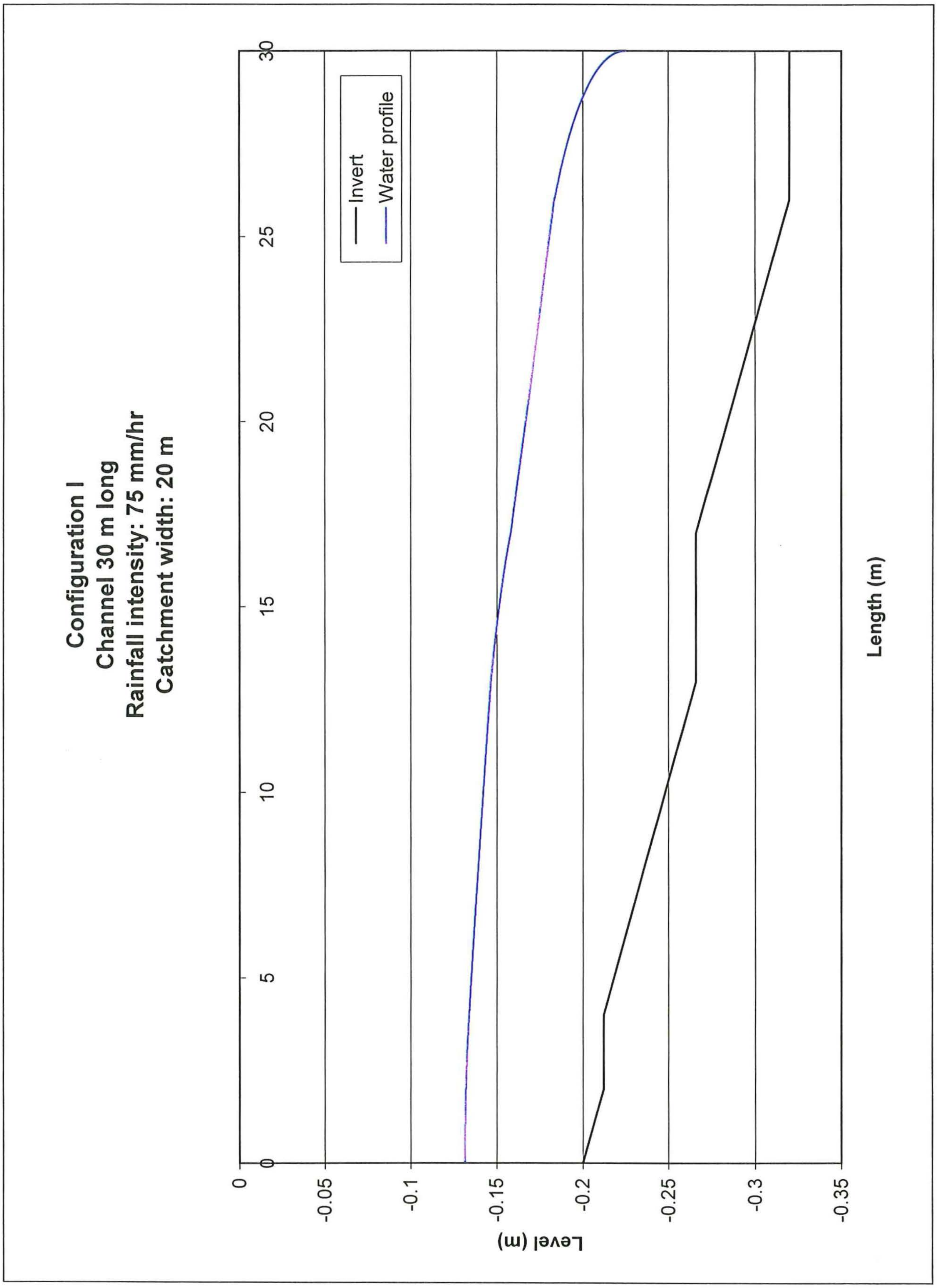

**Figure 34 Numerical simulation of water profile.
System G; Conf. I; rainfall intensity 75mm/hr**

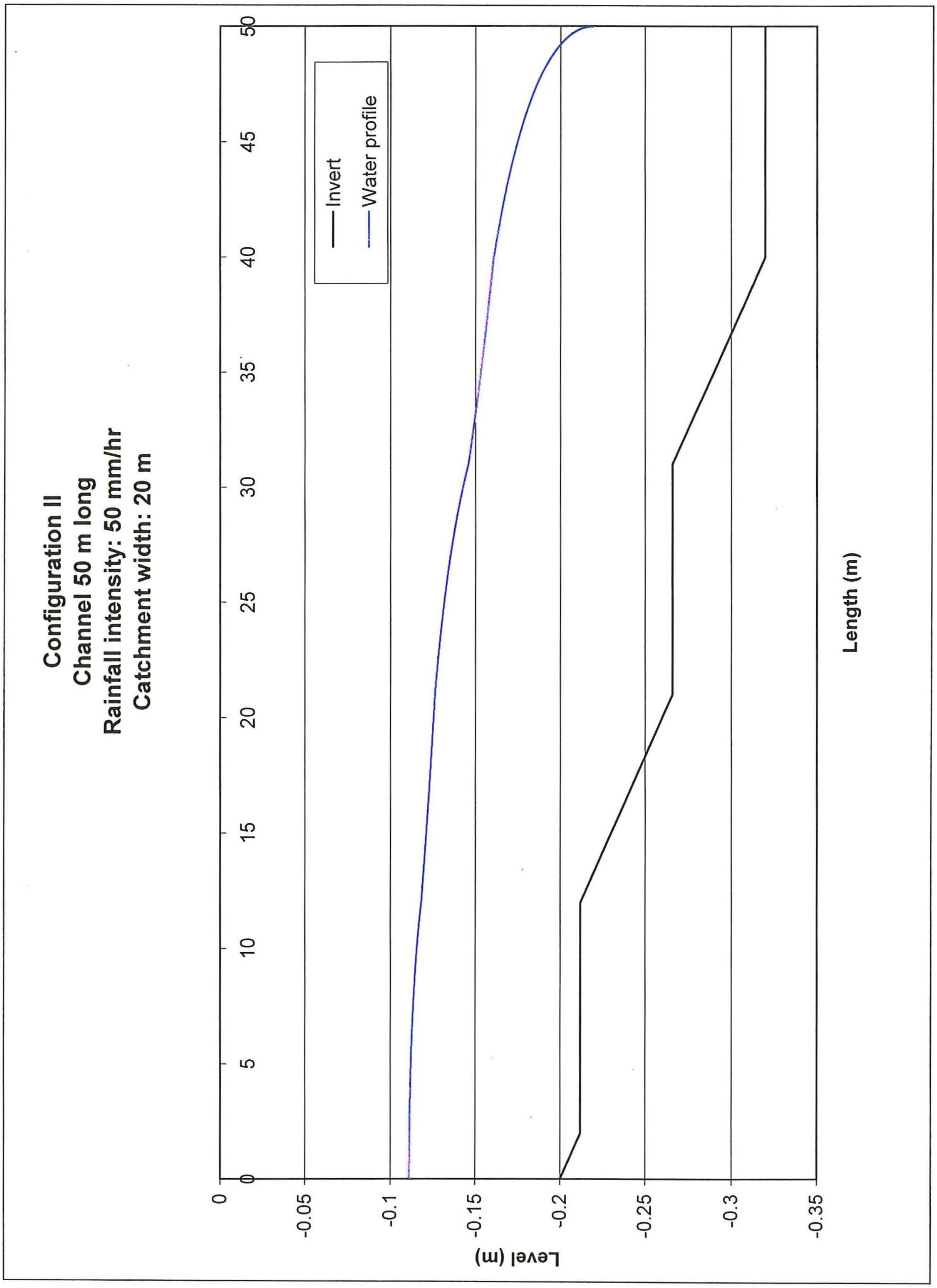

**Figure 35 Numerical simulation of water profile.
System G; Conf. II; rainfall intensity 50mm/hr**

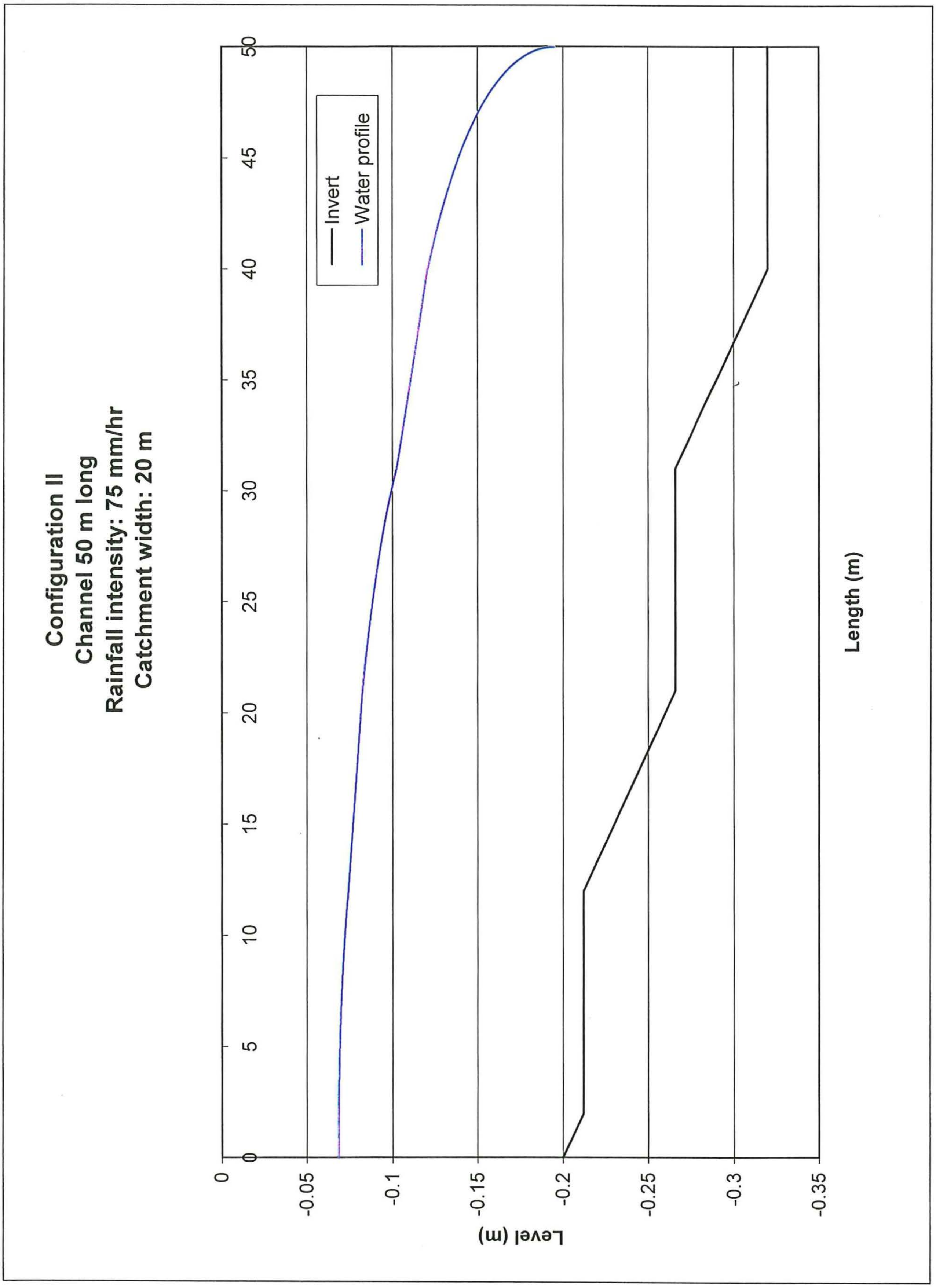

Figure 36 Numerical simulation of water profile.
System G; Conf. II; rainfall intensity 75mm/hr

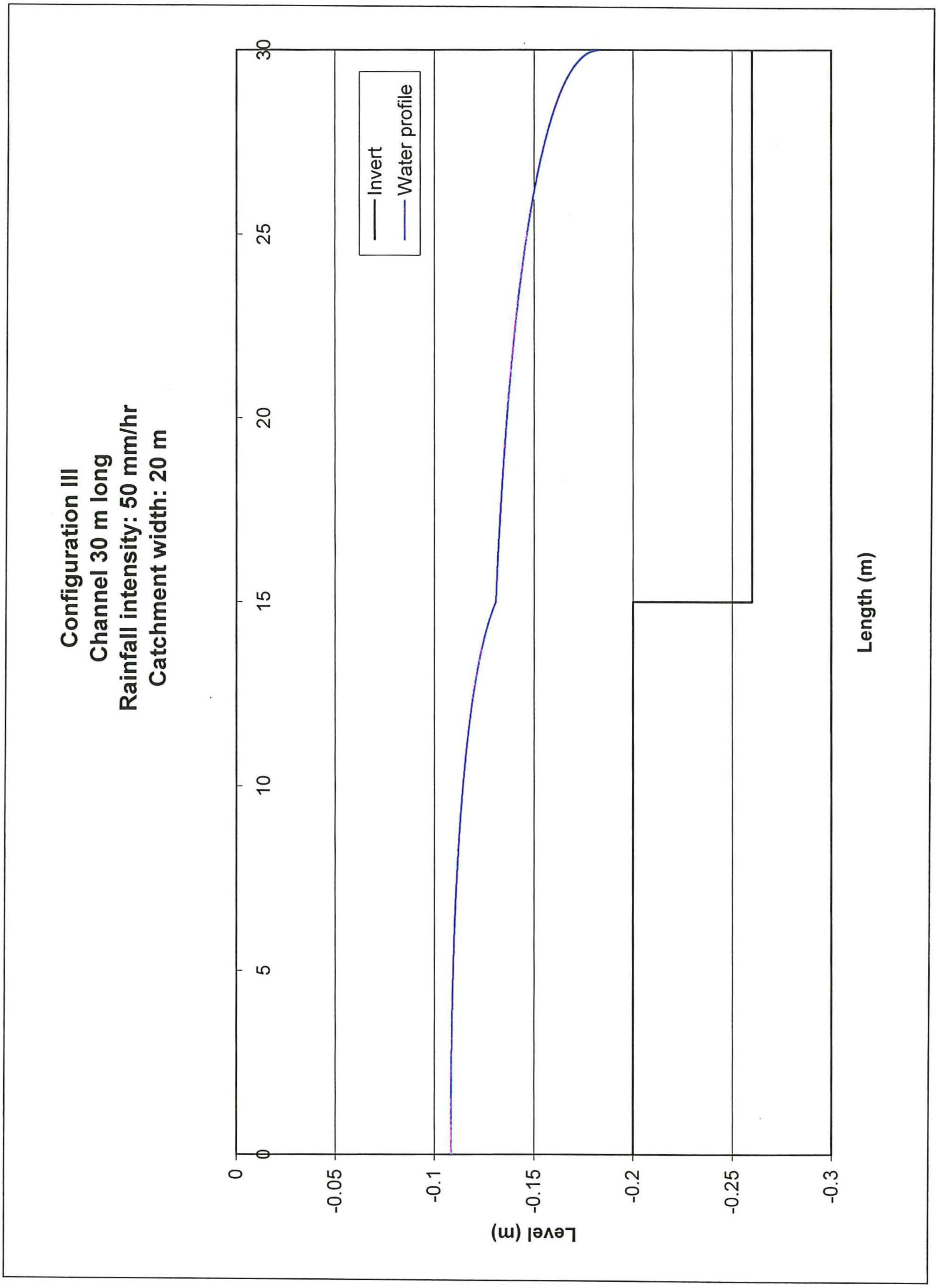

Figure 37 Numerical simulation of water profile.
System G; Conf. III; rainfall intensity 50mm/hr

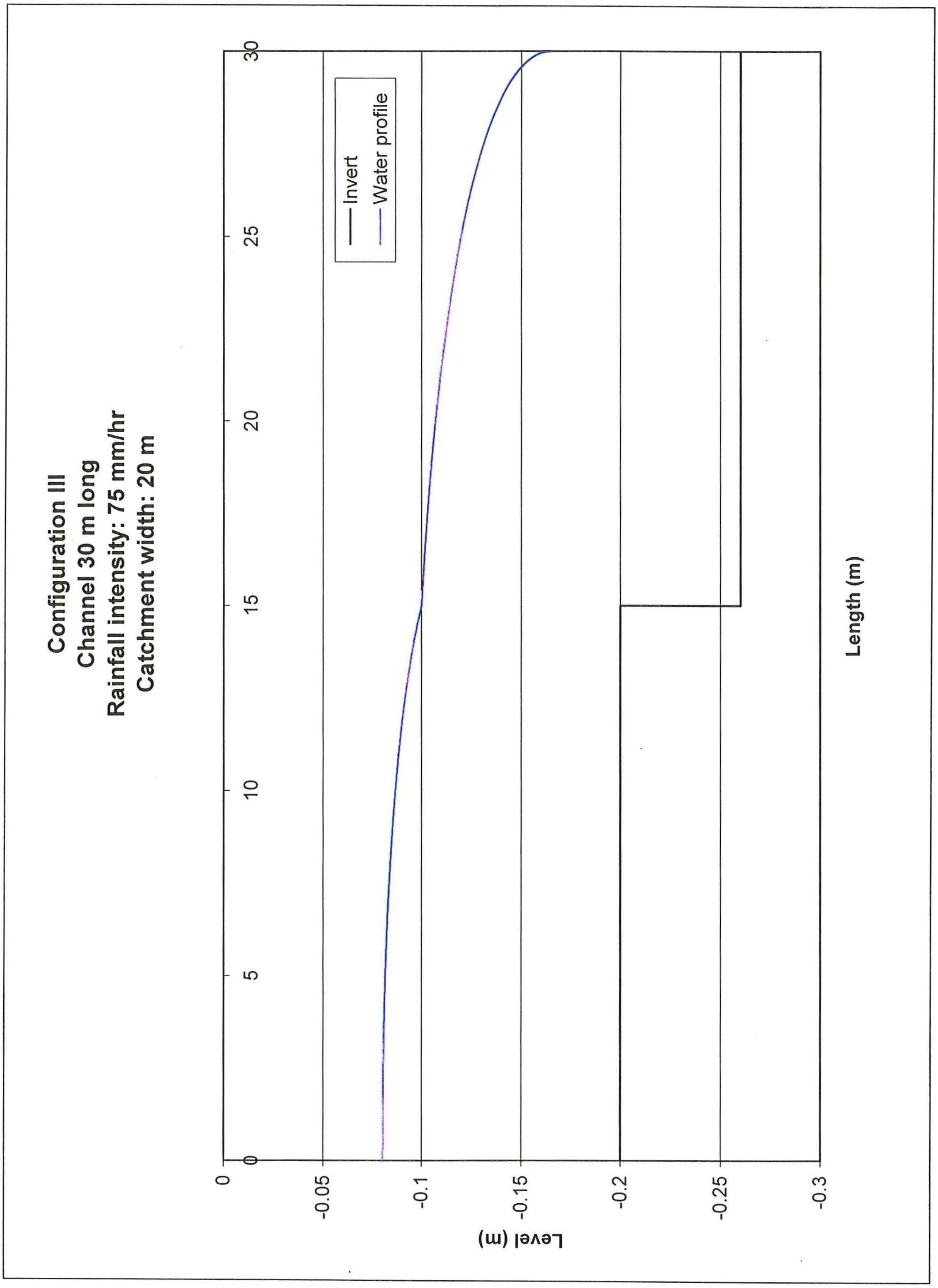

Figure 38 Numerical simulation of water profile. System G; Conf. III; rainfall intensity 75mm/hr

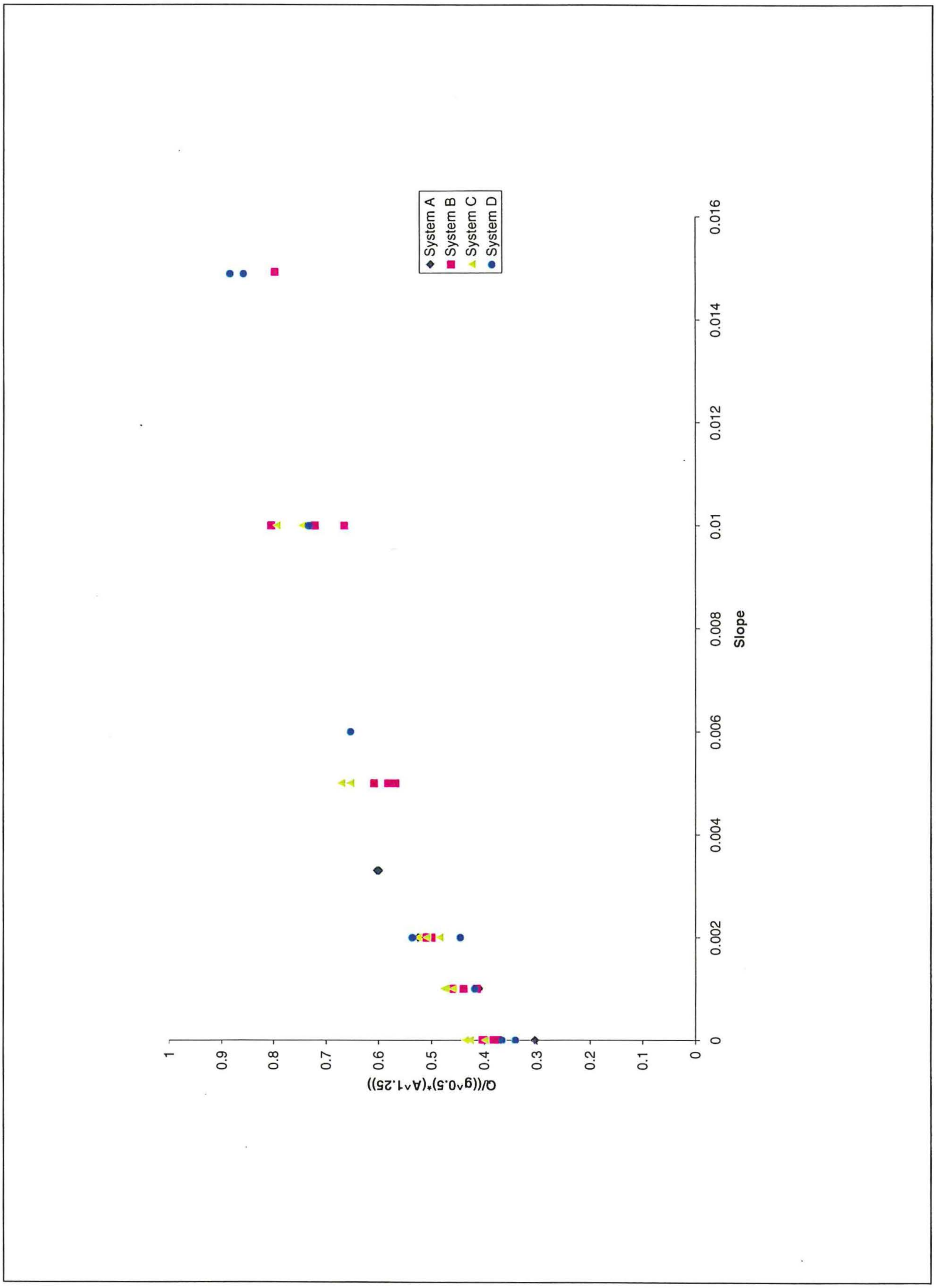

Figure 39 Experimental data; dependency of term $Q/(g^{0.5} A^{1.25})$ on slope

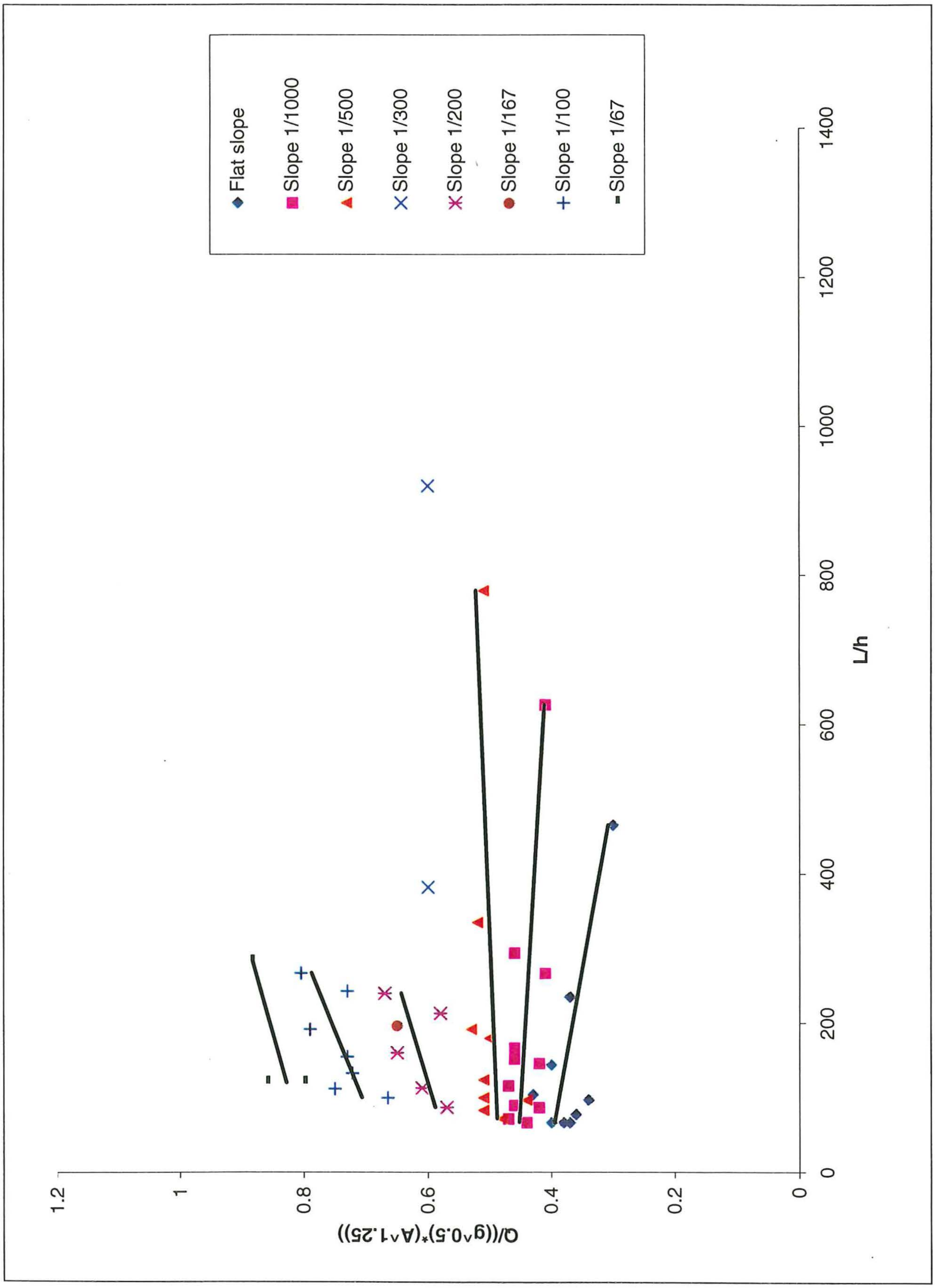

Figure 40 Effect of channel length

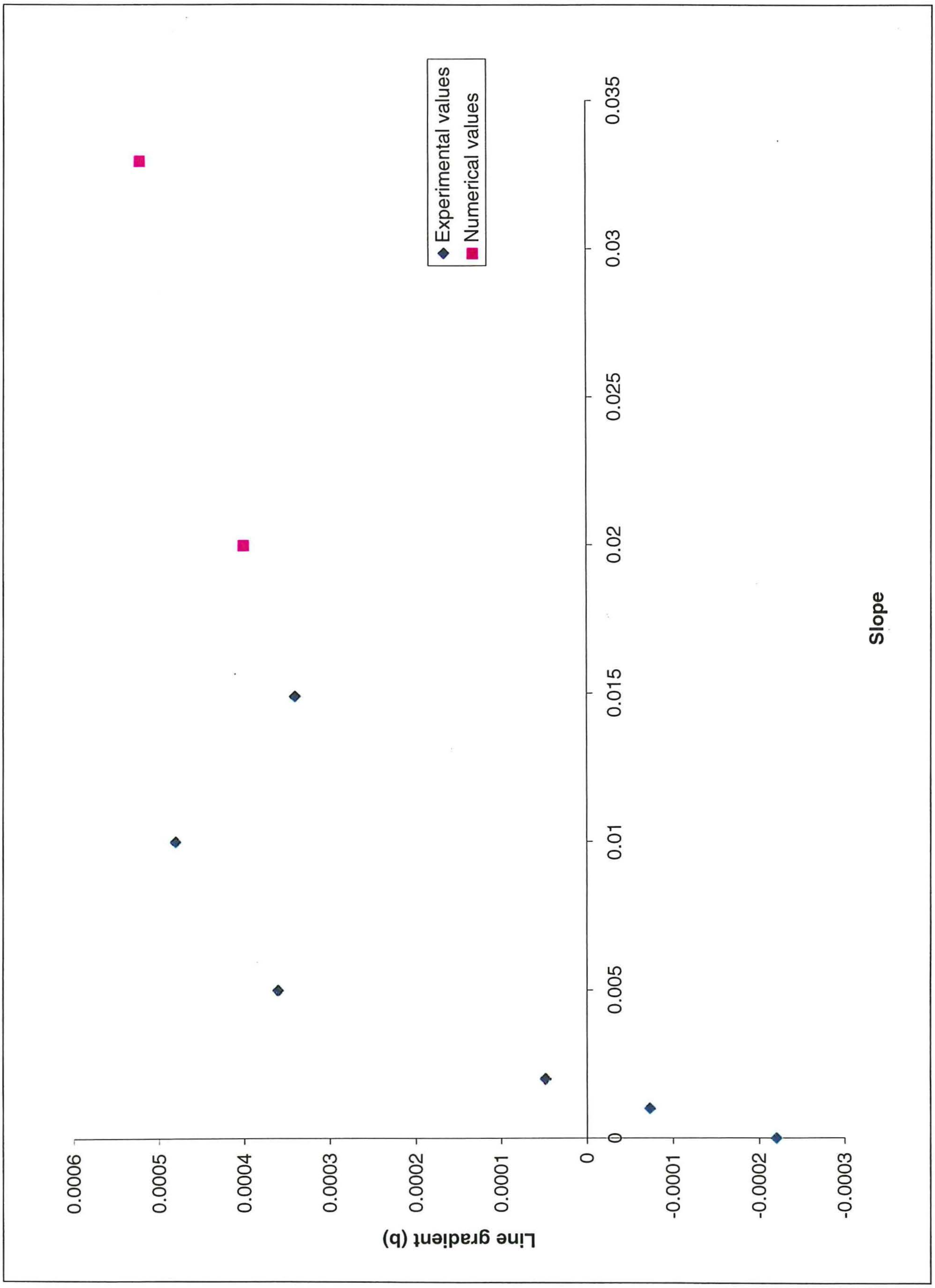

Figure 41 Variation of b with slope

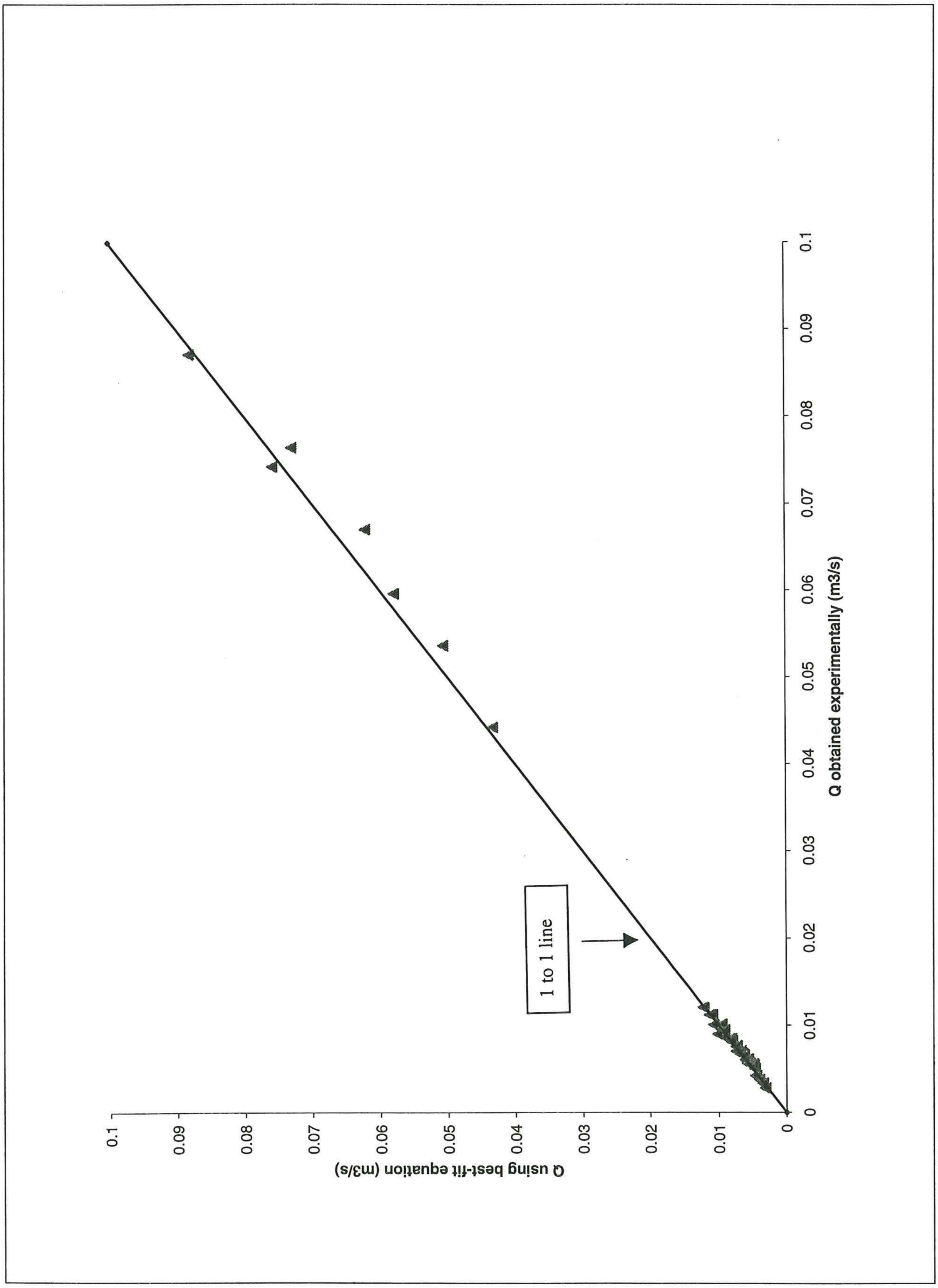

Figure 42 Comparison of measured and predicted flow rates

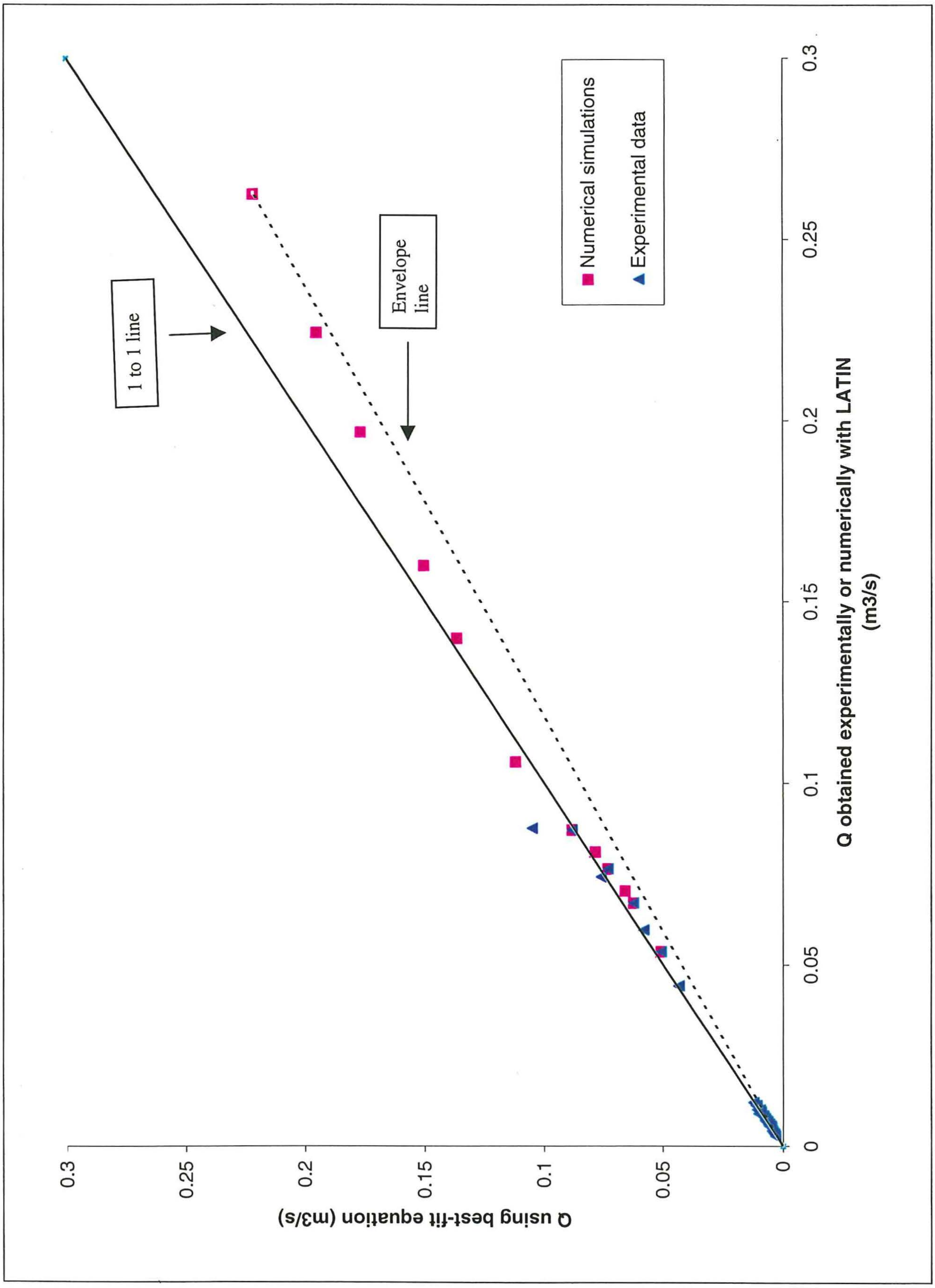

Figure 43 Comparison of measured and numerically simulated flows with predicted flows

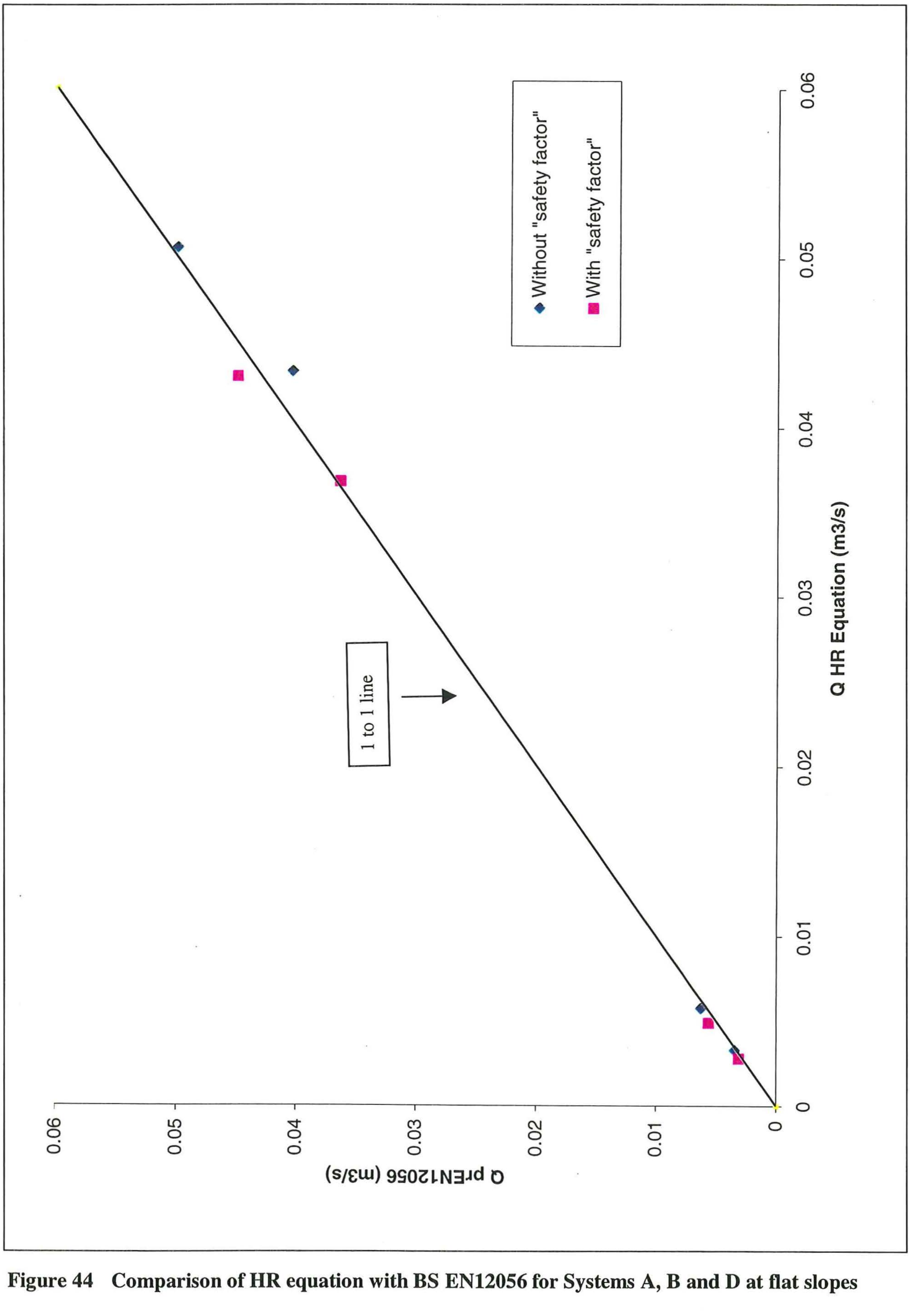

Figure 44 Comparison of HR equation with BS EN12056 for Systems A, B and D at flat slopes

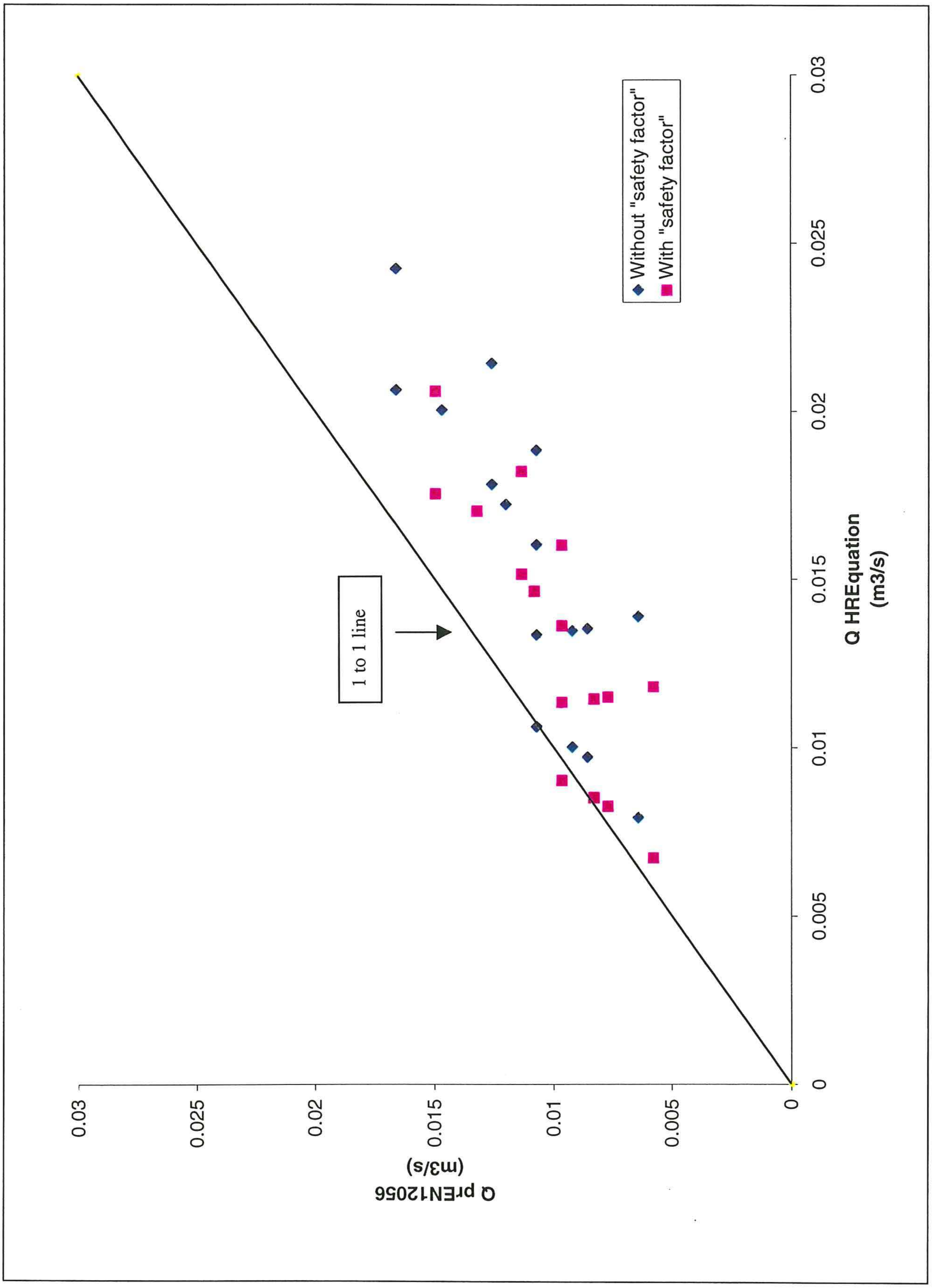

Figure 45 **Comparison of HR equation with BS EN12056 for synthetic data (slopes from 0 to 1/100 and length ratios between 50 and 500)**

Plates

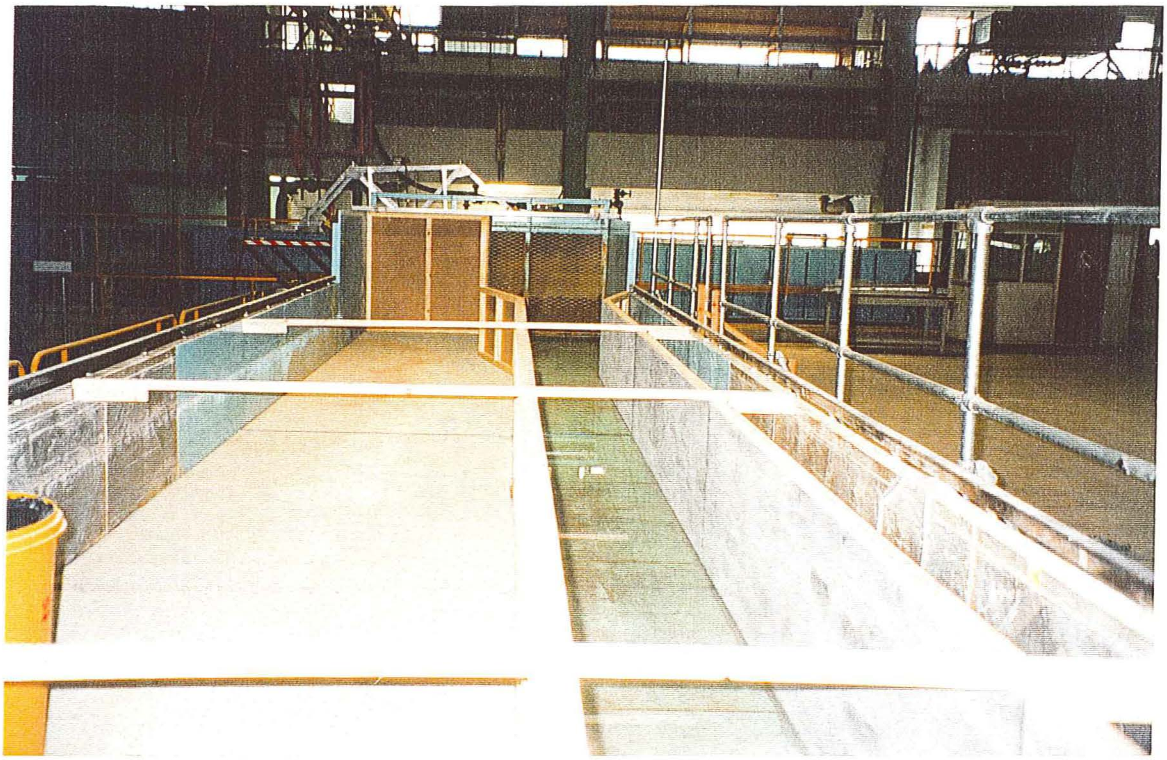

Plate 1a Adaptation of tilting flume
Upstream channel

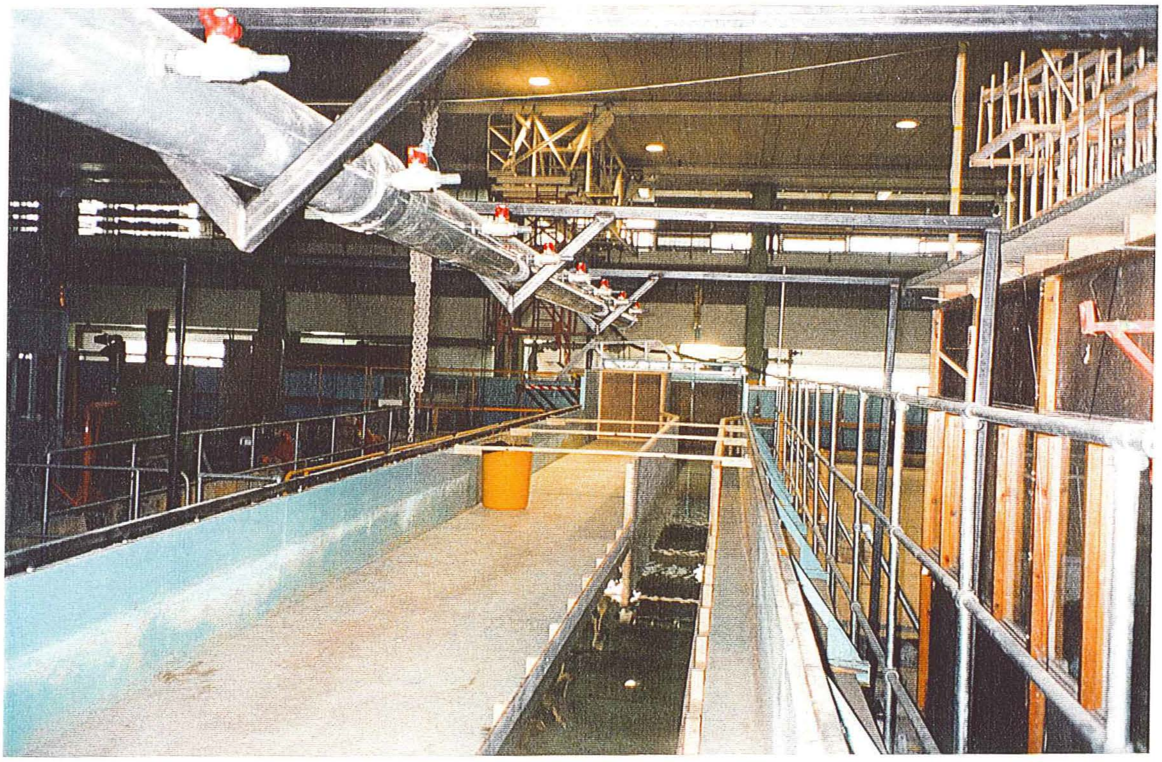

Plate 1b Adaptation of tilting flume
Overhead pipe manifold used to simulate rainfall

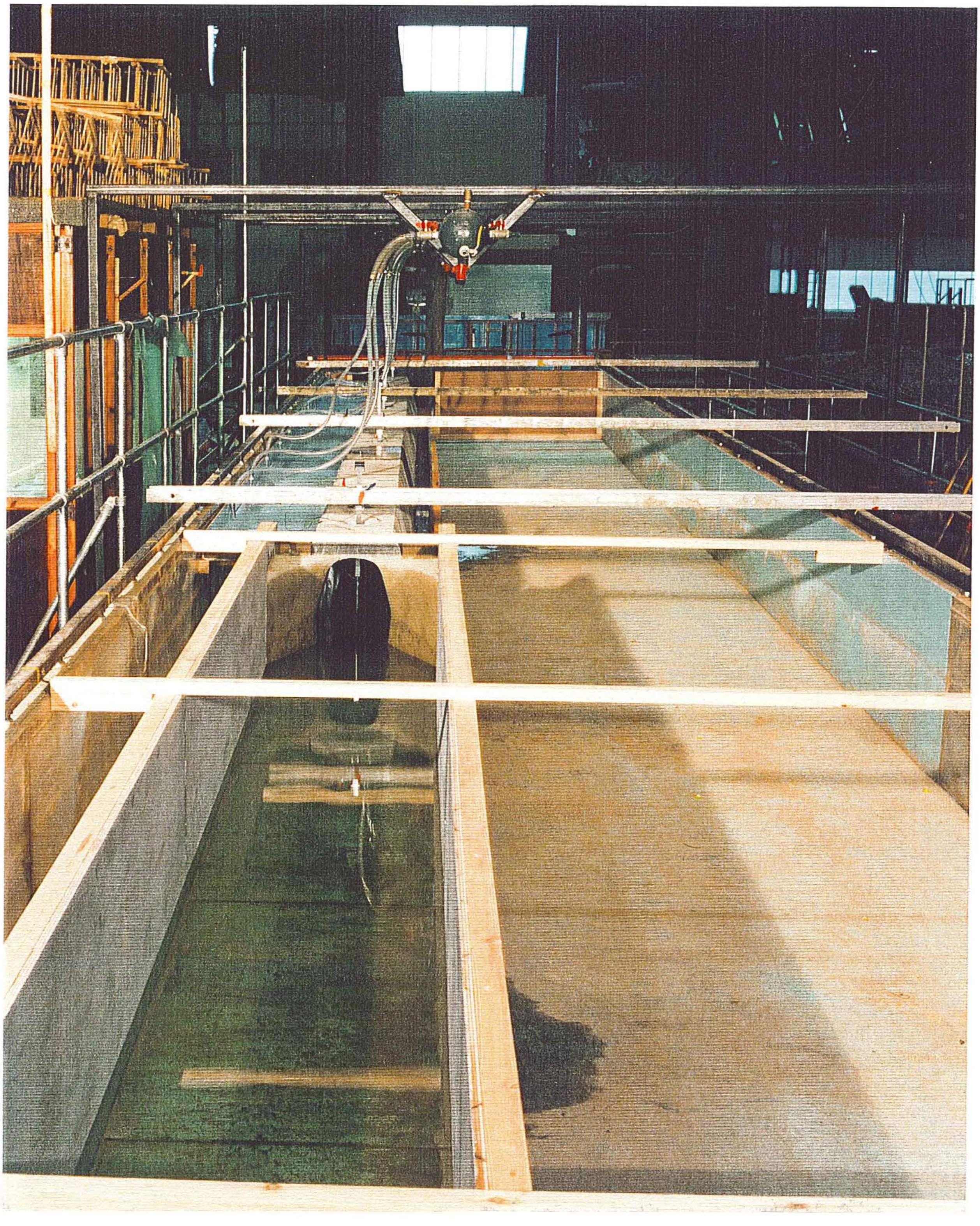

Plate 2 Testing System A

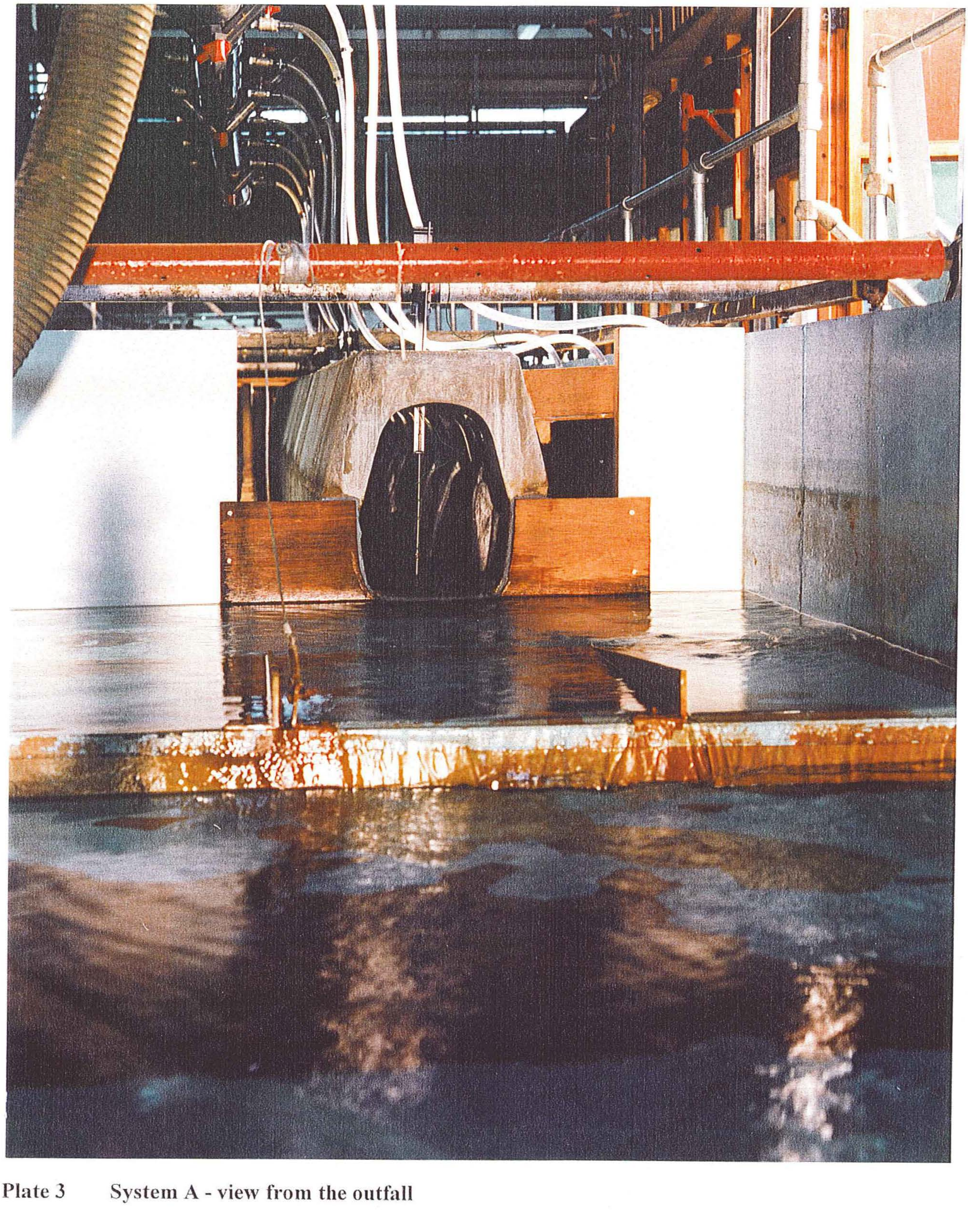

Plate 3 System A - view from the outfall

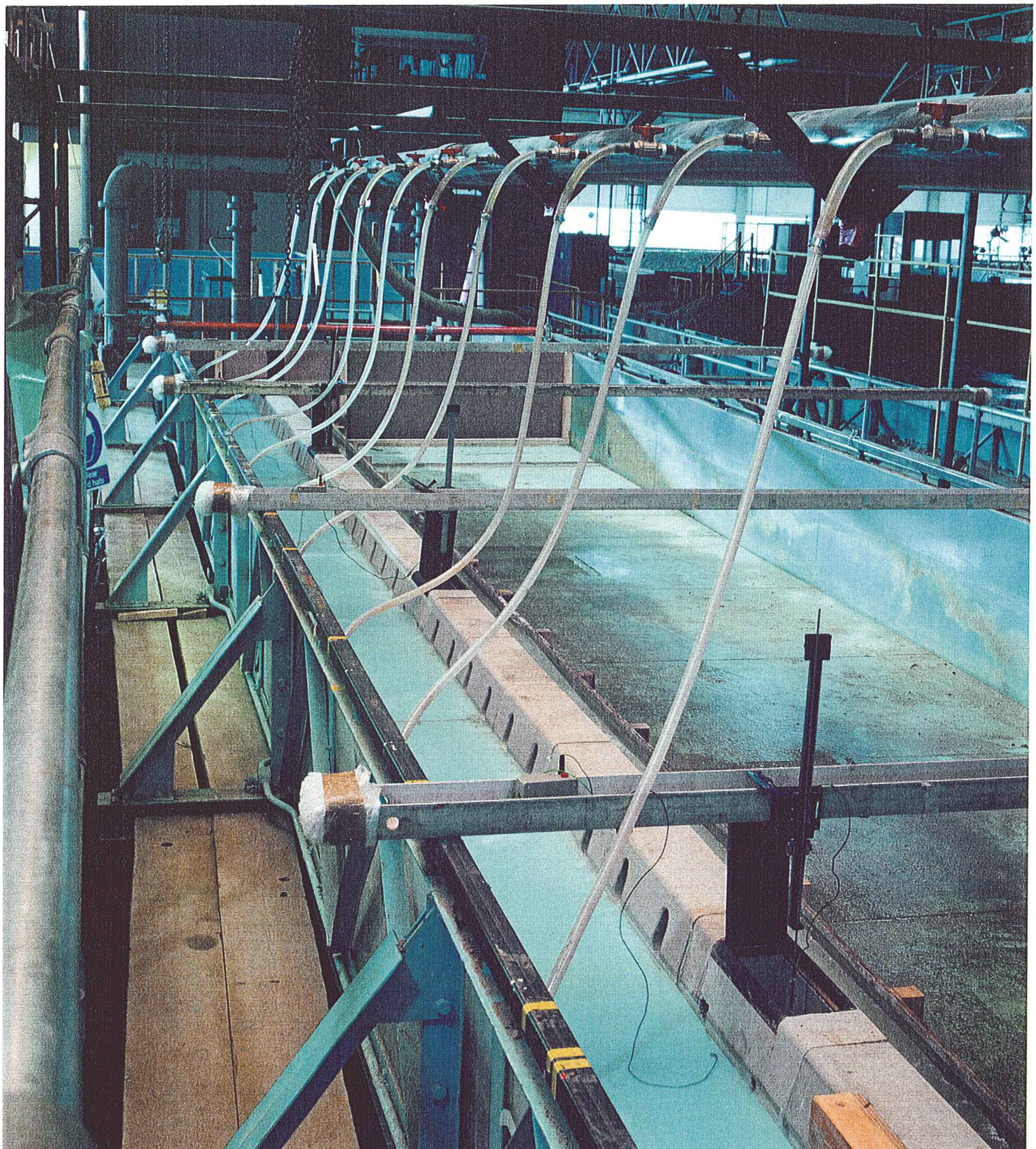

Plate 4 Testing System B

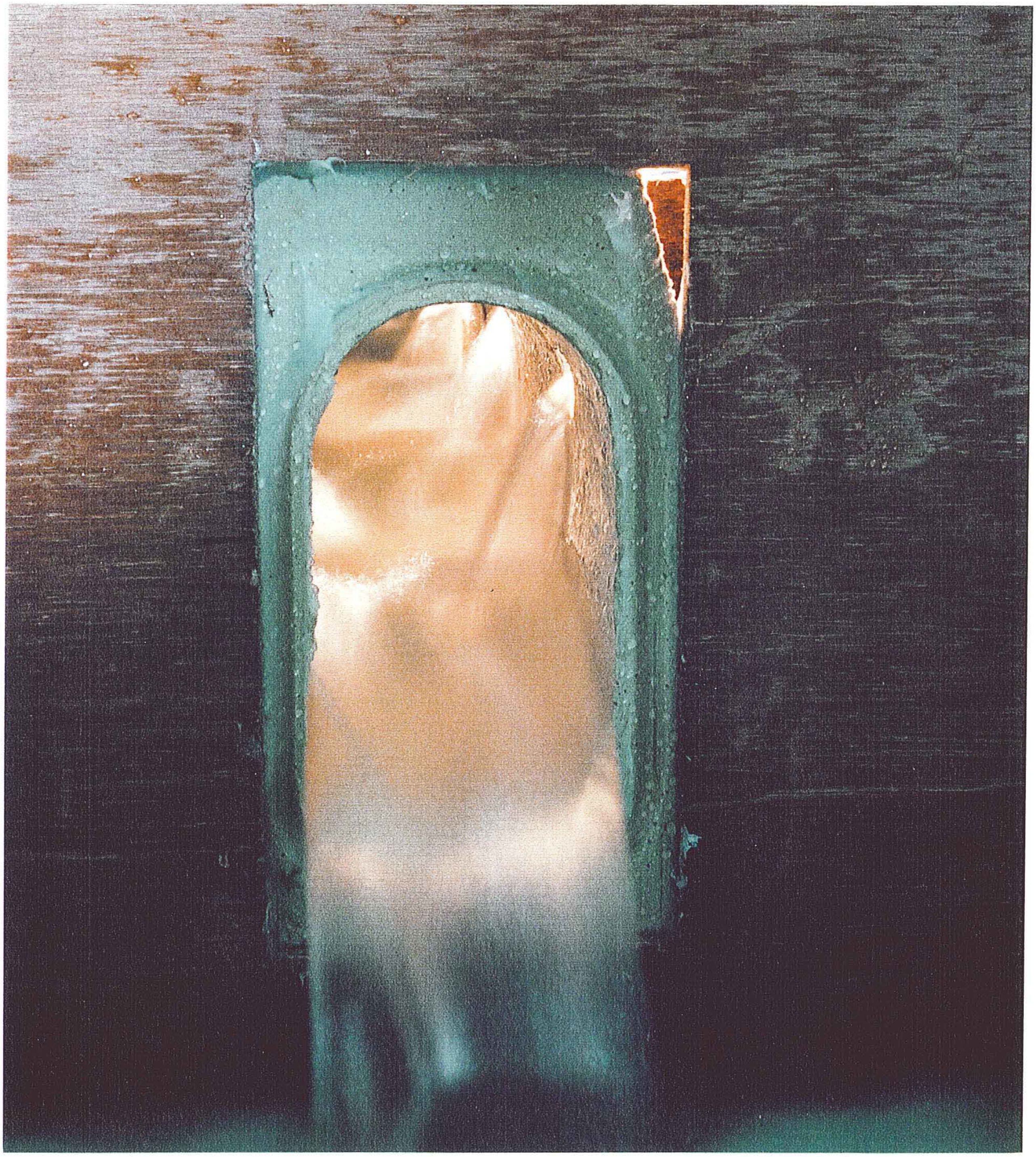

Plate 5 System B – view from the outfall

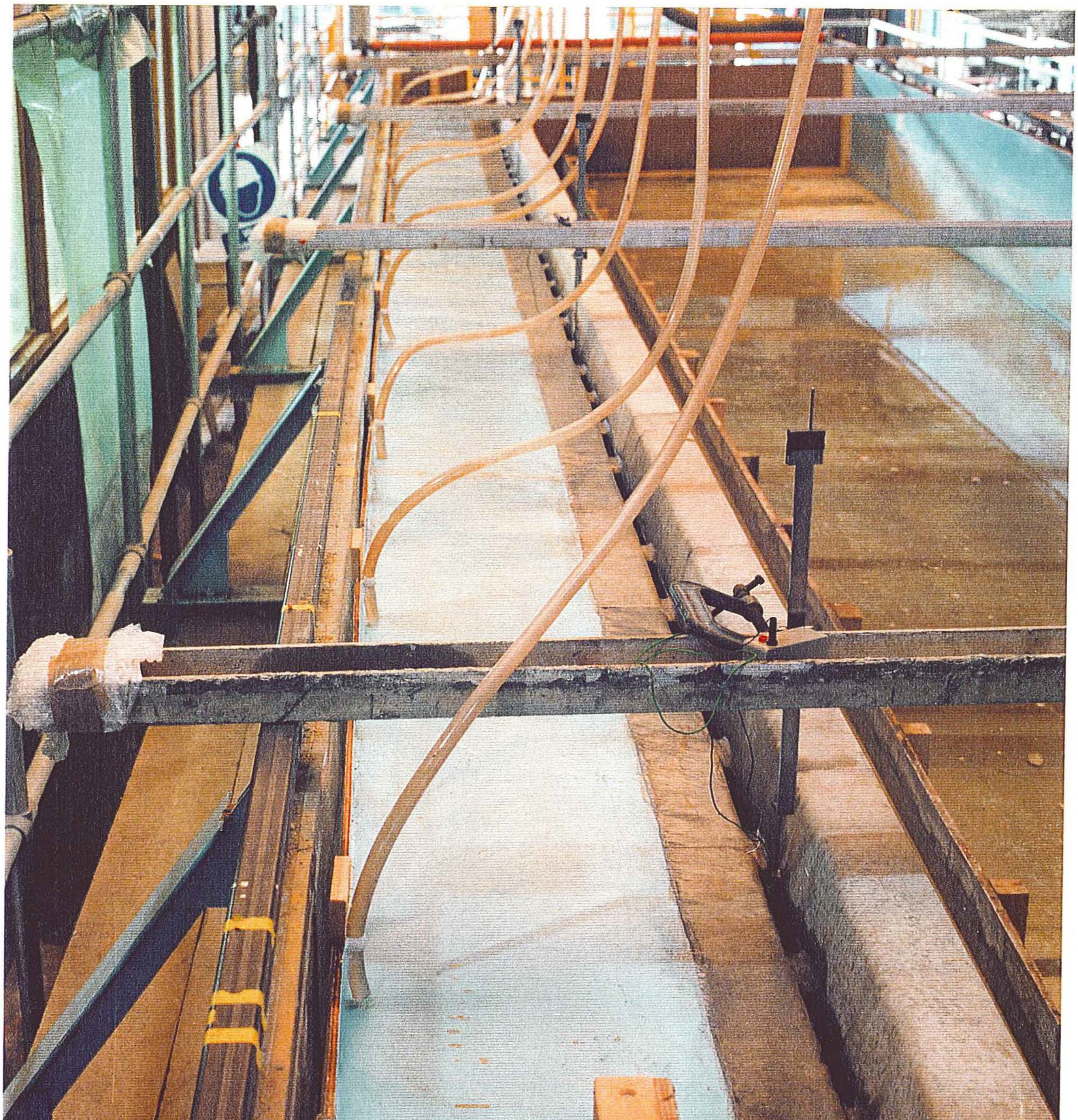

Plate 6 Testing System C

Plate 7 **System C – view from the outfall**

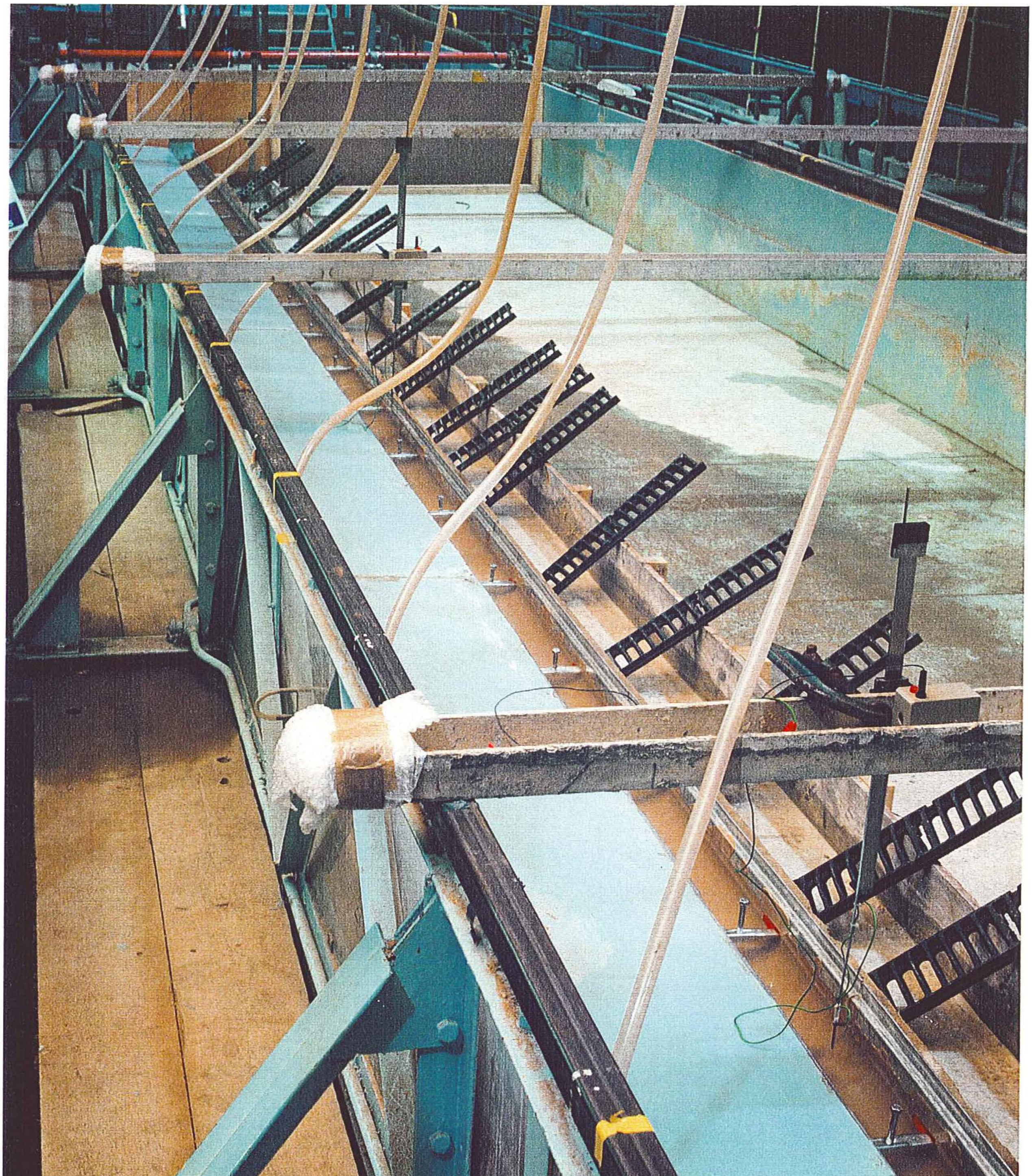

Plate 8 Testing System D

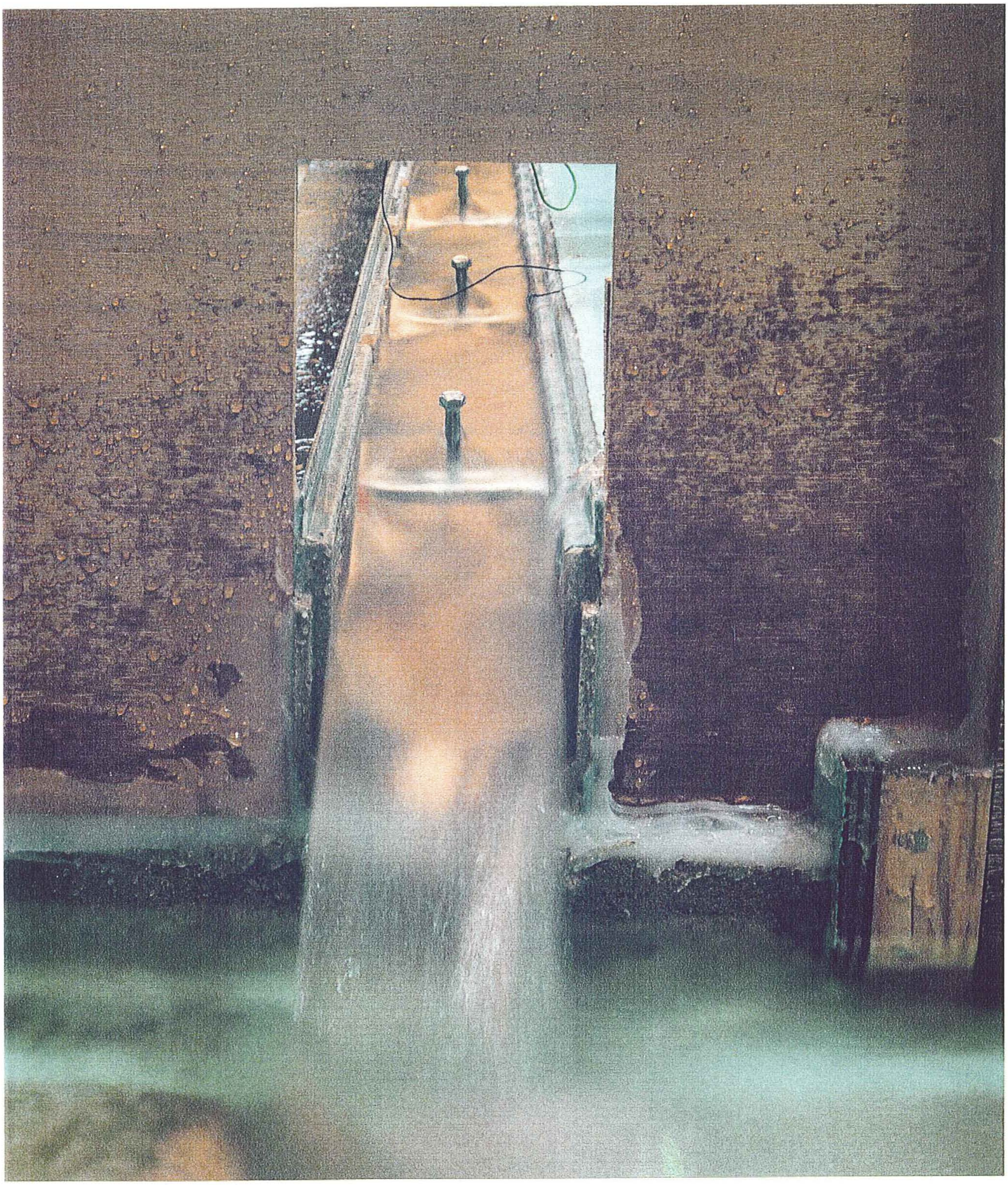

Plate 9 System D – view from the outfall

Plate 10 Eroded sediment bed (view from downstream). System A

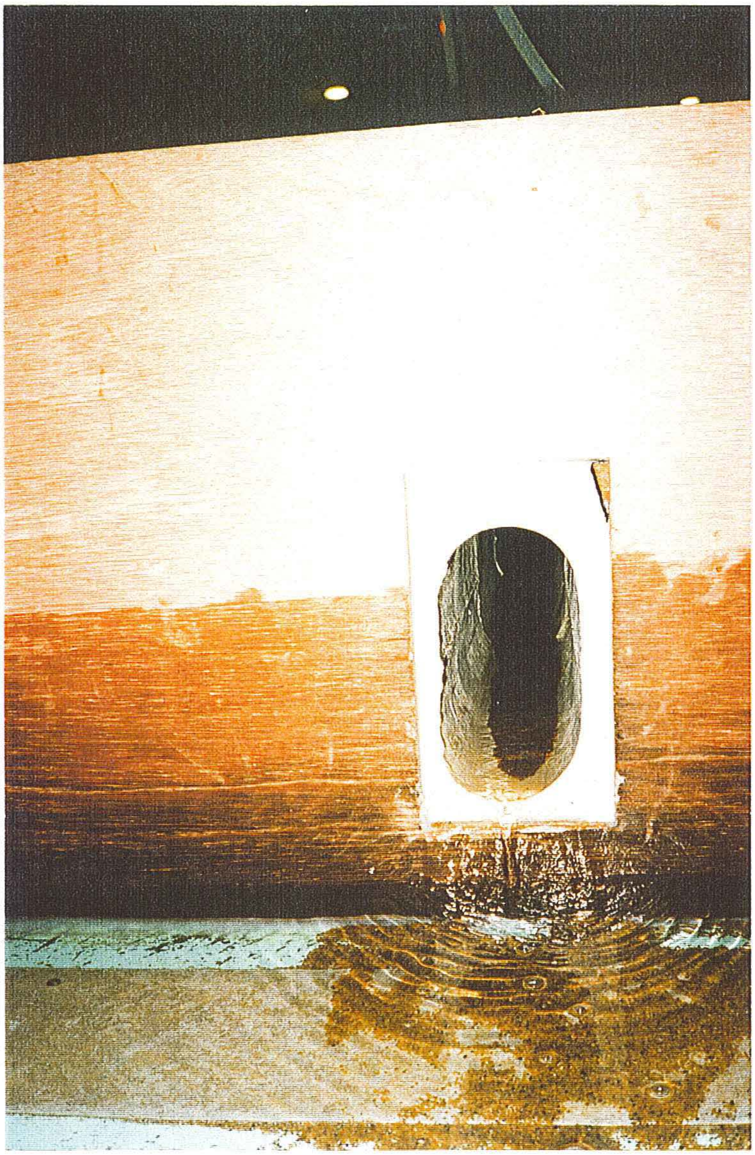

Plate 11 Sediment movement test (view from downstream). System B

Plate 12 Sediment movement (view from upstream). System D

Appendices

Appendix 1

Types of flow profile in sloping gutters (from May, 1982)

Appendix 1 Types of flow profile in sloping gutters (from May, 1982)

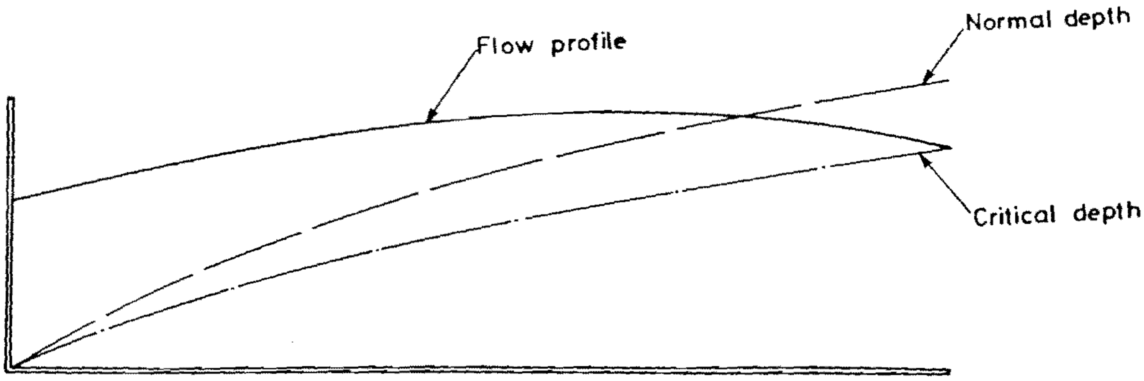

(a) $\frac{8S_0}{\lambda} < 1$

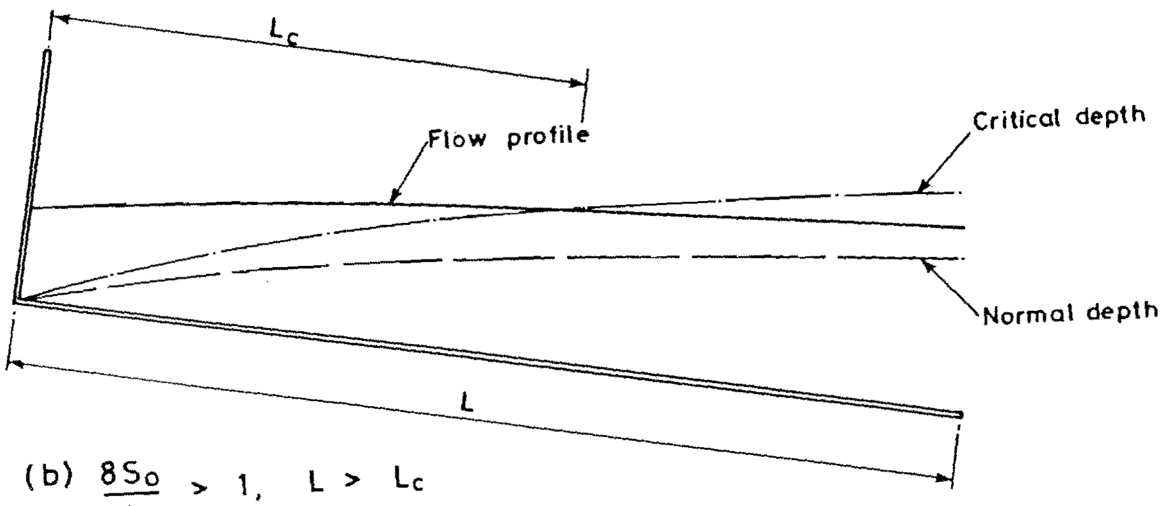

(b) $\frac{8S_0}{\lambda} > 1, \quad L > L_c$

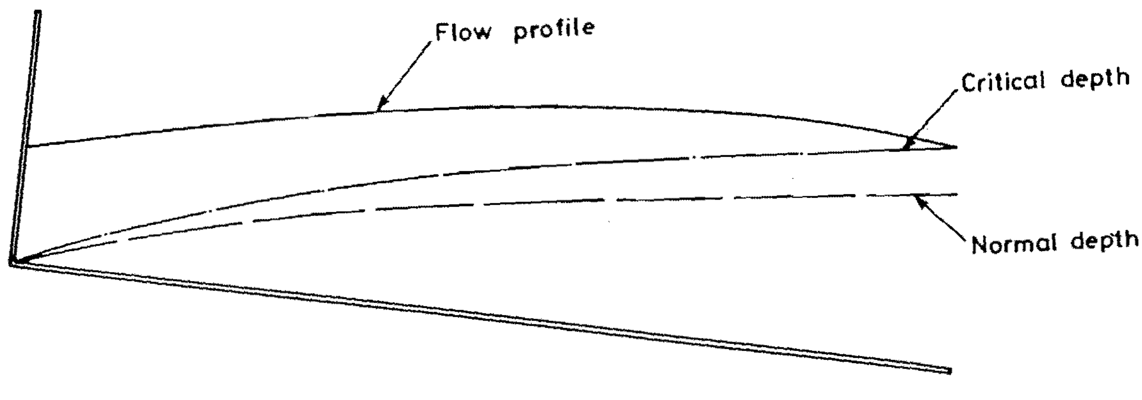

(c) $\frac{8S_0}{\lambda} > 1, \quad L < L_c$

Appendix 2

Friction laws considered in the spatially varied flow program

Appendix 2 Friction laws considered in the spatially varied flow program

The program for spatially varied flows (LATIN) was designed to include the following friction laws:

[See Notation for description of the symbols in these equations]

1. Strickler

$$S_f = \frac{1}{K^2}\frac{Q^2}{A^2 R^{4/3}}$$ K: Strickler's coefficient (A2.1)

2. Manning

$$S_f = n^2 \frac{Q^2}{A^2 R^{4/3}}$$ n: Manning's coefficient (A2.2)

3. Chézy

$$S_f = \frac{1}{Ch^2}\frac{Q^2}{A^2 R}$$ Ch: Chézy's coefficient (A2.3)

4. Colebrook-White

$$S_f = \lambda \frac{Q^2}{8\,g\,A^2 R}$$ λ: Darcy's coefficient (A2.4)

where

$$\frac{1}{\sqrt{\lambda}} = -2\log_{10}\left(\frac{k_s}{14.8R} + 2.52\frac{1}{Re\sqrt{\lambda}}\right)$$ k_s is the roughness and Re is the Reynolds number

Appendix 3

Mathematical solution of the slope at a singular section

Appendix 3 Mathematical solution of the slope at a singular section

The solution can be computed for the different friction laws (see Appendix 2). In the following example, the Colebrook-White equation is used.

[See Notation for description of symbols used in the following equations]

$$\frac{dy}{dx} = \frac{S_o - S_f - \frac{2\beta qQ}{gA^2}}{1 - Fr^2} \tag{A3.1}$$

$$\frac{dy}{dx} = m = \frac{So - \frac{\lambda Q^2}{8gRA^2} - \frac{2\beta qQ}{gA^2}}{1 - \frac{\beta BQ^2}{gA^3}} \tag{A3.2}$$

When the Froude number is equal to one the denominator is equal to zero but so is also the numerator. To compute the ratio, the solution is to use the derivative of the numerator upon the derivative of the denominator.

The friction coefficient, the slope, β and q are considered constant.

$$m = \frac{-\frac{\lambda}{8g}\frac{d}{dx}\left(\frac{Q^2}{RA^2}\right) - \frac{2\beta q}{g}\frac{d}{dx}\left(\frac{Q}{A^2}\right)}{-\frac{\beta}{g}\frac{d}{dx}\left(\frac{BQ^2}{A^3}\right)} = \frac{\frac{\lambda}{8\beta R^2}\left[2\left(\frac{q}{Q}\right)RA^2 - \left(mrA^2 + 2ARma\right)\right] + 2\left[\left(\frac{q}{Q}\right)^2 A^2 - 2ma\frac{q}{Q}\right]}{Amb + 2B\frac{q}{Q}A - 3amB} \tag{A3.3}$$

$$\frac{dR}{dx} = \frac{dR}{dy}\frac{dy}{dx} = rm \quad \text{with} \quad \frac{dR}{dy} = r$$

$$\frac{dA}{dx} = \frac{dA}{dy}\frac{dy}{dx} = am \quad \text{with} \quad \frac{dA}{dy} = a$$

$$\frac{dB}{dx} = \frac{dB}{dy}\frac{dy}{dx} = bm \quad \text{with} \quad \frac{dB}{dy} = b$$

$$m^2\left(\frac{Ab}{aB}-3\right)+m\left(\frac{2Aq}{aQ}+\frac{\lambda A}{8\beta RB}\left(\frac{rA}{Ra}+2\right)+\frac{4Aq}{BQ}\right)-\left[\frac{2\lambda A^2}{8\beta RaB}\frac{q}{Q}+\frac{2A^2q^2}{aBQ^2}\right]=0$$

Defining

$$Z=\frac{A}{B}$$

$$U=\frac{q}{Q}Z$$

$$E=\frac{\lambda}{8\beta}\frac{A}{BR}$$

the above equation can be written as follows:

$$m^2\left(\frac{b}{a}Z-3\right)+m\left[2U\left(\frac{b}{a}+2\right)+E\left(2+\frac{rA}{Ra}\right)\right]-2\frac{B}{a}U(E+U)=0$$

This equation can have two solutions.

Appendix 4

Illustration of water profiles

Appendix 4 Illustration of water profiles

Flat slope: Subcritical flow along the channel with a free exit

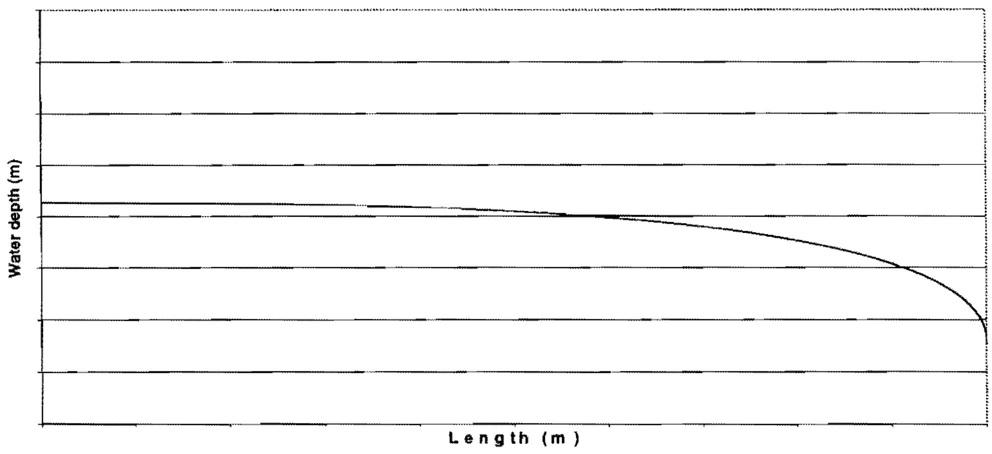

Mild slope: The flow could be either subcritical or subcritical, supercritical and subcritical

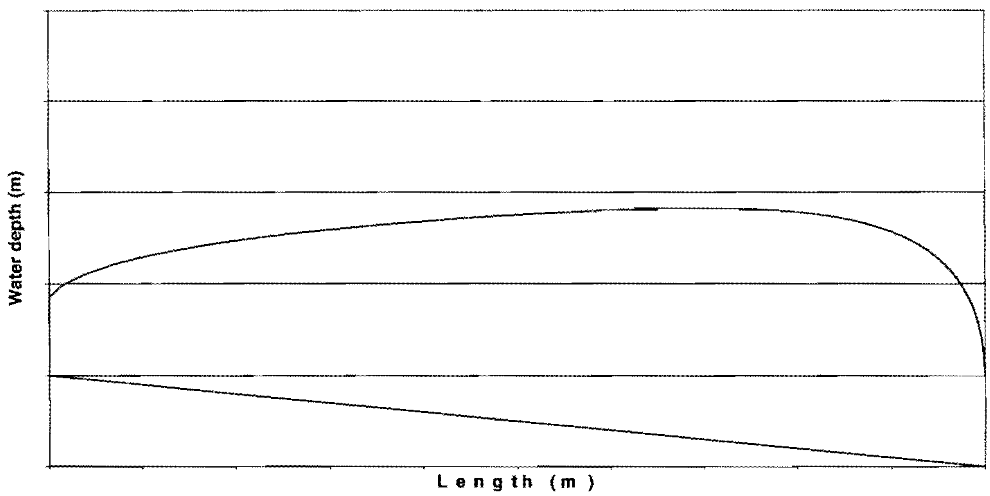

Steep slope (subcritical and supercritical)

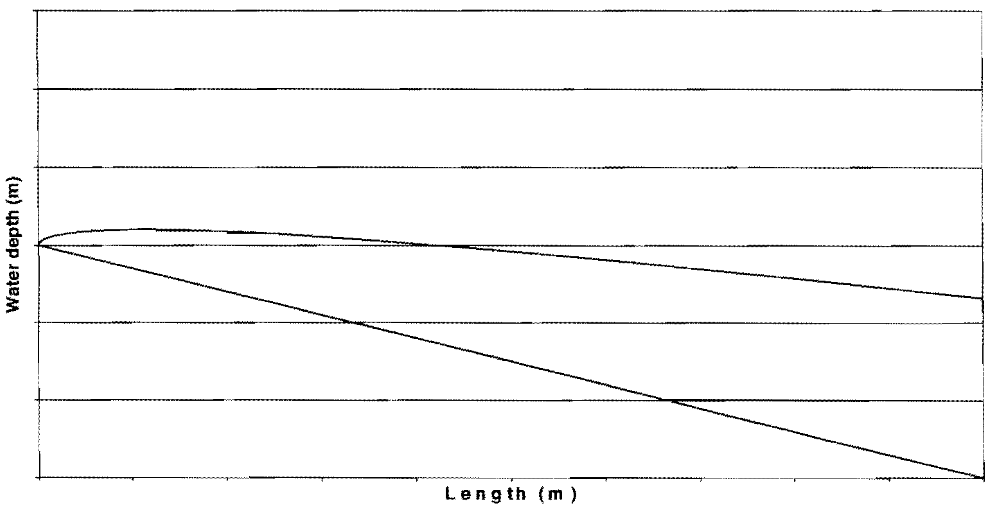

Appendix 5

Theoretical dependency of term $Q/(g^{0.5}A^{1.25})$ on L/h and slope

Appendix 5 Theoretical dependency of term $Q/(g^{0.5} A^{1.25})$ on the length ratio L/h and on the slope